Observations of Soil Moisture Dynamics Associated with Hydrocarbon Affected and Layered Coarse Textured Soils

A Thesis Submitted to the College of Graduate Studies and Research
in Partial Fulfillment of the Requirements
for the Degree of Master of Science
in the Department of Soil Science
University of Saskatchewan
Saskatoon, Saskatchewan, Canada

By
Meghan E. M. Rosso

PERMISSION TO USE

In presenting this thesis in partial fulfillment of the requirements for a Postgraduate degree from the University of Saskatchewan, I agree that the Libraries of this University may make it freely available for inspection. I further agree that permission for copying of this thesis in any manner, in whole or in part, for scholarly purposes may be granted by the professor or professors who supervised my thesis work or, in their absence, by the Head of the Department or the Dean of the College in which my thesis work was completed. It is understood that any copying, publication, or use of this thesis or parts thereof for financial gain shall not be allowed without my written permission. It is also understood that due recognition shall be given to myself and the University of Saskatchewan in any scholarly use which may be made of any material in this thesis. Requests for permission to copy or to make other use of material in this thesis, in whole or in part, should be addressed to:

Head of the Department of Soil Science
51 Campus Drive
University of Saskatchewan
Saskatoon, Saskatchewan
Canada, S7N 5A8

ABSTRACT

The Aurora Soil Capping study, located in northern Alberta, was constructed to evaluate reclamation practices on lean oil sands dumps. The challenges relating to its success includes determining the appropriate soil cover design(s) for the coarse textured reclamation soil, while utilizing available salvaged natural soils, some of which contain residual bitumen in the form of aggregate oil sand material (AOSM). Limited research on this material raises key questions as to the impact it will play on transport and retention processes, along with potential contamination from hydrocarbon leaching. The research conducted sought to answer these questions.

This thesis describes laboratory studies conducted on four soils; the upper organic LFH layer, Bm, BC and subsoil material while varying the amount of AOSM and implementing layering schemes. Material characterization through organic carbon and particle size analysis as well as hydrophobicity studies on AOSM through contact angle analysis were performed. A tension table and pressure plates, along with columns equipped with Time Domain Reflectometry probes, were used for water retention studies. Hydraulic conductivity was measured through constant head methods. To address hydrocarbon leaching concerns, chloride tracer studies were performed and the column outflow was analyzed using Gas Chromatography to detect the hydrocarbon type and concentration.

Results from water retention and hydraulic conductivity studies indicated that although the AOSM was hydrophobic, its placement at varying concentrations and forms did not create consistent significant differences in the amount of moisture retained or transported. Results from the column studies showed that under steady state and transient conditions AOSM could result in decreasing infiltration rates and increasing chloride retention. The integration of soil layers further slowed the infiltration rate and delayed chloride transport.

Under saturated conditions the presence of higher concentrations of AOSM appeared to increase the rate of water movement. Although these differences were minimal, further studies are required to explore this behavior.

Overall, it can be concluded that with appropriate material placement, the addition of layering schemes and hydrocarbon material, the potential exists to increase soil water content in the upper layers of the soil, thereby increasing soil water storage for plant use.

ACKNOWLEDGEMENTS

I would like to thank my supervisors, Dr. Bing Si and Dr. Lee Barbour, for providing the opportunity to work on this project, for the financial support, and for the guidance through the course of my graduate studies. I would also like to thank my supervisory committee, Dr. Jeffrey Schoenau and Dr. Derek Peak who have been supportive in helping me to complete my thesis. I would like to extend my appreciation and gratitude to the students of the soil physics lab and all students and staff of the Department of Soil Science for their assistance and guidance throughout my thesis. Thanks to Dr. Dirk de Boer for his contributions as an external examiner.

I would also like to express my sincere appreciation towards my husband and family for their continual encouragement, guidance and support throughout this process. Without your involvement this work would not have been possible.

TABLE OF CONTENTS

LIST OF TABLES

LIST OF FIGURES

ABBREVIATIONS

ACS	Aurora Soil Capping study
ANOVA	Analysis of Variance
AOSM	Aggregated Oil Sand Material
BTC	Breakthrough Curve
CA	Contact Angle
$CaSO_4$	Calcium Sulphate
CEC	Cation-Exchange Capacity
CEMA	Cumulative Environmental Management Association
CCME	Canadian Council of Ministers of the Environment
CWS	Canada-Wide Standards
EC	Electrical Conductivity
FID	Flame Ionisation Detection
GC	Gas Chromatography
Jw	Flux
K	Potassium
KCl	Potassium Chloride
KPa	Kilopascals
Ksat	Saturated Hydraulic Conductivity
LFH	Topsoil Material Containing Varying Levels of Decomposed Forest Litter
LOS	Lean Oil Sands
MDLs	Method Detection Limits
Na_2SO_4	Sodium Sulphate
NH_4^+	Ammonium
PAH	Polycyclic Aromatic Hydrocarbons
P	Phosphorus
PSD	Particle Size Distribution
PWP	Permanent Wilting Point
SOM	Soil Organic Matter
TDR	Time Domain Reflectometry
TOC	Total Organic Carbon
WDPT	Water Droplet Penetration Time
d_{wb}	Drainage Water
e	Void Ratio
ρb	Bulk Density
t_b	Breakthrough Time
θ	Soil Water Content
h_m	Matric Head
n	Porosity

1. INTRODUCTION

The Aurora Soil Capping study (ACS), located on the Syncrude Aurora mine, was designed to evaluate the impact of soil capping depth, reclamation material selection and the presence of coarse textured hydrocarbon-affected material on reclamation performance. The ACS is constructed over mining overburden dumps of lean oil sands (LOS). The challenges faced in reclaiming LOS include determining the appropriate coarse textured soil cover design(s) required to re-establish an equivalent capability to that of naturally occurring boreal forest ecosystems (Yarmuch, n.d.). Aside from water storage limitations from the coarse textured material, the residual bitumen within its natural state has the potential to contribute to soil water repellency issues (Hunter, 2011). Hunter (2011) indicates that soil water repellency, or hydrophobicity, may pose issues to restricting infiltration and increasing erosion.

Although the Aurora Soil Capping project focuses on integrating various soil capping depths, configurations and reclamation materials on a larger scale, the individual materials that comprise the study must be characterized to assist in identifying the extent of water storage limitations and hydrophobicity issues. An increased understanding of each of the reclamation material characteristics will provide insight into which material will increase reclamation success in the Athabasca Oil Sand region. Further studies into the effect of material layering and varying percentages of hydrocarbon material will indicate whether the presence of disturbed, naturally occurring aggregate oil sand material (AOSM) within a reconstructed reclamation soil profile will further impact nutrient and soil water dynamics.

The focus of this study is on characterizing the transport and water retention behavior of potential reclamation soils, including the potential release of contaminants from the naturally

present hydrocarbons in the form of AOSM, as a measure of future reclamation performance. The specific objectives of this study include:

1.) Evaluating soil water retention, saturated hydraulic conductivity and water repellency of reclamation materials

2.) Determining the effect of varying hydrocarbon concentrations, in the form of AOSM, on soil water retention, saturated hydraulic conductivity and water repellency

3.) Assessing transit times associated with leaching potential of nutrients and hydrocarbons in coarse textured, hydrocarbon affected soils

In order to meet these objectives, a series of laboratory studies were conducted. This thesis focused on four soils; the upper organic LFH layer, Bm, BC and subsoil material from below one meter. In some cases the hydrocarbon content of these materials was altered to produce a range of hydrocarbon contents. The hydrocarbon was present primarily in the form of aggregate oil sand material (AOSM). Material characterization by organic carbon and particle size analysis, along with tension table and pressure plate methods to determine the water retention and hydraulic conductivity of each soil is described in Chapter 3. The hydrophobicity of the reclamation soils and the naturally occurring bitumen was assessed through contact angle analysis and the water droplet penetration time (WDPT) test. Larger scale column studies were utilized in Chapter 4 to assess the effect of varying hydrocarbon concentrations along with soil layering on water flow and storage. This was achieved through the use of Time Domain Reflectometry (TDR) probes equipped within the columns which measured the moisture content under field capacity conditions. Water and nutrient transit time were also measured using constant head methods and chloride tracer Breakthrough Curves (BTC). The outflow solution

was further analyzed using Gas Chromatography (GC) with FID (Flame Ionisation Detection) to detect the hydrocarbon type and concentration leached through the columns.

2. LITERATURE REVIEW

Canada retains the only large-scale commercial oil sands industry with the largest oil sand deposits in the world found in northern Alberta (U.S. Department of the Interior, Bureau of Land Management (BLM), 2012). According to the U.S. Department of the Interior, Bureau of Land Management (2012), the extraction of the oil-rich bitumen for refinement, through strip or open pit mining techniques, leads to significant land destruction through removal of natural vegetation, as well as disturbance and extraction of the soil material from functioning ecosystems.

This chapter will review current reclamation practices used to address the extracted soil material, along with the challenges and influence this material has on water storage and transport processes.

2.1 Overview of Current Reclamation Research Practices: Aurora Soil Capping Study

Current multi-company reclamation efforts are taking place within the oil sands region of Northern Alberta. The Aurora Soil Capping Study, led by Syncrude Canada Limited, is located approximately 100 kilometers north of Fort McMurray, Alberta on the Fort Hills overburden disposal area within the Athabasca oil sand deposit area. This research site consists of replicated one hectare plots of various soil prescriptions, configurations, and soil capping depths (Yarmuch, n.d.) as well as re-vegetation species. The soil prescriptions utilized at the Aurora reclamation site are illustrated in Figure 2.1.

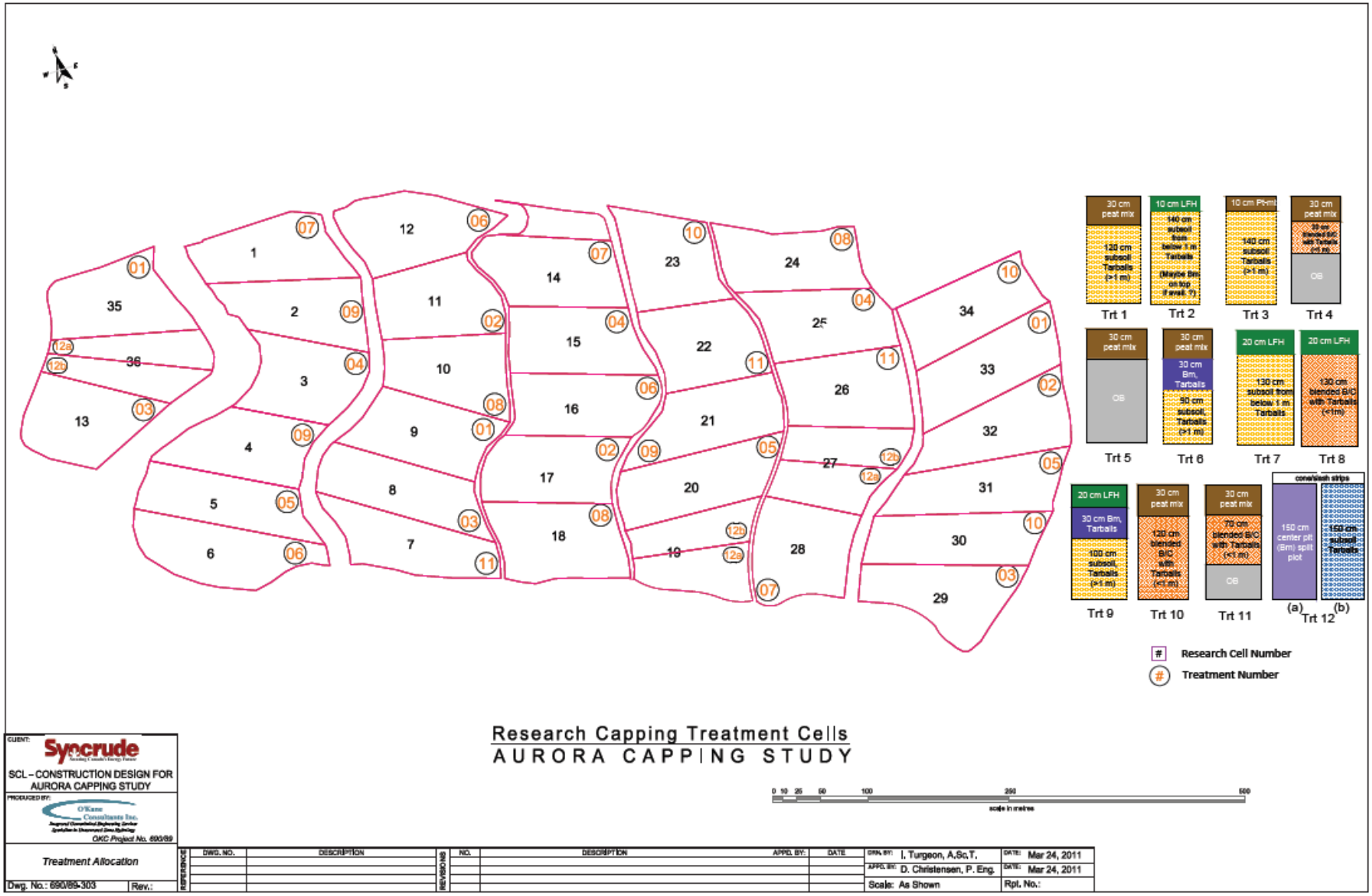

Figure 2.1: Aurora Soil Capping Study Reclamation Prescriptions

The overall focus of the study is to evaluate the various configurations and reclamation materials in an attempt to reduce the challenges associated with the soil material and increase reclamation success.

2.1.1 Key Challenges Associated with Reclamation Success

The oil sands region of Northern Alberta is located within the Boreal Mixedwood Ecoregion (Strong and Leggat, 1981) which can be classified as ecosites a, b (Yarmuch, n.d.) and d (Zettl et al., 2011). The key challenges encountered with reclaiming these sites to the boreal forest ecosystem are in relation to soil profile reconstruction with the organic LFH and coarse textured reclamation soil present, along with the disturbed naturally occurring residual bitumen. This section will review the impact of this material on water storage, transport and nutrient availability.

2.1.1.1 Water Storage

The soil type from ecosites a, b and d can be identified mainly as a dry to very dry sandy soil (Beckingham et al., 1996). Sheoran et al. (2010) indicate that these are soils consisting of high amounts of coarse fragments contain larger pores, also known as macropores, which are unable to store enough plant available water to sustain growth throughout the summer months. This is further identified through ecosite classification in which the soil material ranges from very xeric, xeric, subxeric, submesic, to mesic (Beckingham et al., 1996). These moisture regimes encompass sites in which rates of water release by drainage are much higher than rates of water supply (British Columbia Ministry of Forests (BCMOF) Research Branch, 1998). Due to the rapid removal, water will be available, at most, for only short periods following precipitation events (British Columbia Ministry of Forests (BCMOF) Research Branch, 1998). Although the coarse-textured soil shows limited water storage potential, Sheoran et al. (2010)

indicate that the ability of the soil to provide water is highly correlated to the soil transport processes that occur within the specific soil profile. This is further reported by Zettl et al. (2011) which indicated that the areas of northern Alberta support a range of ecosite types, and subsequently a range of varying moisture regimes, even though the sites exhibit very similar soil texture. The range of moisture regimes within the similar textured naturally coarse soil indicates that there is the potential for natural mechanisms occurring which must be understood. This may include factors such as the presence of organics and textural layering which will be reviewed in the following sections.

2.1.1.2 Water Transport and Nutrient Availability

In addition to the challenges relating to adequate moisture storage, the reclamation soil from the three ecosites of Northern Alberta are also identified as typically rapid to well drained with a poor to medium nutrient regime classification (Beckingham et al., 1996). This further identifies issues relating to moisture storage given the rapid transport rates identified, along with limited nutrient availability present on these well-drained soils.

The ease of water movement, horizontally and vertically, through the soil can be defined by the hydraulic conductivity (McCauley and Jones, 2005). Bouma (2008) indicates that hydraulic conductivity values are highly dependent on the soil pore geometry and water content. It was identified that the hydraulic conductivity decreases with a decrease in water content and pore size of a soil (McCauley and Jones, 2005). Therefore, a coarse textured sand can be characterized as a matrix of large, well-connected pore spaces that are able to transmit water readily (Ritter, 2009; McCauley and Jones, 2005), indicating a high hydraulic conductivity and infiltration rate (McCauley and Jones, 2005; Portage County Government, 2008). Typically the hydraulic conductivity of a coarse sand ranges from 5 m d^{-1} to 20 m d^{-1}(Bouma, 2008), or 20.83

cm hr^{-1} to 83.33 cm hr^{-1}. The large hydraulic conductivity characteristic of coarse textured soils, and the limited proportion of small pores, results in faster water flow rates and increased leaching potential of nutrients. This significantly influences their ability to store water and nutrients for plant growth.

Aside from the influence soil texture has on water storage, external factors that affect the soils ability to store water must be reviewed. One of the factors controlling water transport and nutrient availability is the degree of soil compaction that occurs during soil placement. McCauley and Jones (2005) found that compaction can affect the movement of water through the soil by decreasing the porosity and infiltration and increasing the bulk density of the soil. This results in loss to soil water storage, poor nutrient movement and restrictions to root growth (McCauley and Jones, 2005). McMillan et al. (2007) reported increases in bulk density on reclaimed sites within the Athabasca oil sands region, as compared to naturally undisturbed sites, which they attributed to surface compaction. The extent of compaction on the soil is a function of the soils properties, including the amount of organic matter, water content, texture, bulk density, and structure (McCauley and Jones, 2005). Jones (1995) notes that typically soils with a range of particle sizes are more susceptible to compaction as compared to soils composed mainly of one particle size. In addition, soils that exhibit low organic matter have an increased susceptibility to compaction due to poor structural stability (McCauley and Jones, 2005). Given the elevated field bulk densities observed of 1.69 gcm^{-3} and 1.71 gcm^{-3} at sites within the Athabasca oil sands (Huang et al., 2011) and information that typically bulk densities greater than 1.80 gcm^{-3} restrict root growth within sandy soils (USDA, n.d.), the concern for compaction and its impact on water movement and storage are evident.

2.1.1.3 Presence of Organics: LFH Material

The organic matter integrated into the Aurora Soil Capping Study site includes a mix of soil material with peat and LFH material. In relation to the topsoil layer of the reclamation treatments, Hunter (2011) indicates the independent use of LFH in reclamation prescriptions to be fairly recent. Given its recent use as a reclamation prescription, and for the scope of this thesis, only the LFH material will be reviewed. The LFH components will first be reviewed, followed by their impact on water transport and storage.

The organic horizons of a soil include L, F and H, which consists mainly of forest litter at varying stages of decomposition (Soil Classification Working Group, 1998). The L layer is an accumulation of organic matter in which the original leaf, twig or woody material is easily distinguished. The F and H layers are partly decomposed and fully decomposed organic material, respectively (Soil Classification Working Group, 1998). The H horizon differs from the F horizon by exhibiting greater humification whereby the original structures of the organic material are not identifiable. It is also frequently mixed with mineral grains (Soil Classification Working Group, 1998).

The beneficial use of LFH material as a Soil Organic Matter (SOM) amendment is evident given its contribution to biological activity, providing plant nutrients, improving soil structure, reducing erosion and increasing infiltration (Sheoran et al., 2010; Leeper and Uren, 1993). It can also be noted that the organic carbon stored within the SOM (NRCS et al., 2011) also contributes to the creation of favourable conditions relating to tilth, soil structure development, and the water-holding capacity of the soil (Pennock et al., 1995). Although Leeper and Uren (1993) identified that the organic matter increases the cation-exchange capacity (CEC),

and the sandy soils ability to hold water, results from Hunter's 2011 study indicate that the LFH material from the Athabasca oil sands region does not always increase infiltration.

Hunter (2011) identified that the LFH material has the tendency to fall between wettable and water repellent, indicating that it is not severely water repellent but it has the potential to restrict water infiltration under specific conditions, such as with increased decomposition levels. This was also concluded by Roberts and Carbon (1972), through the identification that the compounds within the humic organic matter fraction contribute to soil water repellency due to skins of organic material forming on the sand grains. This suggests the potential for the LFH material to have a detrimental impact on soil water storage and subsequently decreased infiltration. In addition to interest placed on implementing LFH topsoil material into cover designs, focus has also been on the utilization of the residual bitumen in its natural state. This will be covered within the subsequent sections.

2.2 Influence of Residual Bitumen in the Soil

Bitumen is present in many surficial alluvial soils in the oil sands region, sometimes disseminated but more often in the form of bitumen layers or tarballs (Fleming et al., 2012; Itah and Essien, 2005). For the remainder of this thesis tarball material will be referred to as aggregate oil sand material (AOSM). The range of hydrocarbon-affected material, or AOSM, observed at the Aurora mine site is illustrated in Figure 2.2.

Figure 2.2: Aggregate Oil Sand material at the Aurora Mine Site

These bitumen deposits have been found to occur within layers that range from a few centimeters to half a meter in thickness and stretch horizontally several meters (Fleming et al., 2012). Fleming et al. (2012) indicate that the AOSM found within these deposits also range from a few centimeters to a half a meter and occasionally up to several meters in diameter. It was observed that the AOSM accumulations that are greater than 35 to 40 centimeters in diameter are typically composed of rich, less weathered bitumen interiors. The interiors of these large accumulations contain total hydrocarbon contents that are similar to that of the ore below (Fleming et al., 2012).

The use of larger AOSM within cover designs poses potential issues in terms of disrupting, or fracturing, the stable oil sand material which in turn may result in exposing

unweathered cores (Yarmuch, n.d.). Given limited research into the use of hydrocarbon affected material within reclamation designs, questions remain relating to its influence on soil water storage and transport processes. The AOSM characteristics along with the effects on soil water storage and transport processes are reviewed in section 2.3.

2.2.1 AOSM Form: Degradation Characteristics

Colwell et al. (1978) indicate that aggregates of petroleum with other material such as sand, also known as tar balls, is degraded slowly due to the microorganism's inability to access the oil is in this form. This was confirmed by Fleming et al. (2012) through a column respiration study which monitored oxygen consumption and carbon dioxide production as an indicator of microbial activity within the column. The columns contained AOSM from the top meter of the soil profile, from below one meter of the profile, and clean sand. It was reported that the columns packed with AOSM from the top meter of the profile promoted increased microbial activity as compared to columns packed with AOSM from below one meter of the soil profile. Lower respiration rates were observed with the deeper AOSM. This difference was attributed to a large microbial population present within the top meter of the soil profile. Although microbial hydrocarbon degradation is evident, Fleming et al. (2012) indicated degradation ranges of only 0.64 to 3.8 g per column over a 21 month period. This amount can be compared to the approximate total amount of 860 g of hydrocarbon material present within each column initially. It can be concluded that due to the very slow degradation rate, the majority of the hydrocarbon material will persist within the soil for significant periods of time (Fleming et al., 2012).

While the hydrocarbon material will persist within the soil, it is in a relatively stable aggregate form and studies performed by Fleming et al. (2012) indicate limited environmental concern from hydrocarbon contamination. A column study completed by Fleming et al. (2012)

focused on assessing the potential impacts to groundwater caused by AOSM disturbance. The study layered AOSM and sand into a column and packed these layers using a modified proctor hammer to simulate disturbances associated with large scale excavation and placement of the material. Following the completion of material layering and column packing, 90 mL/day of water was applied to the columns for 11 months. In analyzing the leachate water, it was concluded that F1 hydrocarbons were not detected in the water and very low concentrations of F2 and F3 hydrocarbons were detected. It can be noted that increased hydrocarbon concentration for the F2 fraction was evident when it was exposed to dryness but the F3 fraction showed little response to the same dry conditions. However, Fleming et al. (2012) found that the F2 hydrocarbons rarely occur within AOSM samples and the leachate observed was hypothesized to be products formed during microbial degradation. Although the F2 fractions are thought to be more closely representative of anticipated hydrocarbon concentrations in the field due to microbial degradation and wet dry cycles, the hydrocarbon concentration in the leachate water was still well below clean groundwater standards set by the Province of Alberta. These are referenced as 1.1 mg/L for F1 and F2 fractions; F3 is not regulated (Fleming et al., 2012). Fleming et al. (2012) concluded that the use of hydrocarbon-affected soils within reclamation cover prescriptions causes minimal environmental impacts to surface and groundwater, based on the limited hydrocarbon leachate collected during the column study. Hunter (2011) also supports the recommendation made by Fleming et al. in regards to implementing hydrocarbon-affected materials in reclamation covers.

2.2.2 Hydrophobicity

Soil water repellency, or hydrophobicity, has the potential to restrict water infiltration and increase erosion (Hunter, 2011). The occurrence of water repellency is caused by the soil

particles becoming coated with organic matter. Hunter (2011) indicates that water repellency appears to be naturally occurring in the Athabasca oil sand region, but that coarse textured sandy soils are more susceptible to the challenges associated with soil water repellency.

Doerr et al. (2000) showed that coarse textured soils contain lower particle surface area per unit volume, as compared to fine textured soils, and therefore less organic matter is required to coat the surface. This results in an increased susceptibility of coarse textured material to water repellency issues.

The specific degree of soil material repellency can be described and identified. Doerr (1998) reports that a decline of hydrophobicity can typically be observed in soils, indicating that measuring the delay in droplet infiltration will reflect the length of time in which hydrophobicity persists. Hunter (2011) reviewed various studies and was able to identify criteria for determining water repellency as outlined in Table 2.1. In addition, King (1981) identifies that the severity of repellency can be determined as a function of the soil-water contact angle (CA). The severity of repellency for a 20^{o}C air dried sand with a CA of <75 ^{o} is considered non-significant in terms of its repellence whereas a CA of >101 ^{o} has a level of repellence that is considered very severe (King, 1981).

Table 2.1: Criteria for Determining Water Repellency

Descriptor	King (1981) Time Range (s)	Dekker and Jungerius (1990) Time Range (s)	Doerr (1998) Time Range (s)
Non repellent	≤ 1	0 – 5	≤ 5
			5 – 10
Slightly repellent	1 – 60	5 – 60	10 – 30
			30 – 60
			60 – 180
Strongly repellent	60 – 600	60 – 600	180 – 300
			300 – 600
			600 – 900
Severely repellent	60 – 3600	60 – 3600	
			900 – 3600
		3600 – 10800	
			3600 – 18000
Extremely repellent	≥ 3600	10800 – 21600	
			≥ 18000
		≥ 21600	

Although Hunter (2011) summarized findings that petroleum hydrocarbons contribute to soil water repellency when they coat soil particles, Hunter (2011) was able to conclude through a soil water repellency study that coarse textured hydrocarbon-affected soils, with and without AOSM, from the Athabasca oil sands exhibited less water repellency than the reclaimed mineral soils. These differences in water repellency were likely attributed to the organic content of the soil rather than the hydrocarbon content (Hunter, 2011). In order to assess the potential for hydrophobicity characteristics from the coarse-textured hydrocarbon affected material the hydrocarbon composition of this material must be reviewed.

2.2.3 Hydrocarbon Composition

Gosselin et al. (2010) identify the parent source bitumen contained within the Alberta oil sands as containing heterocyclic PAH (Polycyclic Aromatic Hydrocarbon) compounds. Further studies conducted by Fleming et al. (2012) analyzed the type of hydrocarbons contained within

the AOSM at the Athabasca oil sands through standard chromatographic methods published by the Canadian Council of Ministers of the Environment (CCME) (CCME, 2001a). As illustrated in Table 2.2, it was found that light hydrocarbons comprise less than 1% of the total AOSM hydrocarbons and are rarely present above detectable limits (Fleming et al., 2012). If they are detected, these light hydrocarbons are typically recorded well below the clean soil guidelines, as established by CCME. In contrast, Fleming et al. (2012) identify heavy hydrocarbons as dominating, with F4G hydrocarbon content representing 2% to 5% of the total hydrocarbon concentration of the AOSM.

Table 2.2: AOSM Hydrocarbon Fraction Data Observed for the Athabasca Oil Sands

Fraction	Carbon number	Nominal detection limit	Clean soil guidelines[a] (mg/kg)
F1	C6-C10	20	210
F2	C10-C16	20	150
F3	C16-C34	30	310
F4-HTGC	C34-C50+	30	2800
F4G	C34-C50+	500	2800

Note: [a] as established by Alberta Environment for coarse grained soils in a natural environment

Although the hydrocarbon analysis yielded hydrocarbon fraction data within the AOSM, Fleming et al. (2012) observed significant deviations in hydrocarbon concentrations which are shown in Table 2.3.

Table 2.3: AOSM Hydrocarbon Fraction Deviation Data for the Athabasca Oil Sands

Fraction	Number of Detections	Number of samples analyzed	Mean (mg/kg)	Standard deviation
F1	13	168	3	13
F2	68	276	37	125
F3	272	276	1,730	1,120
F4-HTGC	147	147	6,070	2,550
F4G	220	220	34,700	16,700

In an effort to understand this variability, Fleming et al. (2012) studied three parameters which included depth below ground surface, type of in situ manifestation, and grain size of AOSM. Of these, depth below ground surface and type of in situ manifestation were negligible

in explaining the observed hydrocarbon concentration variability within the AOSM. The grain-size analysis was able to provide some explanation for the variability in hydrocarbon content between the AOSM samples.

Fleming et al. (2012) analyzed 36 samples relating AOSM grain size and hydrocarbon content from the Athabasca oil sands and the mean values (± standard deviation). Correlations between hydrocarbon concentration and moisture content (%), median grain size (D50), item characteristic grain size (D10), uniformity coefficient (Cu), coefficient of gradation (Cc) and silt and clay content (% passing the #200 sieve) were identified by Fleming et al. (2012) in Table 2.4.

Table 2.4: The Influence of Athabasca AOSM on Soil Properties

Category	Upper soil	AOSM soil	Lower soil
Moisture content (%)	3.03 ± 1.84	9.64 ± 3.37	2.58 ± 1.48
D50 (cm)	0.73 ± 0.52	0.53 ± 0.37	0.70 ± 0.53
D10 (cm)	0.29 ± 0.16	0.14 ± 0.06	0.30 ± 0.16
Cu	3.04 ± 2.44	4.49 ± 2.86	2.42 ± 1.04
Cc	1.12 ± 0.38	1.34 ± 0.36	1.10 ± 0.35
Silt and clay (%)	1.95 ± 1.64	4.86 ± 1.92	1.59 ± 1.60

Fleming et al. (2012) were able to conclude that, although weakly correlated, silt and clay content and median grain size may potentially explain the variability. As the AOSM became finer, there was a greater inhibition of weathering and degradation processes, resulting in greater amounts of F3 hydrocarbon fractions. Also, it was reported that as the grain sizes increased, there was an observed decrease in F4G content.

2.3 Increasing Reclamation Success: Addressing Key Challenges

Hunter (2011) identifies that reclamation success is governed by various interdependent components, including the health of microbial, fungal, and plant communities which are dependent on the ability of the soil to absorb and retain water. The coarse textured reclamation material poses challenges relating to limited water storage and rapid transport rates, as identified

previously. In an attempt to increase the reclamation soils ability to absorb and retain water, various soil capping depths, materials and configurations of the coarse textured hydrocarbon affected soil are being studied at the Aurora Soil Capping Study site. Included within this study are various configurations of layering of the coarse textured hydrocarbon-affected or aggregate oil sand material (AOSM). Limited research has been completed into understanding the effect that this layering, with the abundance of naturally-occurring oil sands material, will have on water storage and transport processes. The literature, although limited, will be reviewed in the following section, with focus placed on the impact of hydrocarbon affected material on water storage and the effect of soil layering configurations.

2.3.1 Impact of Textural Layering

The importance of understanding the influence of textural layering is evident given that in nature the soil profile commonly has layered, rather than uniform, textures (Huang et al., 2011). In addition, due to the reported finer texture of the hydrocarbon affected material over adjacent soils, a further attempt can be made to predict hydrocarbon impacts within a soil profile by reviewing the integration of a finer textured material within a coarse textured layering scheme. This will be accomplished using direct comparisons of the influence of textural layering on soil water storage and transport processes, along with a review of the mechanisms governing water transport through layered soil profiles.

2.3.1.1 Transport Mechanisms

McCauley and Jones (2005) identify processes that govern soil water transport which include infiltration, ponding or runoff, and preferential flow. Infiltration can be defined as the process of water entering the soil through the soil surface. It plays a significant role in governing the amount and rate of water that will enter the soil (McCauley and Jones, 2005). The

infiltration rate is defined as the speed at which water enters the soil and is closely correlated to the soils ability to absorb water (McCauley and Jones, 2005). If the soils infiltration capacity is higher than the rate of water applied, the water will infiltrate through the soil and the infiltration rate will be equivalent to the rate that it was applied at. In contrast, if the rate of water applied exceeds the soils infiltration capacity, the water that is in excess will pond on the surface and runoff (McCauley and Jones, 2005). Therefore, the infiltration rate depends on the amount of water delivered, the initial soil water content which affects the soils infiltration capacity, soil properties including hydraulic conductivity, and the amount of time the water is applied for (McCauley and Jones, 2005).

Preferential flow can be defined as the movement of water under the force of gravity through macropore pathways that form as a result of earthworm activity, burrowing insects and animals, plant roots, cracks and fissures, all of which alter the structure of the subsoil (McCauley and Jones, 2005). The process of preferential flow allows water to flow through the large soil pathways, having an impact on infiltration rates and solute transport mechanisms (McCauley and Jones, 2005). The presence of preferential flow poses risks in terms of transporting solutes deep into the profile, increasing the potential for solute contamination (Mori and Higashi, 2009).

Soil textural/structural contrasts create discontinuity in the hydraulic properties of the soil, potentially limiting the downward flow of water and chemical transport (Si et al., 2011). In addition to minimizing nutrient loss, soil layering also contributes to increased soil water storage capacity (Si et al., 2011). This can be explained through two mechanisms: capillary barriers and hydraulic barriers.

Capillary barriers are formed in unsaturated soil profiles of finer overlying coarser textured soil. Aubertin et al. (2009) identify that the difference in unsaturated hydraulic

conductivities between the layered soil tends to restrict the downward flow of water at the interface due to the lower hydraulic conductivity of the unsaturated coarser textured material located below the finer material. This results in the finer textured soil remaining at elevated levels of saturation and therefore increasing soil water storage and residence time. Si et al. (2011) indicate that the soils water storage capacity is greater than the amount that would typically drain under gravity. Burgers (2005) noted that regions with soil moisture deficits can adequately utilize capillary barriers to increase plant available water by restricting percolation. These observations were confirmed by Chaikowsky (2003) who found that layering finer textured topsoil over coarser tailings sands created textural discontinuity resulting in impacts to soil water content. The textural variation results in water accumulating above the layer interface (Chaikowsky, 2003). Further studies performed by Burgers (2005) also concluded that water movement was inhibited by the interface between reclamation soil and tailings sand due to the tailings sand acting as a capillary barrier (Burgers, 2005).

Hydraulic barrier effects are also evident in the case of a coarser material overlying a finer material. In this case, the hydraulic conductivity of the finer textured layer is less than the overlying coarse layer, resulting in water accumulation in the upper layer (Scott, 2000). Scott (2000) indicates that the infiltration rate decreases to that of the finer material and with time the water content will increase significantly in the coarse layer when the wetting front reaches the interface between the layers. Si et al. (2011) report that therefore the water infiltration rate will be reduced and the residence time of water increased due to the hydraulic barrier. The conclusions reached are further confirmed by the results of a column study performed by Gureghian et al. (1979). It was observed that when the wetting front reached the interface of the

coarse over the fine layer, the rate of infiltration at the soil surface and the flux within the column decreased rapidly due to the reduced conductivity of the fine layer.

In the literature cited above, both capillary and hydraulic barrier mechanisms are observed but the material studied showed distinct textural differences. Under natural conditions, soil layers may be from the same textural classes with only slight differences in particle size distribution (Si et al., 2011). Huang et al. (2011) studied the influence of soil layering schemes but reviewed layering with only slight textural differences. The previously identified mechanisms that occurred under drastically differing soil textural layers were also observed by Huang et al. (2011) for sandy soils. In a layered coarse soil, the interface between the finer and coarser sand generates a hydraulic barrier limiting wetting front advance and resulting in non-uniform water infiltration and drainage (Huang et al., 2011). When a finer textured sand is layered above a coarser textured sand, a capillary break occurs resulting in increased water content in the finer-textured layer and reduced percolation (Huang et al., 2011).

Huang et al. (2013) also reviewed the effect of varying layering thicknesses within a soil profile of field capacity. Laboratory columns with 5 or 10 cm thick layers exhibited higher water storage than columns with 25 cm layers and those with a homogenous soil profile. The 5 cm thick layered column consistently had the highest water storage but it was only slightly higher than the 10 cm layered column. The 25 cm layered column and the homogenous column exhibited little difference in water storage when compared to each other (Huang et al., 2013). Huang et al. (2013) indicate that the majority of the water loss in the layered profiles was from the coarse sand layers and that the water content of the medium sand layers only decreased slightly from saturation. This was evident until the thickness of the medium sand layer was greater than 5 cm which resulted in a decrease in water content toward the top of the layer.

Overall, the presence of layers delayed drainage and increased water storage with the amount of water stored increasing, and drainage rate slowing, with the greater number of textural breaks (Huang et al., 2013).

In addition to the capillary and hydraulic barrier mechanisms, Javaux and Vanclooster (2004) indicate that soil layering may generate the development of unstable wetting fronts when a fine textured soil overlays a coarser textured soil. This creates the potential for layers to induce fingering (Javaux and Vanclooster, 2004; Si et al., 2011) or preferential flow. This can reduce soil water storage and chemical residence time in the soil due to water bypassing the majority of the soil profile (Si et al., 2011). This confirms results from a large-scale in situ unsaturated infiltration experiment completed by Javaux and Vanclooster (2004) in which chloride transport was observed through a layered soil profile of sand embedded between two clay layers. The results indicate the occurrence of large velocities immediately below the clay and sand layer interfaces which can be explained by the solute moving through several fingers in the upper part of the layer. In addition, with increased depth, and larger water contents due to the presence of a less conductive underlying clay layer, lateral mixing increased and the resulting transport velocity decreased (Javaux and Vanclooster, 2004).

Additional research is required to determine the exact composition of the AOSM, in terms of fine textured percentage, in order to determine if the fine textured layer scenario that the AOSM was extrapolated to will be representative of the processes occurring within the AOSM layered soil profiles at the Aurora Soil Capping study.

2.3.2 Impact of Hydrocarbon Affected Material on Water Storage

Hydrocarbon materials have a tendency to exhibit water repellency characteristics, but there is limited research into the interaction of these processes when integrated into reclamation

cover designs. Bossert and Bartha (1984) identified the potential for reduced water holding capacity of the soil as a result of the partial coating of the soil surface by hydrophobic hydrocarbons. Hunter (2011) noted that the risk of severe water repellency is not increased with direct contact with the hydrocarbon affected material as indicated by an absence of behavioral differences between the coarse textured soil with AOSM and without AOSM. In contrast, Fleming et al. (2012) were able to conclude that soil with inclusions of AOSM retain increased moisture and are finer textured than the adjacent soils, as a result of an enriched silt and clay fraction as illustrated in Table 2.4. Given the limited research on hydrocarbon affected soils as related to water storage, this thesis will focus on addressing the variability in reported moisture storage capabilities.

2.4 Conclusion

Overall, the specific objectives of the Aurora Soil Capping study are to determine the appropriate reclamation soil cover design(s) required to re-establish the boreal forest ecosystems originally on site (Yarmuch, n.d.). Given challenges arising from limited water storage and rapid transport rates from the coarse textured reclamation material along with tendencies for soil water repellency, alternatives such as textural layering with the naturally-occurring oil sands material are being studied in an attempt to increase water storage and decrease water transport rates.

The effect of hydrocarbon contents, including varying forms, on water retention and flow processes is not well known. There is limited research on the effect of aggregated oil sand material (AOSM) integration within reclamation cover designs and its influence on soil water storage and solute transport within a layered soil profile. This identified gap is addressed in this thesis through a series of laboratory studies.

3. CHARACTERIZATION OF COARSE TEXTURED ATHABASCA OIL SAND MATERIAL FOR USE IN OIL SAND MINE RECLAMATION

3.1 Preface

The goal of the Aurora Soil Capping study is to determine the appropriate soil capping depths and soils to reclaim lean oil sand waste landforms. The reclamation soils being considered include natural, coarse textured hydrocarbon affected soils; consequently, these soils must be characterized in order to fully evaluate their potential use. This characterization includes conventional soil organic carbon content, particle size analysis, water retention and hydraulic conductivity properties as well as a characterization of the hydrophobicity of these soils.

3.2 Introduction

A reclamation cover must store sufficient water and nutrients to support revegetation. As a consequence, the ability of the cover to store water and to transport nutrients must be understood. Reclamation soils at oil sands mine sites are salvaged surficial organic and mineral soils; however, at the Aurora Mine site these soils often contain naturally occurring hydrocarbons in the form of bitumen inclusions, referred to as aggregate oil sand material (AOSM). Therefore it is important to evaluate the impact that the presence of the coarse textured hydrocarbon affected material may have on the water flow and storage properties.

The reclamation soils used for the ACS are sandy soil that has limited ability to store sufficient plant available water to sustain growth throughout the summer months (Sheoran et al., 2010). The ecosite classification for these soils is defined as a, b (Yarmuch, n.d.; Beckingham et al., 1996) and d (Zettl et al., 2011). Soils of this type typically have poor to medium nutrient availability and are rapid to well drained (Beckingham et al., 1996). This limits the ability of the

soil to store water to only a short period following precipitation events (British Columbia Ministry of Forests (BCMOF) Research Branch, 1998). The limited water storage potential of the coarse sand is related to its high hydraulic conductivity, which typically ranges from 5 m d^{-1} to 20 m d^{-1} (Bouma, 2008), or 20.83 cm hr^{-1} to 83.33 cm hr^{-1}, and high infiltration capacity (McCauley and Jones, 2005； Portage County Government, 2008). The large hydraulic conductivity and small water storage capacity of coarse textured soil results in faster water flow rates and increased leaching potential of nutrients. This significantly influences the ability to store water and nutrients for plant growth.

The ability of the reclamation soils to store water and nutrients is controlled not only by their texture but also the presence of organic matter. The organic matter integrated into the Aurora Soil Capping Study includes the LFH topsoil layer. The beneficial use of LFH material as a Soil Organic Matter (SOM) amendment is evident given its contribution to biological activity, providing plant nutrients, improving soil structure, reducing erosion and increasing infiltration (Sheoran et al., 2010; Leeper and Uren, 1993). It should also be noted that the organic carbon stored within the SOM (NRCS et al., 2011) also contributes to the creation of favourable conditions relating to tilth, soil structure development, and the water-holding capacity of the soil (Pennock et al., 1995). Although Leeper and Uren (1993) found that organic matter increases the cation-exchange capacity (CEC) and water storage, results reported by Hunter (2011) indicate that the LFH material from the Athabasca oil sands region does not always increase infiltration.

Hunter (2011) showed that the LFH material has the tendency to fall between wettable and water repellent, indicating that it is not severely water repellent but it has the potential to restrict water infiltration under specific conditions, such as with increased decomposition levels. Roberts and Carbon (1972) found that the compounds within the humic organic matter fraction

contribute to soil water repellency due to skins of organic material forming on the sand grains. Hunter (2011) also reported that the occurrence of water repellency is caused by the soil particles becoming coated with organic matter. Coarse textured sandy soils are more susceptible to the challenges associated with soil water repellency since these soils have a smaller surface area per unit volume, as compared to fine textured soils, and therefore less organic matter is required to coat the surface (Doerr et al., 2000).

It should be noted that the specific degree of soil material repellency can be described and identified. Doerr (1998) reports that a decline of hydrophobicity can typically be observed in soils, indicating that measuring the delay in droplet infiltration will reflect the length of time in which hydrophobicity persists. Hunter (2011) reviewed various studies and was able to identify criteria for determining water repellency as outlined in Table 3.1. In addition, King (1981) concluded that the severity of repellency can be determined as a function of the soil-water contact angle (CA). A CA value of $< 75^{o}$ for an air dried sand at 20^{o}C is considered non-significant in terms of its water repellency whereas a CA of $>101^{o}$ has a level of repellence that is considered very severe (King, 1981).

In addition to organic LFH material, Hunter (2011) noted that the presence of petroleum hydrocarbons also contribute to soil water repellency when they coat soil particles. Bossert and Bartha (1984) identified the potential for reduced water holding capacity of the soil as a result of the partial coating of the soil surface by hydrophobic hydrocarbons. Fleming et al. (2012) concluded that soils with integrated AOSM retain more water due to the enriched silt and clay fraction of the AOSM. It should be noted that in one study, the risk of severe water repellency was not increased with direct contact with the hydrocarbon affected material, as indicated by an

absence of behavioral differences between the coarse textured soil with AOSM and without AOSM (Hunter, 2011).

Given the limited research into the interaction of these processes when integrated into reclamation cover designs, the various reclamation materials must be characterized for soil organic carbon, particle size, water retention and hydraulic conductivity as well as a characterization of the hydrophobicity of these soils. This chapter will focus on identifying these characteristics and assessing the potential soil water storage and repellency interactions within reclamation profiles at the Aurora Soil Capping study.

3.3 Materials and Methods

Laboratory studies were conducted on four soils; the upper organic LFH soil, Bm, BC and subsoil material. Additional treatments implemented within these materials included varying the amount of hydrocarbon-affected material and using different layering schemes. The studies included material characterization through organic carbon and particle size analysis, water retention studies utilizing a tension table and pressure plates, along with saturated hydraulic conductivity studies. Hydrophobicity studies were also performed on the hydrocarbon affected and reclamation soil material through contact angle analysis and the water droplet penetration time (WDPT) test.

3.3.1 Material Extraction

The soil for this study was collected on June 28, 2012 from stockpiles situated in close proximity to the Aurora Soil Capping reclamation study site. The Aurora Soil Capping study is located approximately 100 kilometers north of Fort McMurray, Alberta on the Fort Hills overburden disposal area as shown in Figure 3.1.

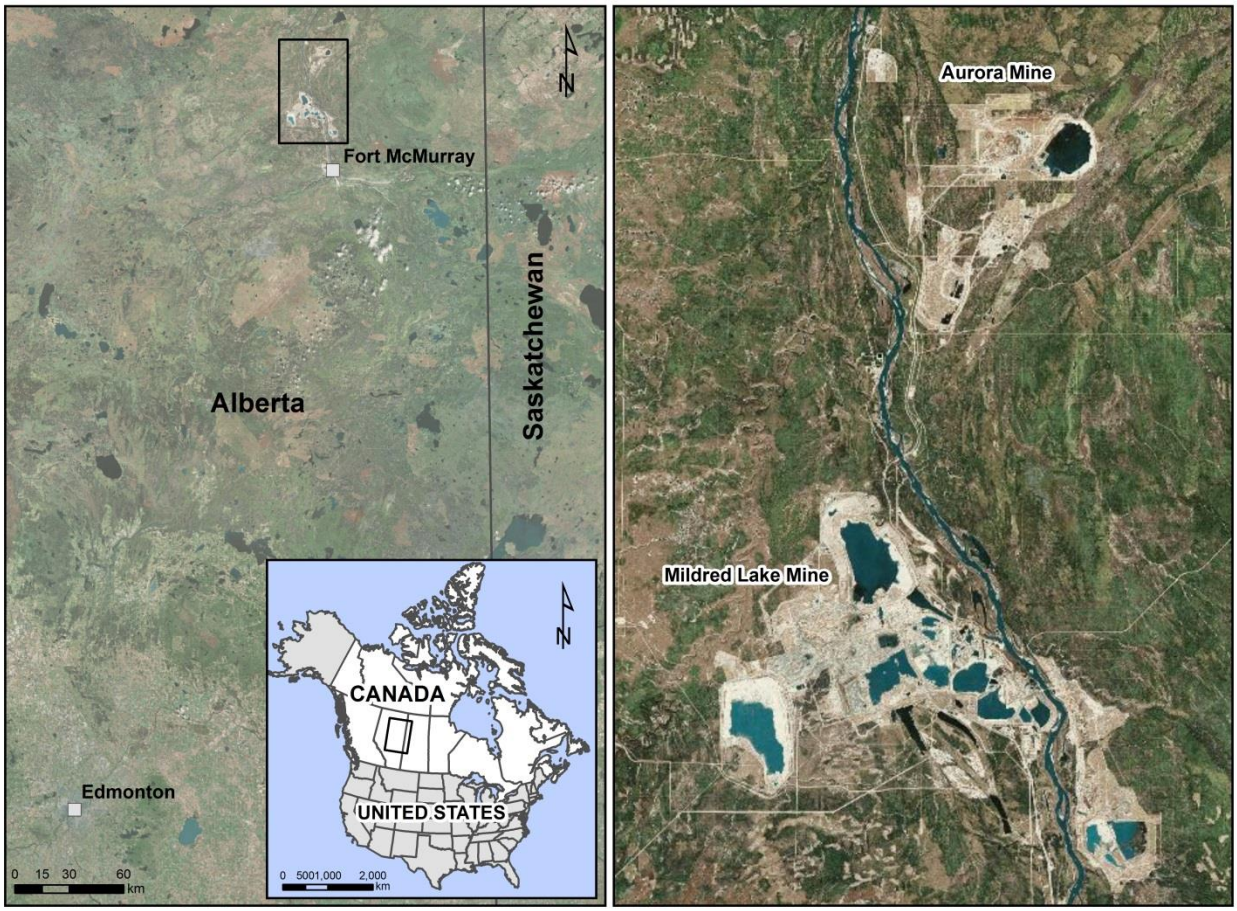

Figure 3.1: Site Geographic Location: Aurora Mine

The Aurora Soil Capping study site consists of replicated one hectare size plots of various soil prescriptions, configurations, and soil capping depths as illustrated in Figure 2.1. The soil material collected for this study consisted of the upper organic LFH soil and various mineral soils, including Bm, blended B and C horizons which will be described as BC or BC with 0% AOSM in this study, and subsoil from below one meter. The material collected corresponds to the treatment designs proposed in section 4.3 (Figure 4.1).

Field surveys to identify the proportion of soil matrix visibly affected by naturally occurring hydrocarbons were conducted by Paragon Soil and Environmental Consulting Inc. (2006). The following trends for the concentrations of hydrocarbons within the study areas of the Athabasca oil-sand deposit were evident:

- 10% and 16% of sites had strong (>25%) levels of hydrocarbons in the top 1 and 1 to 3 m of the soil profile, respectively.
- 14% of sites had medium (5 to 25%) levels of hydrocarbons in both the top 1 and 1 to 3 m of the soil profile.
- 26% and 23% of sites had trace (<5%) levels of hydrocarbons in the top 1 and 1 to 3 m of the soil profile, respectively.
- 50% and 47% of sites had no hydrocarbon levels in the top 1 and 1 to 3 m of the soil profile, respectively.

3.3.2 Water Content and Material Preparation

The water content of each of the mineral soils and surface soil material were determined using the gravimetric method by oven drying the samples at 105°C for 48 hours and re-weighing each sample. The soils were all air dried for a week and passed through a 2.36 mm sieve size opening to remove the large debris present within the samples.

It should be noted that the potential for deviations in moisture content may be evident given that the soil material sampled in the field was collected from stockpiles at the Aurora Soil Capping study site and transported. Thus site soil water content measurements will only act as an indication of potential soil water content at the beginning stages of reclamation placement.

3.3.3 Soil Organic Carbon and Particle Size Analysis

The total organic carbon (TOC) stored within the soil organic matter (SOM) (NRCS et al., 2011) is typically measured due to difficulties in measuring organic matter directly in the laboratory (Pluske et al., 2014). The dried and 2.36 mm sieved soil sample was also ground using a mortar and pestle prior to analyzing the total organic carbon content.

The samples were set in the LECO C632 analyzer for two minutes at a temperature of 840^{o}C using dry combustion (Wang and Anderson, 1998) to determine the total soil organic carbon content in each sample. Wang and Anderson (1998) identified that good results were obtained on sandy soils of low organic carbon content with samples of 2.5 to 5.0 g and measurements completed within 130 seconds. Wang and Anderson (1998) indicate that samples requiring a longer combustion period should be reduced in size. Therefore, significantly smaller samples of around 0.1 g were utilized given limited data on anticipated organic carbon content of these soils and to ensure the analysis could be completed within the 130 second period.

The particle size distribution was measured using a Horiba LA – 950 Laser Scattering Particle Size Distribution Analyzer after air drying and sieving the soil material to 2 mm. The Bm, BC and subsoil material was analyzed along with the BC material with residual hydrocarbons removed. This was accomplished by placing the BC material in a laboratory box furnace (Lindberg/Blue M BF51842 Series) at 550°C for seven hours. The particle size distribution of the crushed up AOSM was also measured. The analysis included measuring the particle size without sonification and then measuring again with sonification to break up any of the aggregates in the sample.

Although Hunter (2011) removed organic matter using 6% sodium hypochlorite from samples obtained from the oil sands sites, Yarmuch (2003) indicates that pretreatment for removal of organic matter are not required for mineral soil samples. This is due to the low amount of organic matter present within the mineral soil which is not extensive enough to impact the results (Yarmuch, 2003). Therefore, the removal of organic matter was excluded for the mineral soils studied.

Yarmuch (2003) reports that particle size analysis measurements are of limited value on material containing high proportions of organic matter relative to mineral matter but after observing a lower organic carbon percentage of the LFH material, particle size analysis was still performed. The process of removing any remaining organic matter was still neglected given the lower percentages of organic carbon present in the LFH material.

Although clay detection is often difficult for laser grain-size measurements (Stefano et al., 2010), the data with sonification was utilized in order to reduce errors relating to underestimating the finer size particle fractions. Although this concern was considered, the data measured will be used given the dominance of the larger size coarse fractions with little physical evidence of fine material present within the reclamation material. The resulting particle size fraction data obtained had soil textures assigned which corresponded to the Canadian System of Soil Classification standards (Soil Classification Working Group, 1998).

3.3.4 AOSM Hydrophobicity

Letey et al. (2000) indicate that a soil is classified as water repellent if a drop of water placed on the soil does not enter the soil spontaneously. A water repellent soil can be classified as having a water–solid contact angle equal to, or greater than, 90^{o} whereas a wettable soil will have differing contact angles between zero and 90^{o} (Letey et al., 2000). To assess the AOSM hydrophobicity, the Low Bond Axisymmetric Drop Shape Analysis method (Stalder et al., 2010) was utilized to determine the contact angle from a photograph of a water droplet on the soil surface. Stalder et al. (2010) indicate that this method assists in analytically solving the Young–Laplace equation according to photographic images of axisymmetric sessile drops. The photographic images were developed using the PGX Measuring Head instrument. The instrument was placed on a slide containing double sided tape with the layer of material to be

studied. The procedure was performed on BC sieved to 2.36 mm and crushed AOSM with five replicates of each material. A photograph was taken every six seconds for a one minute period for the BC material and for a five minute period for the AOSM following the application of a droplet of four microliters of water onto the soil surface. The extended period of time allowed for the assessment of the persistence of hydrophobicity characteristics. As summarized by Hunter (2011), the water droplet penetration time (WDPT) test provides a measure of persistence of the water repellency of the soil. This included applying the droplet of water onto the soil surface and recording the infiltration time (Hunter, 2011).

It was reported by Robichaud et al. (2008) that extreme conditions of soil water repellency can be easily identified through observation. When the soil is strongly water repellent the water drop "beads up" on the soil surface for 300 seconds and when the soil exhibits no water repellency, the water drop infiltrates within five seconds (Robichaud et al., 2008). Although Doerr (1998) reported that a decline of hydrophobicity can typically be observed in soils as the WDPT can vary from instantly infiltrating to many hours, many WDPT tests have been terminated after several minutes due to the very time consuming nature of the test and ultimately the evaporation of droplets which will influence the results. Therefore, it can be summarized that WDPT values over five seconds are considered adequate measures of water repellency.

The resulting contact angle of the droplet on the soil layer was measured utilizing Image J software (Hunter, 2011) and the Low Bond Axisymmetric Drop Shape Analysis (LB-ADSA) plugin.

3.3.5 Soil Water Retention

Water retention properties included five replications of each of the mineral and organic soils using tension table methods as published by Romano et al. (2002). The LFH, Bm, BC and

subsoil material were analyzed along with the BC material with residual hydrocarbons removed. Additional treatments were studied which included BC with 2% and 5% AOSM crushed into powder form and BC with 2% and 5% AOSM in solid form that ranged in size from 0.2 cm to 0.5 cm for each core. The AOSM was added to the soil on a per weight basis. A concentration of 2% and 5% were used based on the higher percentage of sites surveyed in the Athabasca oil sands region showing trace (<5%) levels of hydrocarbons (Paragon Soil and Environmental Consulting Inc., 2006). In addition to the solid AOSM form, questions are raised on the impact that this material would have if it was in the powder form. This form was also studied as it has the potential to occur through frequent mining activity disturbances.

The material was packed in a 4.78 cm high and 5.08 cm diameter copper core with a filter paper (Whatman 5mm #4 Qualitative filter paper) on the bottom secured in place with one layer of cheesecloth and an elastic band. The amount of material and dry bulk density that each of the cores were packed to is summarized in Appendix E. Although the dry bulk density was used within this study, it corresponds to the observed field bulk density of 1.69 gcm^{-3} at sites within the Athabasca oil sand region (Huang et al., 2011). It should be noted that a 0.3 cm rim was left at the top of each of the cores, with the exception of the LFH treatments, to allow for material expansion as well as to avoid material loss through continual core movement. The cores were saturated in distilled water with 0.005 M $CaSO_4$ (Calcium Sulphate) wetting solution (Romano et al., 2002) for a period of ten days and weighed prior to placement on the porous barrier of 60% silt to 40% clay that was mixed on a by weight basis. Although Romano et al. (2002) specify that the wetting solution should be deaerated, distilled water was used given the potential for a greater representation of field retention data due to the absence of fully saturated soils in the field.

The high air entry layer was created at the bottom of each test sample by mixing 600 g silt to 400 g of clay with one liter of distilled 0.005 M $CaSO_4$ water. Prior to core placement, the 60:40 silt clay (MCP ASP100 Kaolin) mixture was poured into a constructed suction table to a 1.5 cm thickness above the microfiber membrane covered channel system and left for a period of nine days to allow for water to evaporate and the porous layer to become denser (Romano et al., 2002). After pressing the cores slightly into the porous barrier to establish good hydraulic contact between the soil and the porous bed, the matric head, h_m, was dropped every four days to -3 cm, -30 cm and -70 cm with the cores weighed at each increment to ensure that the two consecutive masses of a given sample do not differ by more than 0.1 g prior to assuming the hydrostatic equilibrium has been reached (Romano et al., 2002).

For measurements at -3 cm and -30 cm the cores were weighed once prior to altering the suction to avoid material loss from continued core movement throughout the duration of the study. This also reduced the chance that hydraulic contact between the soil water in the sample and the water in the suction table would be lost leading to inaccurate results (Romano et al., 2002). The time period of four days is considered to be a significant period of time to reach hydrostatic equilibrium at -3 cm and -30 cm matric head given that field capacity, exhibiting matric heads of -100 cm and -300 cm (Miller, 2010), can be estimated to be reached within two to three days following the addition of water (Veihmeyer and Hendrickson, 1950). Zettl et al. (2011) also observed that field capacity was reached after 18 hours of drainage in field sites in close proximity to the Aurora Soil Capping study. The -70 cm increment was weighed after four days and reweighed until the two consecutive masses of the sample did not differ by more than 0.1 g.

The remaining soil water retention curve for each material was completed for matric heads of -100 cm and -300cm, which represent field capacity (Miller, 2010) using pressure plate methods. Additionally, the water retention data was collected for -700 cm and -5000 cm to derive a more continuous curve. The 15 Bar Ceramic Plate Extractor apparatus was utilized to derive the remaining soil water retention curve for values of -100 cm, -300cm, -700 cm and -5000 cm. The one Bar ceramic plates were used for the low pressure measurements of -100 cm, -300cm, and -700 cm and the 15 Bar plates used for the high pressure measurements of -5000 cm.

Ali (2010) indicates that after low tension measurements the same samples should be used at the high tensions in the pressure plate to avoid ambiguous results from differing samples used. Thus the soil water retention was measured at -100 cm, -300cm, and -700 cm suctions utilizing the same soil cores from the tension table which were directly transferred from the tension table to the pressure plate apparatus, with the exception of the BC cores containing AOSM, the sieved BC with 0% AOSM and BC material with hydrocarbons removed. These cores were removed from the suction table and saturated immediately with distilled water with 0.005 M $CaSO_4$ wetting solution to allow for saturated hydraulic conductivity tests to be performed. Following the completion of the saturated hydraulic conductivity tests, the cores were re-saturated for a period of three weeks to ensure the cores were fully saturated prior to placement on the pressure plate to complete the soil water retention measurements. In addition, the material in each of the cores was re-packed in rubber cores of 0.9 cm high and a diameter of 5.1 cm for measurement at the high pressure of -5000 cm. This was done as it is recommended to keep small sample heights as the time required to reach equilibrium varies according to the square height of the sample (Soilmoisture Equipment Corp, 2009).

Prior to running the pressure plate system, and core placement, the porous ceramic plates were saturated to remove trapped air from porous spaces in the pressure plate (Soilmoisture Equipment Corp, 2008). The pressure plates were saturated in a deaerated water 0.005 M $CaSO_4$ wetting solution (Dane and Hopmans, 2002a) by submerging the plates in a tub of the wetting solution for a period of 24 hours prior to use (Soilmoisture Equipment Corp, 2008). A hand operated vacuum pump, along with wetting solution, further removed trapped air from the ceramic plate (Soilmoisture Equipment Corp, 2008).

Following saturation the plates were placed into the pressure plate chamber and the valve hooked up to the interior tube located in the chamber. The connecting exterior tube was submerged under water in an Erlenmeyer flask (Dane and Hopmans, 2002a) filled with the deaerated 0.005 M $CaSO_4$ solution. According to Dane and Hopmans (2002a), the burette filled with water will allow for air leaks to be detected. The cores were placed on the pressure plates by applying a slight twist to the core to achieve hydraulic contact between the soil core and the ceramic plate (Ali, 2010). Suctions of -100 cm, -300 cm, -700 cm and -5000 cm were applied at -10 KPa, -30 KPa, -70 KPa and -500 KPa, respectively following information provided by Bonczek (2007) that permanent wilting point, -15000 cm, can alternately be depicted as 15 bars or -1500 Kilopascals (KPa).

To determine if equilibrium has been reached, the cores were weighed and re-weighed prior to switching pressures considering the same criteria and procedure used for the suction table as identified by Romano et al. (2002). Although the procedure identified by Romano et al. (2002) was utilized, consistent weight differences could not be achieved when the final weights were taken for all of the suctions. This was observed in a few of the cores for the LFH material and cores containing AOSM. In these situations the absence of water flowing from a sample was

also monitored and used as supplementary information before determining whether to proceed to the next measurement increment. The absence of water flow was not used as the main indicator of hydrostatic equilibrium given the potential reasons for the water flow to cease. This includes low hydraulic conductivity in the soil sample, soil shrinkage, and clogged pores in the plates (Decagon Devices, Inc., 2013).

An issue occurred when measuring the BC material with 0% AOSM and the cores containing the AOSM at -100 cm because the pressure rose higher than the intended set rate. Therefore, the weight differences observed between the two measurements at -100 cm are larger than a 0.1 g difference. Although the hydrostatic equilibrium had to be assumed for the -100 cm measurements, it is anticipated that the weights reported are close to the equilibrium given the amount of time between the measurements and the absence of water flowing from the samples.

Measurements at -1500 KPa, or permanent wilting point, were ignored due to the compromised soil structure through soil displacement with the pressure applied at this rate. This corresponds with information provided by Dane and Hopmans (2002a) that at the higher applied pressures complete equilibrium within the sample may not be achieved.

Following completion of the pressure plate measurements, the cores were air dried for a period of a week and re-weighed to determine the final moisture content. Typically following measurements after the final suction level, the soil is placed in an oven and dried at 105°C for a period of 24 to 48 hours (Romano et al., 2002) to determine the final water content of the soil. This method was not used given concerns for the stability of the hydrocarbons contained within the soil samples. Thus the air dried weight was utilized to derive the soil water retention curve for all of the soil samples studied.

Given the issues identified, the soil water retention data derived will be utilized as a means for comparison between the samples on the amount of water retained. The values observed will need to be viewed as an approximation of field water retention due to potential variability between the core replicates, as well as natural variability within the oil sands region.

3.3.6 Soil Hydraulic Conductivity

Water flux (Jw) and saturated hydraulic conductivity (Ksat) data was calculated utilizing measurements obtained through constant head methods for LFH, Bm, subsoil, BC with 0% AOSM and BC with residual hydrocarbons removed. Additional treatments were used which included BC with 2% and 5% AOSM in the solid form and crushed into powder form.

Plastic cores of 7.6 cm height and 7.7 cm diameter with a membrane paper bottom secured in place with one layer of cheesecloth and an elastic band were used for the LFH, Bm, subsoil, BC with 0% AOSM and BC with residual hydrocarbons removed. The same copper cores that were used in soil water retention analysis for BC with 2% and 5% AOSM crushed into powder form and BC with 2% and 5% solid AOSM were used for the hydraulic conductivity analysis. The hydraulic conductivity for BC with 0% AOSM was re-measured while measuring the hydraulic conductivity for the BC with 2% and 5% AOSM. The same cores and bulk density were used to allow for a more thorough comparison on the effect of AOSM on hydraulic conductivity, along with water retention information. It should be noted that the larger cores were used for the LFH, BC, Bm and subsoil material because Reynolds and Elrick (2002) indicated that ideally if the Ksat measurements are intended to be representative of field conditions then the cores must be large enough to adequately include the soil structure.

Although there are differences in the bulk density (See Appendix F), it was anticipated that studying a range of bulk density will be more indicative of field conditions, given observed

field bulk densities of 1.52 g cm^{-3} (Zettl et al., 2011) up to 1.71 g cm^{-3} at sites within the Athabasca oil sand region (Huang et al., 2011). The higher bulk density that was studied for the BC with 2% and 5% AOSM in solid and powder form, along with BC with 0% AOSM, corresponds to the observed field bulk density of 1.69 g cm^{-3} (Huang et al., 2011) and will allow for direct comparison to the soil water retention data. In addition, McMillan et al. (2007) also reported increases in bulk density on reclaimed sites within the Athabasca oil sands region as compared to naturally undisturbed sites, in which they attributed these results to surface compaction, further indicating the advantage of studying a range of bulk densities for some of the material used.

Following core packing, the cores were saturated in distilled water with 0.005 M $CaSO_4$ wetting solution for a period of four days prior to performing the study. Dane and Hopmans (2002b) recommend a deaerated 0.005M $CaSO_4$ wetting solution and indicate that wetting with distilled water can promote dispersion of the clays in the sample. Reynolds et al. (2002) further indicated that distilled or deionized water should never be used for measuring saturated hydraulic conductivity of a natural porous medium due to the encouragement of clay dispersion from these sources. Therefore, local tap water was used for this study. It can be noted that chemical additions, such as thymol, have been recommended for the wetting solution in order to inhibit biological activity (Skaggs et al., 2002) but Reynolds et al. (2002) indicate that chemicals currently available can potentially cause as much disturbance to the soil as biological activity and may cause changes to water viscosity, water surface tension and/or soil wettability. Therefore, chemicals to inhibit biological activity were avoided for soil hydraulic conductivity tests, as well as soil water retention tests.

The saturated hydraulic conductivity data was derived by maintaining a constant head and measuring the water outflow from the cores over a five minute period. Three replicates of each of the LFH, BC, Bm, Subsoil and BC with hydrocarbons removed were packed into the cores with three measurements taken for each core whereas the BC material with a range of hydrocarbon material had five replicates packed and one measurement taken for each replicate. The head maintained for each of the cores can be viewed in Tables F.0.1 and F.0.2 (See Appendix F). The calculations used to derive the flux (cm s^{-1}) and saturated hydraulic conductivity (cm hr^{-1}) for each of the materials is as follows:

$$J_w = \frac{V}{A \cdot t} \qquad \text{(Eq. 3.1)}$$

$$K_{sat} = \frac{J_{w \cdot L}}{(L+H)} \qquad \text{(Eq. 3.2)}$$

where V is the volume (cm^3) of water collected from the core area (A) (cm^2) for the specified time interval (t) (seconds). The L and H are the core height (cm) and the constant head height (cm) of water above the core, respectively.

3.4 Results and Discussion

3.4.1 Material Characterization: Water Content, Organic Carbon and Particle Size

The resulting site gravimetric water content, soil carbon percentage, particle size and soil texture for each of the reclamation materials can be viewed in Table 3.1. A detailed report of gravimetric moisture content, soil organic carbon percentage and particle size analysis is presented in Appendix A, B and C.

Table 3.1: Aurora Soil Capping Study Material Characterization

Material	Gravimetric Water Content† ($g\ g^{-1}$)	Organic Carbon† (g/100g)	Particle Size (g/100g) † Sand	Silt	Clay	Soil Texture††
reclaimed site material						
BC	0.033 (0.0006)	0.75 (0.17)	92.7 (2.32)	6.3 (1.74)	0.3 (0.48)	Sand
Subsoil	0.051 (0.0015)	0.54 (0.15)	94.9 (1.06)	5.1 (1.06)	0.0 (0.00)	Sand
Bm	0.037 (0.0017)	1.43 (0.14)	88.5 (4.47)	10.3 (2.85)	0.1 (0.07)	Sand/Loamy Sand
LFH	0.093 (0.0212)	2.07 (0.03)	92.2 (1.36)	7.8 (1.36)	0.0 (0.00)	Sand
AOSM (Crushed)			95.0 (0.86)	5.0 (0.86)	0.0 (0.00)	Sand
hydrocarbons removed						
BC			98.0 (0.24)	2.0 (0.24)	0.0 (0.00)	Sand

Note : †Values are reported as average and standard deviation
†† Canadian System of Soil Classification standards (Soil Classification Working Group, 1998).

The majority of the Aurora Soil Capping material can be identified as sand texture, coinciding with observations made by Beckingham et al. (1996) which identified the material to be a dry to very dry sandy soil.

The AOSM shows comparable grain size to the other materials studied (Table 3.1). This varies from results obtained by Fleming et al. (2012) which showed that AOSM soils were finer textured than the adjacent soils as a result of an enriched silt and clay fraction.

Overall, the dominating coarse nature and low soil organic carbon levels indicate potential issues relating to the reclamation soils ability to retain water. The ability of the soil organic carbon to aggregate mineral particles (NRCS et al., 2011) and create favourable conditions relating to tilth, soil structure development and the soils water-holding capacity (Pennock et al., 1995) is likely hindered by the low soil organic carbon levels observed. The sand texture of the soil further limits its ability to retain water as Kramer (1944) indicates that sandy soils have a very low water holding capacity.

3.4.2 AOSM Hydrophobicity

The data obtained for determining AOSM hydrophobicity and potential hydrophobicity in the mineral BC soil can be viewed in Appendix D. Summarized data can be viewed in Table 3.2 and 3.3 with one minute increments reported for the AOSM and 30 second increments for the BC soil. An example of the photographs taken using the PGX instrument and resulting contact angles reported for the AOSM are illustrated in Figure 3.2.

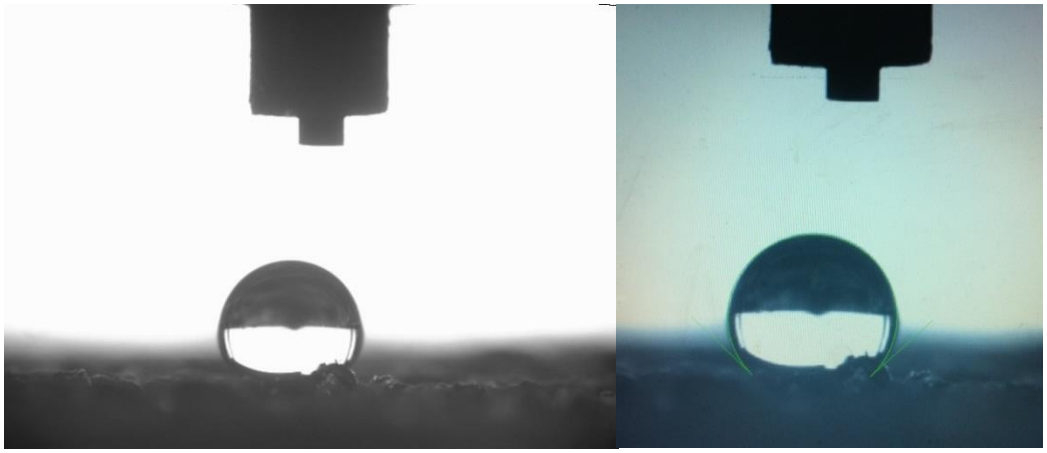

Figure 3.2: Photograph Taken (Left) with PGX instrument at 84 seconds for AOSM Replication One and Resulting Contact Angle Fit (Right)

Table 3.2: Contact Angle Analysis for the Crushed AOSM over a One Minute Increment

Time Interval (seconds)	AOSM-Rep 1 (°)	AOSM-Rep 2 (°)	AOSM-Rep 3 (°)	AOSM-Rep 4 (°)	AOSM-Rep 5 (°)
0	137	139	143	140	152
60	136	138	140	140	152
120	134	138	140	137	148
180	134	136	140	137	148
240	132	136	137	137	150
300	131	134	136	134	145

Table 3.3: Contact Angle Analysis for the BC Material over a 30 Second Increment

Time Interval (seconds)	BC-Rep 1 (°)	BC-Rep 2 (°)	BC-Rep 3 (°)	BC-Rep 4 (°)	BC-Rep 5 (°)
0	42	45	42	20	11
30	32	17	26	19	10
60	25	14	25	18	9

Following the criteria identified by Letey et al. (2000) the BC reclamation material is wettable and non-repellent while the AOSM is water repellent given the large contact angles measured. King (1981) identifies that the severity of repellency for a 20°C air dried sand with a CA of <75° is considered non-significant in terms of its repellence and a CA of >101° has a severity of repellence that is considered very severe. Following the above criteria, along with categories outlined by Hunter (2011) in Table 2.1, the AOSM can be characterized as

hydrophobic with strong to very severe water repellency given the water droplet did not infiltrate within 300 seconds (Robichaud et al., 2008) and had a contact angle greater than 101°.

Hunter (2011) stated that petroleum hydrocarbons contribute to soil water repellency when they coat the soil particle. However, the BC material used in this study, which is in direct contact with hydrocarbon material, did not show elevated soil water repellency. Therefore, the risk of severe water repellency is not increased with direct contact of the soil with the hydrocarbon-affected material.

3.4.3 Soil Water Retention

The average volumetric water content retained at each of the suction levels can be viewed in Table 3.4 and the resulting volumetric water retention curves with standard error bars can be viewed in Figures 3.3 and 3.4. See Table E.0.2 (Appendix E) for the corresponding average gravimetric water content at the varying suction levels. It should be noted that the calculated and measured saturated porosity is plotted at 1 cm of suction.

Statistical analysis was conducted using the R Program System version 3.0.2. Initially an exploratory analysis was performed on the data using the Cleveland dot plot in which outliers were removed. The Analysis of Variance (ANOVA) model was used to compare the multiple means between water retention curves as suction changes. Following that the significance level is set at 5%; a p-value less than 0.05 is thus considered a significant difference. The p-values and average soil water contents are reported for each of the analyzed suctions for the treatments without AOSM and with AOSM inclusions and are summarized in Tables 3.5 and 3.6, respectively.

Table 3.4: Average Volumetric Water Content Measured at Varying Pressures for Five Replicates of Each Material

Material	Θw-0 cm† (cm^3/cm^3)	Θw-3 cm† (cm^3/cm^3)	Θw-30 cm† (cm^3/cm^3)	Θw-70 cm† (cm^3/cm^3)	Θw-100 cm† (cm^3/cm^3)	Θw-300 cm† (cm^3/cm^3)	Θw-700 cm† (cm^3/cm^3)	Θw-5000 cm† (cm^3/cm^3)
LFH	0.521 (0.007)	0.471 (0.006)	0.376 (0.012)	0.189 (0.013)	0.180 (0.020)	0.170 (0.018)	0.150 (0.026)	0.121 (0.028)
Bm	0.450 (0.004)	0.397 (0.002)	0.263 (0.008)	0.092 (0.011)	0.095 (0.003)	0.070 (0.015)	0.053 (0.010)	0.034 (0.002)
Subsoil	0.446 (0.009)	0.390 (0.003)	0.292 (0.009)	0.099 (0.005)	0.095 (0.011)	0.089 (0.009)	0.068 (0.010)	0.034 (0.005)
----------BC Soil Material----------								
0% AOSM	0.419 (0.017)	0.378 (0.012)	0.239 (0.023)	0.084 (0.012)	0.063 (0.010)	0.032 (0.019)	0.027 (0.014)	0.037 (0.003)
2% AOSM Powder	0.430 (0.007)	0.380 (0.005)	0.258 (0.016)	0.083 (0.007)	0.062 (0.018)	0.043 (0.018)	0.031 (0.017)	0.035 (0.003)
2% AOSM Solid	0.427 (0.010)	0.378 (0.010)	0.245 (0.015)	0.089 (0.004)	0.062 (0.020)	0.043 (0.019)	0.039 (0.005)	0.033 (0.002)
5% AOSM Powder	0.427 (0.006)	0.374 (0.002)	0.256 (0.008)	0.087 (0.005)	0.076 (0.003)	0.033 (0.004)	0.035 (0.002)	0.036 (0.001)
5% AOSM Solid	0.439 (0.005)	0.386 (0.004)	0.242 (0.010)	0.091 (0.004)	0.084 (0.005)	0.046 (0.008)	0.042 (0.002)	0.037 (0.003)
----------hydrocarbons removed----------								
BC	0.457 (0.005)	0.408 (0.005)	0.250 (0.021)	0.087 (0.009)	0.080 (0.011)	0.072 (0.010)	0.054 (0.010)	0.030 (0.006)

Note : †Values are reported as means with standard deviation below in parenthesis.

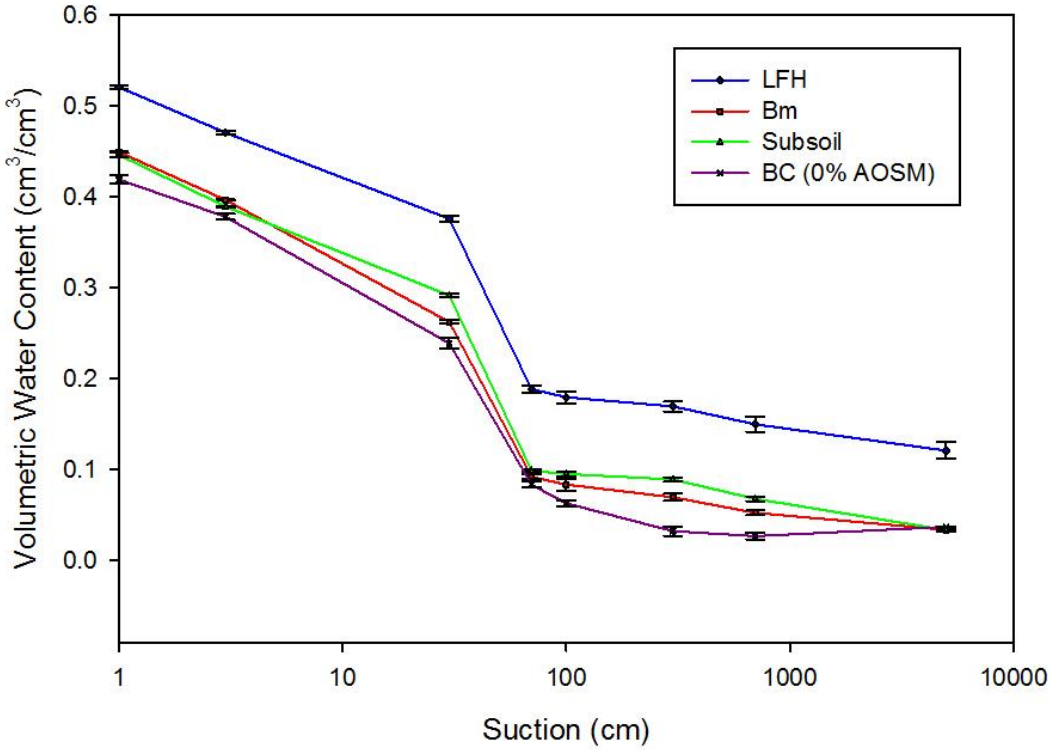

Figure 3.3: Measured Average Soil Water Retention Curves and Standard Error Bars for Five Replicates: Organic and Mineral Soil

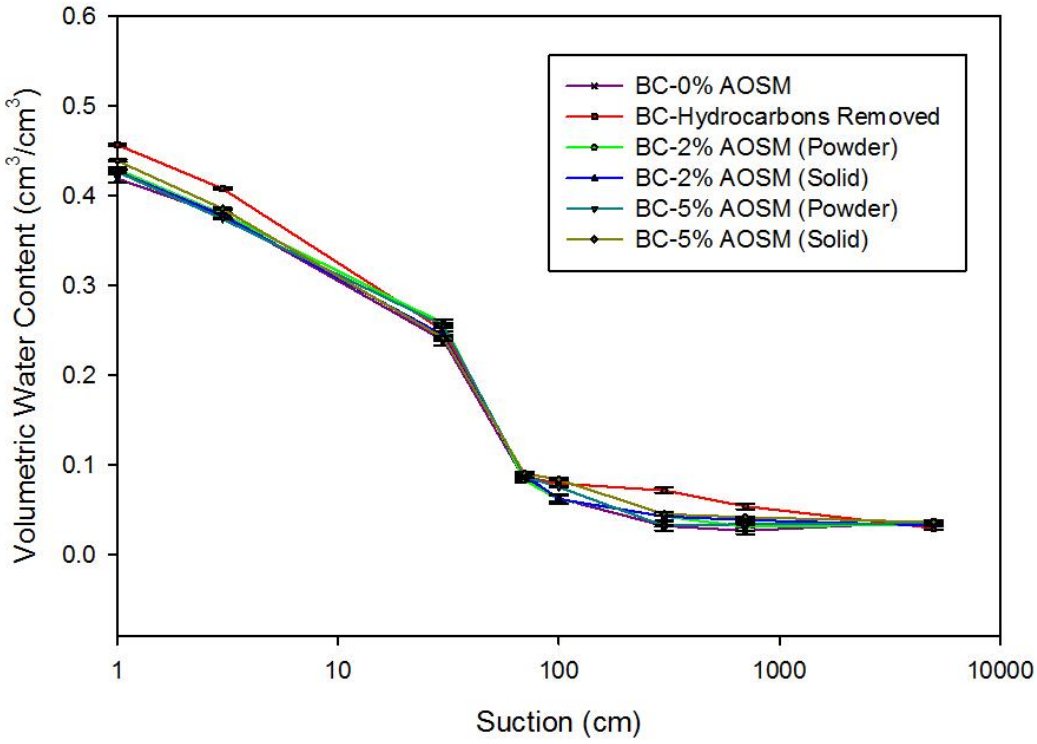

Figure 3.4: Measured Average Soil Water Retention Curves and Standard Error Bars for Five Replicates: AOSM Cores

Due to concerns on whether the soil samples were originally fully saturated, calculations were performed based on the core density and particle density of the soil and bitumen. The calculations used to derive the saturated porosity, or saturated water content, for each of the materials is as follows:

$$V_s=M_s/G_s \quad \text{(Eq. 3.3)}$$

$$V_b=M_b/G_s \quad \text{(Eq. 3.4)}$$

$$V_v=V-V_s-V_b \quad \text{(Eq. 3.5)}$$

$$n=V_v/V \quad \text{(Eq. 3.6)}$$

where V_s is the volume of the soil (cm^3), M_s is the mass of soil (g), G_s is the specific gravity or particle density of the soil ($g\ cm^{-3}$), V_b is the volume of the bitumen (cm^3), M_b is the mass of bitumen (g), V_v is the volume of voids (cm^3), V is the total volume of the soil sample (cm^3) and n is the porosity. It should be noted that the specific gravity (G_s) of most soils ranges from 2.5 to 2.9 with cohesionless soils, such as sand, assumed to be 2.65 (Murthy, 2003). The specific gravity of bitumen typically ranges from 0.9 to 1.04 (Ancheyta and Speight, 2007). The range in variation is usually a result of local conditions which affect the material close to the exposures in surface oil sands deposits and bitumen found in deposits that have not been exposed to weathering (Speight, 2000). One study found that the specific gravity of bitumen of the Athabasca region to be 1.03 (Speight, 2010). This value was used for porosity calculations within this study. The resulting adjustments to the average soil water retention curves based on the porosity at saturation can be viewed in Figures 3.5 and 3.6.

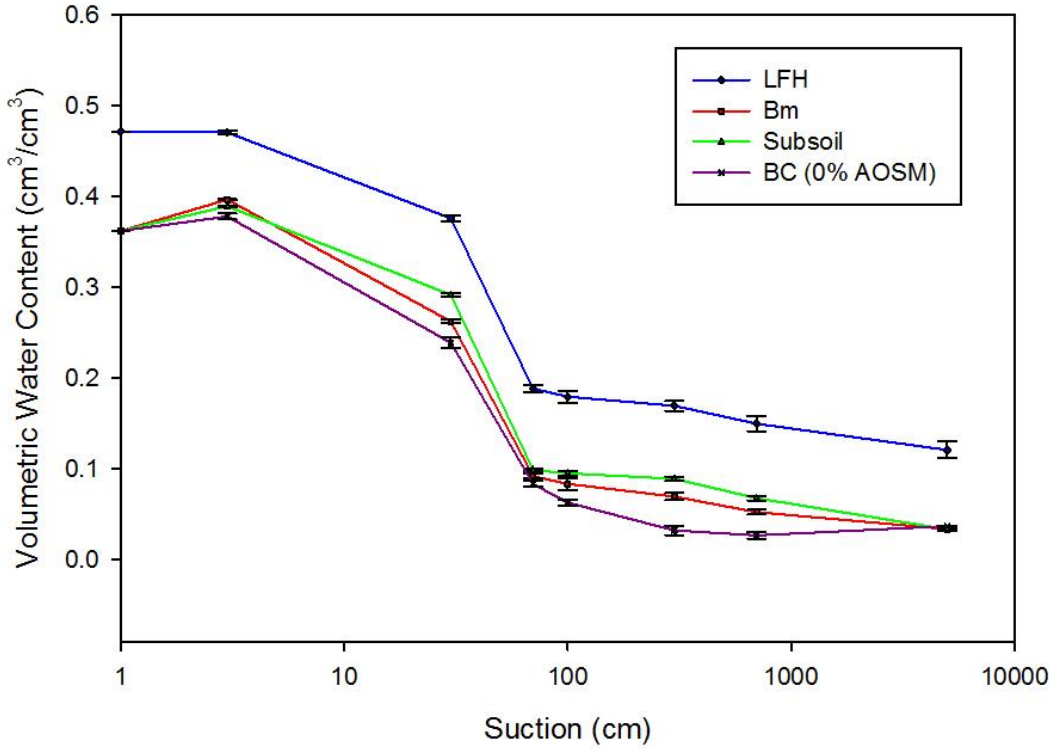

Figure 3.5: Calculated Soil Water Retention Curve with the Standard Error Bars for Five Replicates: Organic and Mineral Soil

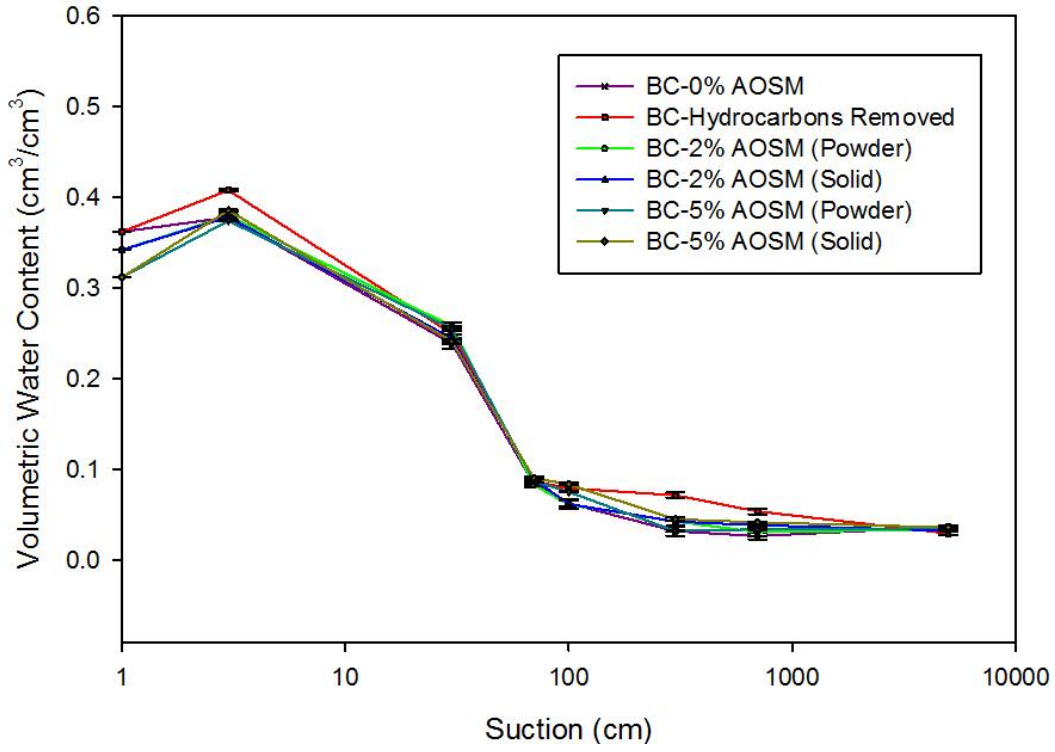

Figure 3.6: Calculated Soil Water Retention Curve with the Standard Error Bars for Five Replicates: AOSM Cores

Based on the results illustrated in the calculated soil water retention curves in Figures 3.5 and 3.6, it appears that the samples were able to reach saturation given the higher measured saturated porosity as shown in Figures 3.3 and 3.4. Although the air-entry value, or "the matric suction where air starts to enter the largest pores in the soil" (Fredlund and Xing, 1994, p.522), is not detectable in the measured water retention curves (Figures 3.3 and 3.4), it is anticipated from the calculated curves (Figures 3.5 and 3.6) that the air-entry value falls between the first two measured points at around 10 cm of suction, or 1 KPa, but due to the lack of measurement within this range it was not detected.

In reviewing the measured water retention curves and statistical analysis (Table 3.5) there were significant differences ($p<0.05$) detected between the organic and mineral materials studied. The LFH material retained higher water contents as compared to the mineral soils. This can be attributed to the higher organic matter content (Table 3.1). It should be noted that the LFH was packed to a 1.4 g cm^{-3} dry bulk density, as compared to the dry bulk density of 1.69 g cm^{-3} for all the other treatments. Soils with lower bulk density would have higher soil water contents close to saturation. However, soils with slightly higher bulk density would have an increase in the retained moisture content at field capacity. Therefore, it is anticipated that if the bulk density was increased to 1.69 g cm^{-3} the LFH material will retain even more water over the mineral soil.

The average bulk density observed at the Aurora Soil Capping study site is 1.52 g cm^{-3} as identified by Zettl et al. (2011), which was lower than bulk densities of up to 1.69 gcm^{-3} and 1.71 gcm^{-3} respectively, for sites north of Fort McMurray, Alberta, as reported by Huang et al. (2011). The sites that exhibited a higher bulk density had a large coarse sand content but contained a greater percentage of fine sand over medium sand. The data presented in Figures 3.3 and 3.4 is

comparable to the fine sand drying soil water characteristic curve obtained by Yang et al. (2004) for a bulk density of 1.56 g cm^{-3}.

Of the mineral soil treatments, the subsoil appears to retain the highest water content at the various suction levels over the Bm and BC material without hydrocarbons removed. Sheoran et al. (2010) indicate that soils consisting of high amounts of coarse fragments contain larger pores. Typically, there is a decrease in water content with larger pore sizes of a soil (McCauley and Jones, 2005) but this is not evident with the subsoil material. This has the potential to be attributed to the presence of a greater fine sand fraction within the subsoil material which will result in greater water retention over a medium or coarse textured sand (Yang et al., 2004) or water repellency issues.

The coarse textured sandy soils are more susceptible to the challenges associated with soil water repellency (Hunter, 2011) because of their smaller specific surface area, thus requiring less organic matter to coat the surface (Doerr et al., 2000). Bossert and Bartha (1984) identify the potential of partial coating of the soil surface by the hydrophobic hydrocarbons can lead to reduced water holding capacity of the soil. However, Hunter (2011) indicates that soil water repellency has the potential to restrict infiltrating water. Given that the cores were saturated prior to placement on the tension table and the subsoil material had a greater sand fraction, the bottom of the cores may have dried first, creating elevated water repellency. This restricted downward water flow and consequently increased the water content in the subsoil cores over the Bm and BC material without hydrocarbons removed.

In reviewing the treatments with hydrocarbon material in Table 3.6, significant differences in water content for suctions of 0 cm, 3 cm, 100 cm, 300 cm, 700 cm and 5000 cm are evident whereas for suctions of 30 cm and 70 cm there is no significant difference. Due to the soil water

retention curves falling close together as shown in Figure 3.4, assumptions cannot be made on which treatments are significantly different. Therefore, an ANOVA was performed on the data for two of the six treatments at a time for suctions of 0 cm, 3 cm, 100 cm, 300 cm, 700 cm, and 5000 cm to determine which treatments are significantly different. The ANOVA output is summarized in Table 3.7.

The BC with hydrocarbon material removed retained higher amounts of water when compared to the BC treatments containing 0% AOSM (Table 3.7). It can also be identified that the BC with hydrocarbons removed retains increased moisture over the BC treatments with 2% and 5% AOSM, at many of the suctions, given the water retention curves illustrated in Figure 3.4. This indicates that residual hydrocarbons coating the soil particles present in the BC treatments resulted in reduced water storage in the soil as previously indicated by Bossert and Bartha (1984).

Overall, the BC cores containing 0%, 2% and 5% AOSM concentrations showed limited significant differences across the majority of the suctions studied (Table 3.7). Significant differences are detected when comparing solid forms of BC with 5% AOSM to BC with 2% AOSM at saturation and 100 cm suctions. In comparing BC with 5% AOSM in the solid form to BC with 0% AOSM there are significant differences between the two treatments at saturation, 100 cm and 700 cm. This indicates that under certain conditions the implementation of concentrations of 5% AOSM in the solid form will actually increase the water retained. Although significant differences are detected, it is not significant across all of the suctions studied. Due to the similarity between each of the water retention curves for the BC material with AOSM, it can be concluded that increasing AOSM concentrations did not have a large physical effect on the water retention properties of the soil. The exception to this is in comparing

the BC with 5% AOSM in the solid form to BC with 5% AOSM in the crushed powder form which reveals significant differences in retained moisture for the AOSM in the solid form at all suctions except 30 cm, 70 cm and 5000 cm.

In comparing the water retention for the Bm and subsoil treatments to those of the BC cores with AOSM, it was observed that the Bm and subsoil treatments still retained higher water contents. Given that the subsoil retained the highest moisture levels for all the mineral soil treatments studied, it is anticipated that the integration of higher concentrations of AOSM in the solid form into this treatment would provide the best potential for increasing moisture content for revegetative success.

Table 3.5: Reported P-values from ANOVA Analysis on Organic and Mineral Soil

Suction (cm)	P-Value	Volumetric Water Content † (cm^3/cm^3)			
		LFH	Bm	Subsoil	BC (0%)
0	3.450×10^{-15}*	0.521	0.450	0.446	0.419
3	2.200×10^{-16}*	0.471	0.397	0.390	0.378
30	4.189×10^{-13}*	0.376	0.263	0.292	0.239
70	1.851×10^{-12}*	0.189	0.092	0.099	0.084
100	3.232×10^{-9}*	0.180	0.095	0.095	0.063
300	2.104×10^{-10}*	0.170	0.070	0.089	0.032
700	2.918×10^{-9}*	0.150	0.053	0.068	0.027
5000	2.138×10^{-8}*	0.121	0.034	0.034	0.037

Note : †Values are reported as average
*****Indicates significance at $p<0.05$

Table 3.6: Reported P-values from ANOVA Analysis on the Treatments with AOSM

Suction (cm)	P-Value	Volumetric Water Content † (cm^3/cm^3)					
		0%	2% Powder	2% Solid	5% Powder	5% Solid	Hydrocarbon Removed
0	3.317×10^{-5}*	0.419	0.430	0.427	0.427	0.439	0.457
3	1.748×10^{-6}*	0.378	0.380	0.379	0.374	0.386	0.408
30	0.392600	0.239	0.258	0.245	0.256	0.242	0.250
70	0.569100	0.084	0.083	0.089	0.087	0.091	0.087
100	0.034940*	0.063	0.062	0.062	0.076	0.084	0.080
300	0.001512*	0.032	0.043	0.043	0.033	0.046	0.072
700	0.011650*	0.027	0.031	0.039	0.035	0.042	0.054
5000	0.019000*	0.037	0.035	0.033	0.036	0.037	0.030

Note : †Values are reported as average
*Indicates significance at $p<0.05$

Table 3.7: Reported P-values from ANOVA Analysis on AOSM Treatment Comparisons

Contrast	0 cm	3 cm	100 cm	300 cm	700 cm	5000 cm
BC with hydrocarbon removed VS BC with 0% AOSM	0.0016*	0.0009*	0.07076	0.0116*	0.0256*	0.0353*
BC with 0% AOSM VS BC with 2% AOSM-powder	0.2415	0.7822	0.9103	0.3815	0.6755	0.1721
BC with 2% AOSM-powder VS BC with 2% AOSM-solid	0.6498	0.7761	0.9715	0.9932	0.9977	0.2940
BC with 2% AOSM-solid VS BC with 5% AOSM-solid	0.0461*	0.1788	0.04427*	0.7837	0.2175	0.0632
BC with 5% AOSM-powder VS BC with 5% AOSM-solid	0.0078*	0.0007*	0.0110*	0.0111*	0.0007*	0.5923
BC with 0% AOSM VS BC with 5% AOSM-solid	0.0382*	0.2260	0.0036*	0.1899	0.04114*	0.7612

Note : Rounded to four decimal places from original output

*****Indicates significance at $p<0.05$

3.4.4 Soil Hydraulic Conductivity

Table 3.8 depicts the bulk density, average flux, average saturated hydraulic conductivity and corresponding void ratio for each of the soil materials studied.

Table 3.8: Bulk Density (ρb), Flux (Jw) and Saturated Hydraulic Conductivity (Ksat)

Material	**ρb (gcm^{-3})**	**Jw† ($cm^3s^{-1}cm^{-2}$)**	**Ksat† ($cmhr^{-1}$)**	**Void Ratio**
LFH	1.38	0.0125	27.72	0.9210
	1.42	0.0126	28.89	0.8682
	1.54	0.0122	26.95	0.7237
Bm	1.59	0.0131	29.94	0.6665
	1.61	0.0169	38.19	0.6416
Subsoil	1.51	0.0111	24.61	0.7539
	1.60	0.0108	25.18	0.6540
	1.61	0.0110	24.82	0.6497
----------BC Soil Material----------				
0% AOSM	1.60	0.0123	27.13	0.6584
	1.61	0.0138	32.35	0.6422
	1.63	0.0115	25.67	0.6247
	1.69	0.0150	20.43	0.5682
2% AOSM Powder	1.69	0.0120	17.37	0.5204
2% AOSM Solid	1.69	0.0134	20.09	0.5204
5% AOSM Powder	1.69	0.0117	16.64	0.4540
5% AOSM Solid	1.69	0.0170	23.04	0.4539
----------hydrocarbons removed----------				
BC	1.61	0.0247	58.33	0.6490
	1.62	0.0269	60.53	0.6380

Note : †Values reported as means

The typical hydraulic conductivity ranges of 20.83 cm hr^{-1} to 83.33 cm $hr^{-1}$for a coarse sand identified by Bouma (2008) is comparable to the hydraulic conductivity values observed for the soil materials studied in Table 3.8, with the exception of the cores containing AOSM in the crushed powder form.

Due to the differences in void ratio at the measured saturated hydraulic conductivity, the data was modeled to determine the extent that the saturated hydraulic conductivity for a particular soil is changing as a result of changes in void ratio. A modified Kozeny-Carman equation was used as reported by Newman (2002). The equation is as follows:

$$Ks^*/Ks = [e^{*3}/(1+e^*)]/[e^3/(1+e)] \qquad \text{(Eq. 3.7)}$$

where Ks* is the value determined for a given void ratio e* and Ks is the estimated value for other void ratios (e). The void ratio can be presented as:

$$e = Vv/Vs \qquad \text{(Eq. 3.8)}$$

where Vv is the volume of voids (cm^3) and Vs is the volume of the soil (cm^3). The resulting modeled saturated hydraulic conductivity curves, in $cmhr^{-1}$, with standard error bars can be viewed in Figures 3.7 and 3.8.

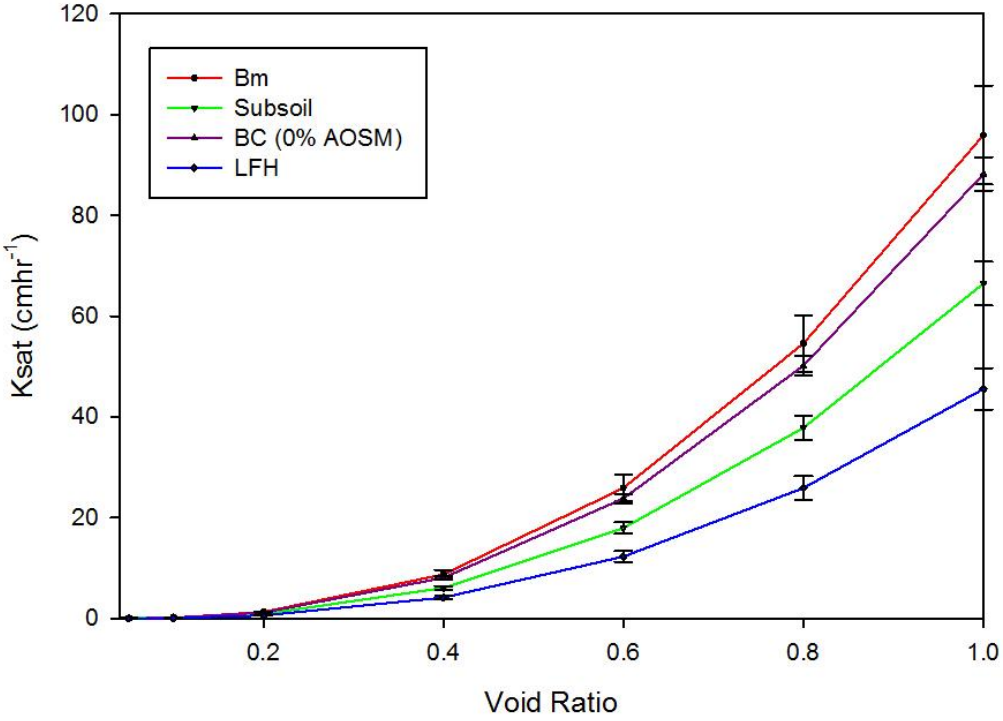

Figure 3.7: Modeled Saturated Hydraulic Conductivity for Nine Replicates: Organic and Mineral Soil

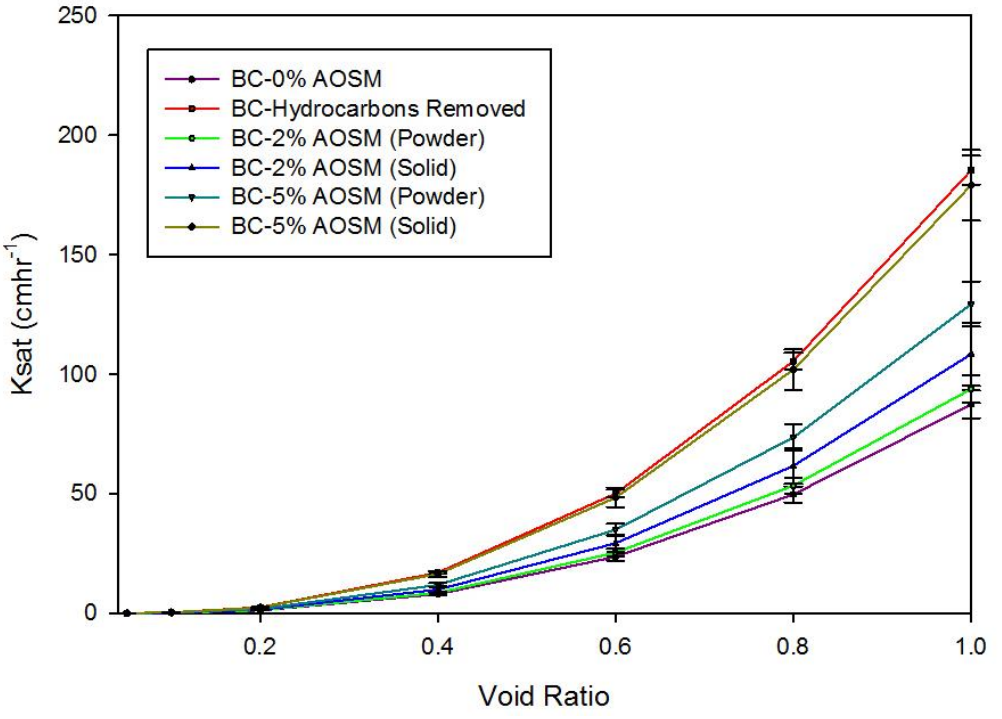

Figure 3.8: Modeled Saturated Hydraulic Conductivity for Five Replicates: AOSM Cores

Statistical analysis was conducted using the R Program System version 3.0.2. The Analysis of Variance (ANOVA) model was used to compare the multiple means between the modeled saturated hydraulic conductivity values at a void ratio of 0.6. A p-value of less than 0.05 is considered a significant effect. The averaged modeled results and deviance at all the void ratios calculated can be viewed in Tables 3.9 and 3.10 for treatments without and with hydrocarbon inclusions, respectively. The significance at void ratios of 0.6 is also indicated within the tables.

Significant differences in saturated hydraulic conductivity were detected in the organic and mineral soil, with the exception of the BC material with 0% hydrocarbon inclusions, at a void ratio of 0.6 (Table 3.9). The LFH material had slower flux and saturated hydraulic conductivity values. This coincides with observations made by Hunter (2011) in which the LFH material has the potential to restrict water infiltration under specific conditions, such as with increased decomposition levels.

In comparing the saturated hydraulic conductivities for the mineral soils, there were significant differences between the Bm and subsoil treatments. The subsoil material exhibited the lowest saturated hydraulic conductivity compared to the other reclamation materials. Given that the subsoil material has the greatest coarse sand content (Table 3.1), and that hydraulic conductivity decreases with decreased pore size of a soil (McCauley and Jones, 2005), the lower saturated hydraulic conductivity was not anticipated. This might be related to a greater fine sand fraction compared to other materials studied or the potential for water repellency issues in the subsoil material. Hunter (2011) identified that the presence of water repellency has the potential to restrict infiltrating water and the coarse textured sandy soils are more susceptible to the challenges associated with soil water repellency.

Table 3.9: Average Modeled Saturated Hydraulic Conductivity at Varying Void Ratios for Organic and Mineral Soil

Material	Ksat-0.05† (cm/hr^{-1})	Ksat-0.10† (cm/hr^{-1})	Ksat-0.20† (cm/hr^{-1})	Ksat-0.40† (cm/hr^{-1})	Ksat-0.60† (cm/hr^{-1})	Ksat-0.80† (cm/hr^{-1})	Ksat-1.00† (cm/hr^{-1})
LFH	0.011	0.083	0.607	4.163	12.295*	25.905	45.536
	(0.003)	(0.022)	(0.164)	(1.125)	(3.323)	(7.002)	(12.308)
Bm	0.023	0.174	1.279	8.769	25.896*	54.563	95.911
	(0.007)	(0.053)	(0.391)	(2.683)	(7.923)	(16.694)	(29.344)
Subsoil	0.016	0.121	0.886	6.079	17.951*	37.822	66.484
	(0.003)	(0.023)	(0.172)	(1.178)	(3.480)	(7.332)	(12.888)
----------BC Soil Material----------							
0% AOSM	0.021	0.160	1.176	8.065	23.817	50.182	88.211
	(0.002)	(0.018)	(0.133)	(0.913)	(2.697)	(5.683)	(9.989)

Note : †Values are reported as average with standard deviation
*****Indicates significance at $p<0.05$

Table 3.10: Average Modeled Saturated Hydraulic Conductivity at Varying Void Ratios for AOSM

Material	Ksat-0.05† (cm/hr^{-1})	Ksat-0.10† (cm/hr^{-1})	Ksat-0.20† (cm/hr^{-1})	Ksat-0.40† (cm/hr^{-1})	Ksat-0.60† (cm/hr^{-1})	Ksat-0.80† (cm/hr^{-1})	Ksat-1.00† (cm/hr^{-1})
----------BC Soil Material----------							
0% AOSM	0.021	0.159	1.165	7.986	23.583*	49.690	87.345
	(0.003)	(0.024)	(0.177)	(1.211)	(3.577)	(7.537)	(13.248)
2% AOSM Powder	0.022	0.170	1.250	8.569	25.306	53.319	93.726
	(0.003)	(0.024)	(0.173)	(1.188)	(3.508)	(7.390)	(12.991)
2% AOSM Solid	0.026	0.197	1.445	9.907	29.256	61.642	108.355
	(0.007)	(0.054)	(0.397)	(2.721)	(8.037)	(16.934)	(29.766)
5% AOSM Powder	0.031	0.235	1.724	11.821	34.908	73.550	129.288
	(0.005)	(0.038)	(0.280)	(1.923)	(5.679)	(11.966)	(21.033)
5% AOSM Solid	0.043	0.326	2.388	16.372	48.350	101.873	179.073
	(0.008)	(0.060)	(0.442)	(3.034)	(8.961)	(18.880)	(33.187)
----------hydrocarbons removed----------							
BC	0.044	0.337	2.470	16.936	50.015	105.382	185.242
	(0.004)	(0.033)	(0.242)	(1.660)	(4.903)	(10.331)	(18.160)

Note : †Values are reported as average with standard deviation
*****Indicates significance at $p<0.05$

As shown in Table 3.8, it appears that with hydrocarbon present in the soil, the flux rates were reduced and lower hydraulic conductivities were evident as compared to the BC soil with 0% hydrocarbon concentration, but this did not take into account the differences in void ratio. When the saturated hydraulic conductivity for soils with the same void ratio are compared (Table 3.10), limited significant differences were observed among BC materials with varying hydrocarbon percentages and forms. The only significant difference detected was the BC material with no hydrocarbon inclusions (0%) when compared to the BC material with AOSM at 2%, 5% and BC with all hydrocarbons removed.

The cores with hydrocarbons in the solid form showed higher mean flux rates over the corresponding hydrocarbon percentages in the crushed powder form (Table 3.10). However, the lack of a statistically significant effect may be attributed to the large variability among replicates present with the hydrocarbons in the solid form. This creates difficulty in identifying the behavior of hydrocarbons in the solid form under saturated conditions given the instability and range in the measured data.

3.5 Conclusion

The observed sand texture of the reclamation material, along with lower organic carbon present, indicates challenges related to soil water storage that ultimately will influence revegetation success. Of the mineral reclamation materials studied, the subsoil appears to provide the best possibility for reclamation success given the higher retained moisture levels, slower flux rates and lowest hydraulic conductivity, thereby increasing soil water storage for plant use. The ability of the subsoil material to exhibit these characteristics, given it has the greatest coarse fragments, may be attributed to water repellency processes which have the ability to restrict infiltration, thereby increasing water content, or the presence of a greater fine sand

fraction within the subsoil material. It should be noted that the coarse materials are more susceptible to water repellency due to the lower particle size area and therefore reduced organic matter, or hydrocarbon material, required to coat the surface.

The opposite trend was observed when comparing the BC material with hydrocarbons removed and the BC material with 0% AOSM in terms of water retention. It was concluded that water repellency can also cause reduced storage due to the residual hydrocarbons coating the soil particles. This may potentially have minimal effects, and can only be detected when comparing to a material where all hydrocarbons had been removed, as soil water repellency was not detected through contact angle studies on the BC reclamation material with 0% AOSM.

Although the AOSM was determined to be hydrophobic with strong to very severe water repellency, its placement at varying concentrations and forms did not create consistent significant differences in the amount of retained moisture. This further indicates that the previous observation of reduced moisture storage with hydrocarbon integration does not occur with an increase in hydrocarbon material, thus showing the hydrocarbon material as having minimal impacts to moisture storage. The absence of increasing moisture storage from AOSM integration may potentially be attributed to the lack of an enriched silt and clay fraction in the AOSM.

Limited significant differences were also observed when the saturated hydraulic conductivity of the BC material with varying hydrocarbon percentages and forms were reviewed under the same void ratio. The lack of statistical differences may be attributed to the large deviations in data present with the hydrocarbons in the solid form. This raises questions on the behavior of the hydrocarbon material given the larger inconsistency in results under saturated conditions.

In conclusion, given that the LFH and subsoil retained the highest moisture levels and had the highest site gravimetric moisture contents for all the treatments studied, it is anticipated that a reclamation design with these soils would be the best scenario for increasing moisture content for revegetative success. In addition, although not significant, the integration of higher concentrations of AOSM in the solid form may provide increased potential for moisture retention.

4. ASSESSING THE ROLE OF LFH, AGGREGATE OIL SAND MATERIAL AND SOIL LAYERING ON NUTRIENT AND SOIL WATER DYNAMICS IN COARSE-TEXTURED RECLAMATION MATERIAL

4.1 Preface

The previous chapter compared the soil water retention characteristics of the individual soil reclamation materials and the water repellency of the naturally occurring aggregate oil sand material (AOSM), or hydrocarbon-affected material. The results suggested that the subsoil material exhibited increased moisture storage over the other treatments. In an attempt to further understand soil water and nutrient retention in reclamation designs at the Aurora Capping Study (ACS) site, a column study was performed using different combinations of AOSM and soil reclamation soils. Nutrient and hydrocarbon leaching potential were also examined.

4.2 Introduction

The reclamation soils used for the ACS are from ecosites a, b (Yarmuch, n.d.; Beckingham et al., 1996) and d (Zettl et al., 2011) and can be identified mainly as a dry to very dry sandy soil (Beckingham et al., 1996). Sheoran et al. (2010) indicate that soils consisting of high amounts of coarse fragments contain larger pores that are unable to store enough plant available water to sustain growth throughout the summer months. Zettl et al. (2011) further confirmed that the areas of northern Alberta support a range of ecosite types, and subsequently a range of varying moisture regimes, even though the sites exhibit very similar soil texture. The range of moisture regimes with soils of similar texture indicates that there may be other mechanisms controlling soil water storage and possibly nutrient availability which need to be understood. This may include factors such as the presence of organics and textural layering.

Aside from reclamation soils at oil sands mine sites consisting of salvaged mineral soils, surficial LFH material and naturally AOSM are also present. These materials may create soil

water storage and water and chemical transport behavior similar to those associated with texturally variable soils through capillary barrier and fingering flow mechanisms. The integration of AOSM has also raised question on the potential for hydrophobicity interactions as well.

In addition, due to the limited research into the interaction of hydrocarbon-affected coarse textured material on soil water and transport processes, questions have been raised as to the contamination risks from potential leaching of the integrated hydrocarbon material in reclamation cover designs. Although Yarmuch (n.d.) identifies that the use of the naturally-occurring oil sands material within cover designs poses potential issues in terms of disrupting, or breaking up, the stable oil sand materials which may result in exposing unweathered cores, the CEMA Hydrocarbon Task Group for soil salvage concluded that surficial materials containing oil sands materials do not pose a severe risk.

As a result of limited research from integrating AOSM, soil layering schemes and LFH material into a reclamation profile, the objective of this study is to investigate the anticipated effects of AOSM concentrations and soil layering influences on soil water and nutrient retention. The potential for leaching of nutrients and hydrocarbons will also be identified and thus the scope of hydrocarbon contamination originating from the AOSM can be estimated. This will be accomplished through a column study which involves a series of three phases which focus on measuring the field capacity and the changes in water storage as affected by artificial rainfall and evaporation patterns as well as the leaching of nutrients and hydrocarbons from reclamation covers consisting of AOSM.

4.3 Background

Soil textural/structural contrasts create discontinuity in the hydraulic properties of the soil, potentially limiting the downward flow of water and chemical transport (Si et al., 2011). Aside from minimizing nutrient loss, soil layering also contributes to increased soil water storage capacity (Si et al., 2011). This can be explained through two mechanisms: capillary barriers and hydraulic barriers.

Capillary barriers are formed in unsaturated soil profiles of finer overlying coarser textured soil. Aubertin et al. (2009) identify that the difference in unsaturated hydraulic conductivities between the layered soil tends to restrict the downward flow of water at the interface due to the lower hydraulic conductivity of the unsaturated coarser textured material located below the finer material. This results in the finer textured soil remaining at elevated levels of saturation and therefore increasing soil water storage and residence time. Burgers (2005) noted that regions with soil moisture deficits can adequately utilize capillary barriers to increase plant available water by restricting percolation.

Javaux and Vanclooster (2004) indicate that soil layering may also generate the development of unstable wetting fronts at the interface of a fine textured soil over a coarser textured soil. This creates the potential for layers to induce fingering (Si et al., 2011). This can reduce soil water storage and chemical residence time in the soil due to water bypassing the majority of the soil profile (Si et al., 2011).

Hydraulic barrier effects are also evident in the case of a coarser material overlying a finer material. The hydraulic conductivity of the finer textured layer is less than the overlying coarse layer, resulting in water accumulation in the upper layer (Scott, 2000). Scott (2000) indicates that the infiltration rate decreases to that of the finer material and with time the water

content will increase significantly in the coarse layer when the wetting front reaches the interface between the layers. Si et al. (2011) report that the water infiltration rate will be reduced and the residence time of water increased due to the hydraulic barrier.

Under natural conditions, soil layers from the same textural class but with only slight differences in particle size distribution (Si et al., 2011) can create enhanced soil water storage (Huang et al., 2011; Huang et al., 2013). Huang et al. (2011) showed that in a layered coarse soil, the interface between the finer and coarser sand generates a hydraulic barrier limiting wetting front advance and resulting in non-uniform water infiltration and drainage (Huang et al., 2011). They also showed that when a finer textured sand is layered above a coarser textured sand, a capillary break occurs resulting in increased water content in the finer-textured layer and reduced percolation (Huang et al., 2011).

Huang et al. (2013) also examined the effect of varying layering thicknesses within a soil profile at field capacity. Laboratory columns with five or ten cm thick layers exhibited higher water storage following gravity drainage than columns with 25 cm layers and those with a homogenous soil profile. The five cm thick layered column consistently had the highest water storage but was only slightly higher than the ten cm layered column. The 25 cm layered column and the homogenous column exhibited little difference in water storage when compared to each other (Huang et al., 2013). Overall, the presence of layers delayed drainage and increased water storage with the amount of water stored increasing, and drainage rate slowing, with the greater number of textural breaks (Huang et al., 2013).

In addition to the mechanisms associated with texturally variable soils, hydrophobicity interactions may also influence water storage and water and chemical transport behavior. Hunter (2011) found that the LFH material from the Athabasca oil sands region does not always increase

infiltration. It has the tendency to fall between wettable and water repellent, indicating that it is not severely water repellent but it has the potential to restrict water infiltration under specific conditions, such as with increased decomposition levels. Hunter (2011) noted that, in conjunction with the organic LFH topsoil material, the presence of petroleum hydrocarbons also contribute to soil water repellency when it coats soil particles. The coarse textured sandy soils are more susceptible to the challenges associated with soil water repellency since these soils have a smaller surface area per unit volume, as compared to finer textured soils, and therefore require less organic matter to coat the surface (Doerr et al., 2000). Bossert and Bartha (1984) identified the potential for reduced water holding capacity of the soil as a result of the partial coating of the soil surface by hydrophobic hydrocarbons. Through a soil water repellency study, Hunter (2011) was able to conclude that coarse textured hydrocarbon-affected soils, with and without AOSM, exhibited less water repellency than the reclaimed mineral soils. These differences in water repellency were likely attributed to the organic content of the soil rather than the hydrocarbon content (Hunter, 2011). This shows the potential for reduced impacts from AOSM integration when compared to the naturally occurring organic matter in the reclaimed mineral soils. Hunter (2011) also reports that the risk of severe water repellency is not increased with direct contact with the hydrocarbon-affected soil.

Conclusions reached by Fleming et al. (2012) indicate that the use of AOSM within reclamation cover prescriptions contributes minimal environmental impacts to surface and groundwater, based on the limited hydrocarbon leachate collected during column studies. Hunter (2011) also supports the recommendation made by Fleming et al. (2012) in regards to implementing AOSM in reclamation covers.

The studies conducted by Fleming et al. (2012) analyzed the type of hydrocarbons contained within the AOSM at the Athabasca oil sands. It was found that light hydrocarbons comprise less than a fraction of 1% of the total AOSM hydrocarbons and are rarely present above detectable limits. If they are detected, they typically are recorded well below the clean soil guidelines, as established by Canadian Council of Ministers of the Environment (CCME). The F4G heavy hydrocarbon represents 2% to 5% of the total hydrocarbon concentration of the AOSM and can be identified as the dominating type of hydrocarbon. It was observed that as the AOSM became finer, there was a greater inhibition of weathering and degradation processes, resulting in greater amounts of F3 hydrocarbon fractions and decreased F4G content (Fleming et al, 2012).

Fleming et al. (2012) were also able to reduce the cause for concern given the results of a column study that focused on assessing the potential impacts to groundwater caused by AOSM disturbance. The study involved layering AOSM and sand into a column and packing these layers using a modified proctor hammer to simulate disturbances associated with large scale excavation and placement of the material. Following the completion of the material placement and column packing, 90 mL/day of water was applied to the columns for 11 months. In analyzing the leachate water, it was concluded that F1 hydrocarbons were not detected in the water and very low concentrations of F2 and F3 hydrocarbons were detected. It can be noted that increased hydrocarbon concentration for the F2 fraction were evident when it was exposed to dryness but the F3 fraction showed little response to the same dry conditions. Fleming et al. (2012) indicate that the F2 hydrocarbons rarely occur within AOSM samples and the leachate observed was hypothesized to be products formed during microbial degradation. Although the F2 fractions observed are to be more closely representative of anticipated hydrocarbon

concentrations in the field due to exposure to microbial degradation and wet dry cycles, the hydrocarbon concentration in the leachate water was still well below that of the clean groundwater standards set by the Province of Alberta; 1.1 mg/L for F1 and F2 fractions (Fleming et al., 2012). It should be noted that the F3 fraction is not regulated (Fleming et al., 2012).

4.4 Materials and Methods

The ACS site consists of numerous reclamation design prescriptions, as illustrated in Figure 2.1. The scope of this column study will focus on the reclamation treatments consisting of varying AOSM concentrations and layering schemes illustrated in Figure 4.1

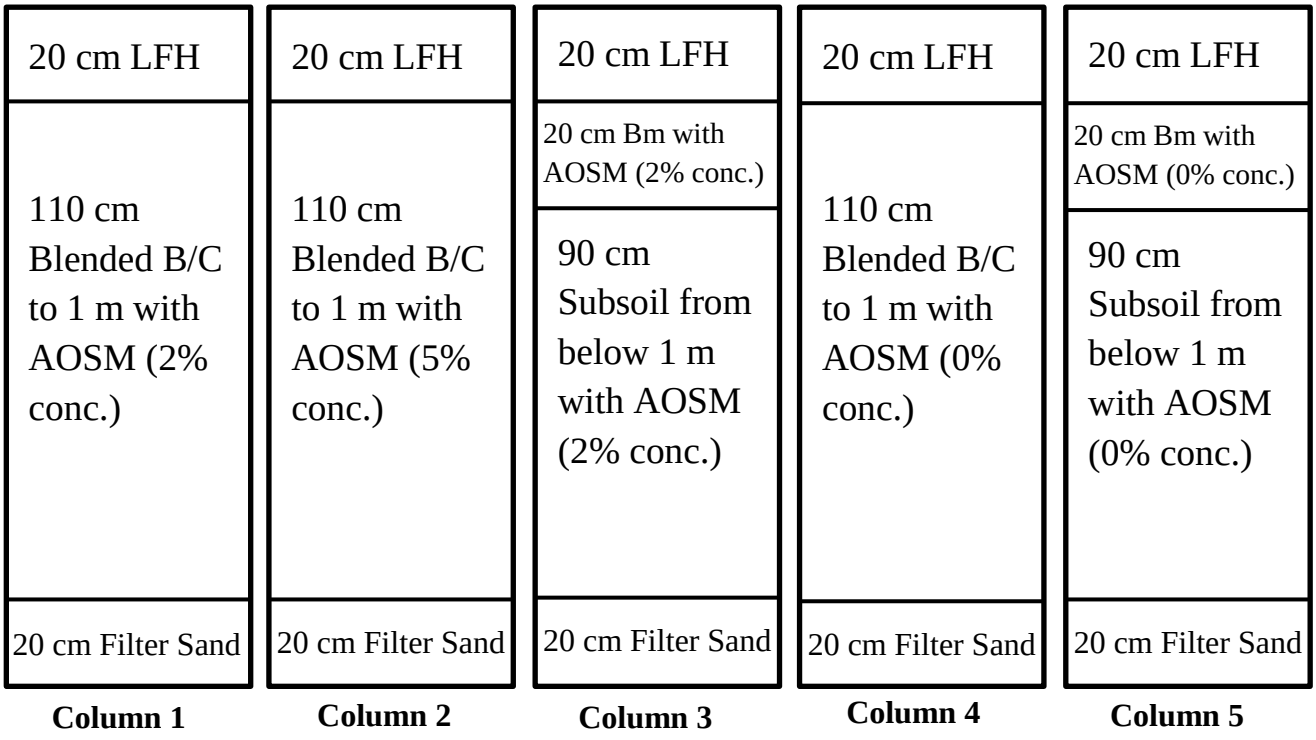

Figure 4.1: Reclamation Treatments for the Three Phase Column Study

The soil material collected from the Aurora Soil Capping study location, corresponding to the treatments illustrated in Figure 4.1, is utilized for the column study and packed into columns that are 20 cm in diameter and 150 cm in length.

The total amount of soil to be packed into the corresponding layer height for each treatment was determined by attempting to pack to a bulk density of 1.52 gcm^{-3} which corresponds to the average Aurora Soil Capping study bulk density observed in the field, as identified by Zettl et al. (2011). Although bulk densities of up to 1.69 gcm^{-3} and 1.71 gcm^{-3} are reported at sites within the Athabasca oil sands (Huang et al., 2011), the lower bulk density was chosen in an attempt to reduce influences from potential compaction scenarios.

Lewis and Sjöstrom (2010) indicate that the goal of repacking is to restore the bulk density of the soil to a similar value to that of naturally observed, while avoiding the formation of preferential flow pathways. The damp packing method was used and involved loading small amounts or "lifts" of damp material into the column and then mechanically packing it either by hand or with a type of ram or pestle (Lewis and Sjöstrom, 2010). Oliviera et al. (1996) indicate that in order to produce homogenous sand packing, dry deposition must be in increments of 0.2 cm followed by compaction. Due to the size of the columns and accurate results obtained by Plummer et al. (2004) while utilizing 15 cm lifts, five cm lifts were utilized for this study. The soil columns were packed to a 5% gravimetric water content. This water content was selected based on information reported by Lewis and Sjöstrom (2010) on compacting damp soil and difficulties incurred within initial trials associated with the settlement of dry placed material following water applications.

The material was prepared in 2000 g increments in order to achieve easier placement with a smaller amount of material at one time until the total amount of material for the five cm layer amount was reached. The 2% hydrocarbon AOSM treatment required an addition of 40 g of AOSM to the 2000 g dry soil without AOSM material while the 5% hydrocarbon AOSM treatment required 100 g of AOSM for 2000 g of dry soil without AOSM material (See

Appendix G for calculations). The 5% moisture content was accomplished by mixing 2000 g of soil with 102 mL of water and 40 g of AOSM for the columns containing 2% AOSM concentrations and 105 mL of water with 2000 g of soil and 100 g of AOSM for the columns containing 5% AOSM concentrations (See Appendix H for calculations). Following placement of the prepared soil within the column, the material was packed with a modified soil packing tool similar to a soil tamper but with rounded plastic base. According to Fleming et al. (2012), the blows required for packing will simulate the disturbances associated with large scale field excavation and placement of the soil material. Following methods indicated by Plummer et al. (2004), the lift soil surface was scarified to a depth of about 0.5 to one cm after compaction and prior to further soil addition in order to avoid layering or segregation by particle size. Coarse filter sand (Target 10-20 Filter Sand) was placed at the bottom of the column to allow for leachate to be collected under free drainage conditions.

The complete column study consisted of two replicates of each of the five treatments illustrated in Figure 4.1, resulting in a total of ten columns. Each replicate followed the three phases as described in the following sections with new material packed in each of the columns for each replicate studied.

4.4.1 Phase I: Soil Water Storage at Field Capacity

Time Domain Reflectometry (TDR) probes were placed throughout each of the column prescriptions illustrated in Figure 4.1. The two stainless steel TDR probes were configured as two parallel rods that are 15 cm long and 3.5 cm apart and have a diameter of 0.3 cm. The TDR rods were placed horizontally within the columns at the depths of 2.5, 5, 15, 30, 50, 80, 110 and 130 cm.

TDR measures the travel time, which is subsequently converted to distance that electromagnetic waves would travel within that time. The apparent dielectric constant can be calculated from the travel distance and soil water contents derived from the apparent dielectric constant through the equation developed by Topp et al. (1980). The soil water content was measured by TDR every two minutes for the first hour during the advance of the wetting front and then switched to a five minute measurement increment for the second hour. The remainder of the phase was measured every 20 minutes. The measured moisture content was recorded with a CR10X data logger utilizing the Loggernet 2.1 Datalogger Support Software.

The set of columns were brought to column saturation by maintaining a five cm constant head of distilled water on the surface layer until the TDR data reported water contents that stayed constant for at least an 80 minute period. This time period along with the observation that a significant proportion of water that was added to the column had drained from the bottom of the column was also used to determine when column saturation was reached. It is anticipated that full saturation was unable to be reached due to the possibility of entrapped air in the columns but the saturation reached would be comparable to saturated field conditions. For the remainder of the chapter column saturation will be referred to as saturation.

The soil water content was monitored during drainage until field capacity had been reached. According to Veihmeyer and Hendrickson (1950), it can be estimated that field capacity will be reached within two to three days following the addition of water. Zettl et al. (2011) observed that field capacity was reached after 18 hours of drainage in field sites in close proximity to the Aurora Soil Capping study site. Therefore, the moisture content observed after both 18 hours and a two day period were assessed to determine the moisture content at field capacity.

4.4.2 Phase II: Artificial Rainfall and Enhanced Field Capacity Scenario

Hillel (1998) indicates that field capacity can be estimated as the volumetric water content at a matric suction of 10 or 33 KPa. Given the height of the column and potential concerns for field capacity to be reached at the column base, a pressure of 20 KPa was applied to the top of the column following artificial rainfall applications. It is anticipated that the repeated wetting and drainage with applied air pressure will enhance field capacity by potentially helping a greater portion of the column to approach field capacity conditions.

The air pressure of 20 KPa was applied to the top of each of the soil columns utilizing airlines secured to an air supply and a pressure regulator with manifold to supply all five columns simultaneously.

The amount of artificial rainfall was determined by examining the natural rainfall patterns for Fort McMurray, Alberta. The data for Fort McMurray, Alberta (See Appendix I) was analyzed for the months of May, June, July and August from 2009-2011 for larger rainfall events. Two rainfall events of 31.5 mm which occurred on June 22, 2009 and 27.5 mm on August 24, 2009 were applied to the columns. The first rainfall simulation was applied to the columns at field capacity and the second rainfall simulation was applied four days after the first rainfall event. Although the precipitation patterns applied are much higher than the averages experienced at Fort McMurray, Alberta, a larger amount was utilized in attempt to predict the impact of AOSM and soil layering interactions under worst case scenario events. The duration of this phase of the column study lasted for a two week period in which soil moisture measurements were obtained using TDR probes following the same methods mentioned in Section 4.4.1.

4.4.3 Phase III: Nutrient and Hydrocarbon Leaching Potential

Given studies indicating that some hydrocarbons are sensitive to wetting and drying cycles (Fleming et al., 2012), the columns were subjected to a cycle of wetting and drying by completing Phases I and II of the column study prior to measuring hydrocarbon and nutrient leaching in Phase III.

Concerns may be raised relating specifically to the hydrocarbon concentration measurements becoming compromised due to the previous exposure of the AOSM to water infiltration. However, it is presumed that this scenario will be a greater representation of the actual amount of hydrocarbon material being leached in natural long term field conditions.

Nutrient Leaching

A tracer was selected to represent nutrient movement in the columns. Rowland et al. (2009) indicated that reclaimed soils were low in ammonium (NH_4^+), phosphorus (P) and potassium (K). The NH_4^+ and P are indicated to be immobile in the soil (Jensen, 2008; Johnson and Cole, 1979) leading to reduced leaching as compared to K which has the potential to be an issue in sandy soils (University of Nebraska-Lincoln, 2013). In addition fertilizer applications of K, in the form of potassium chloride (KCl), increase soil Cl substantially (White and Broadley, 2001). Due to little adsorption of Cl to the soil, and that it is not chemically altered by soil organisms, it is often used as a tracer for soil water movement (White and Broadley, 2001).

KCl was chosen to act as a nutrient index tracer given the increased relative mobility of this compound as compared to using compounds with higher adsorption and reduced mobility. Dyck et al. (2003) performed solute leaching studies in which KCl was utilized at application rates that varied from 0.11 to 2.24 kg KCl m^{-2}. It was identified that the average background Cl in sand soil is 0.005 kg Cl m^{-3} (Dyck et al., 2003).

Ten mL of a chemically saturated KCl solution was prepared and added to each column. This solution contained 310 g/L of KCl based on the solubility at 10°C (Speight, 2005). The mass of Cl added in this spike was at a rate of 100 g m^{-2} (See Appendix J for calculation) which corresponds to the lower rate applied in similar experiments by Dyck et al. (2003). This was considered sufficient given the smaller scale column study performed and the coarse nature of the soil with lower average background Cl present. The KCl solution was applied to the surface of the column using a syringe to attempt to evenly distribute the solution over the column surface.

A final amount of 4.64 g of KCl in 30 mL of distilled water was used due to the inability to develop a clear breakthrough curve by initially spiking each column with 3.14 g of KCl in 10 mL of distilled water. It should be noted that the amount of 3.14 g of KCl originally applied was higher than the amount of 3.10 g KCl calculated (Appendix J) as a measurement error occurred during the application process for the first set of columns.

The nutrient leachate was collected from the base of the column under free drainage scenarios, under a five cm constant head boundary condition on the column surface. The effluent was initially collected every four minutes for a 100 minute period once the water had started to drain from the column after the spike solution was applied. After 100 minutes the effluent was collected every 10 minutes for an additional 40 minute period. The volume of effluent was not collected in the first replication of the columns.

The chloride concentration in each of the columns outflow solution, collected over a time interval, was measured using an Electrical Conductivity (EC) meter (Fisher Scientific Accument AP85). The EC meter does not directly measure the concentration of the chloride solution in the water, but the EC value will linearly correlate with the chloride concentration (UNEP, 2012).

The breakthrough curves, defined as the resulting outflow chloride concentrations as a function of time for each column, indicate how long it takes the chloride tracer to filter through each of the columns. The peak time in the breakthrough curve is one of many indices to measure how fast the solute will pass through the entire column. In addition to the chloride breakthrough curves developed, the BTC's were plotted as EC concentration versus the cumulative infiltration for each column. This was accomplished by first obtaining the water content measured by the TDR at 15 cm, 30 cm, 50 cm, 80 cm, 110 cm and 130 cm for each of the columns over the constant head period. The measured water content was then used to calculate the weighted volume of water over each depth-increment in the column. The total accumulated volume of water across all of the column depths was then divided by the total column volume to obtain an average water content. The pore volume was obtained by multiplying the total column volume by the average weighted water content for each column.

The cumulative inflow was then calculated as follows:

$$Vt*T/T_{final}-PV_{FC} \quad \text{(Eq. 4.1)}$$

where Vt is the total volume of water added to the column (m^3), T is the time (min) that the EC and water content measurements were taken at, T_{final} is the time (min) that the last measurement was taken for each column and PV_{FC} (m^3) is the calculated pore volume at field capacity. The resulting cumulative infiltration was calculated as follows:

$$CF/PV_{ave} \quad \text{(Eq. 4.2)}$$

where CF is the cumulative inflow (m^3) and PV_{ave} (m^3) is the average pore volume for each column once the constant head was applied.

The time the first effluent was collected from the base of the column following the initiation of the constant head, the EC measurement, the average weighted water content for the

entire column volume, the calculated pore volume, cumulative inflow and cumulative infiltration can be viewed in Appendix L.

The results obtained in this study show potentially what will occur at the ACS study site under a worst case scenario approach with constant water infiltration. The results allow for conclusions to be drawn directly as to the impact that AOSM and layering can have on nutrient leaching.

Hydrocarbon Leaching

To assess the hydrocarbon concentration leached from each of the columns, the outflow solution was collected from the bottom of the column following the nutrient index tracer study. At the time of outflow collection it was anticipated that the columns were at, or near, saturation given reported water contents that remained constant from the TDR measured data.

The outflow solution was collected in glassware with tight fitting Teflon-lined lids (CCME, 2001b) that had been triple-rinsed with acetone solvent, followed by tap water and a final deionized water rinse as indicated by the University of Delaware Department of Chemistry and Biochemistry (n.d.). As indicated by the CCME (2001b), the samples were immediately stored at 4°C following collection until analysis with no chemical preservation used.

The analysis method used included Gas Chromatography (GC) with FID (Flame Ionisation Detection) as utilized by Fleming et al. (2012) which follows the benchmark method published by the CCME (2001b). The liquid form of the outflow solution required samples to be liquid-liquid extracted (LLE) to remove hydrocarbons from the outflow solution. The Ontario Ministry of the Environment (2001) indicates that the F2, F3 and F4 fractions are determined by extraction with hexane prior to column cleanup and GC-FID analysis. The procedure was similar to the Direct Hexane Extraction procedure indicated by Horvath (2009), with the

exception of the removal of the filter paper, given its initial use when adding the outflow solution to the separatory funnel and dry filtered air component. Following liquid-liquid extraction, the samples were cleaned up using sodium sulphate (Na_2SO_4) and silica gel columns following procedures published in section 11.4 of the CCME (2001b). The final volumes of samples were recorded prior to analyzing using a Varian CP-3800 GC with FID detector. The columns utilized for analysis were CP8673. The methods used to extract for the columns and settings on the GC were based on CCME guidelines (CCME, 2001b). In addition to the outflow from the five varying column prescriptions from both replications one and two, a blank was prepared using all reagents and equipment but with no sample. The method blank is part of quality control samples and must report results that are less than the Method Detection Limits (MDLs) (CCME, 2001b). A spike sample was also run to determine the efficiency of the process. Although Fleming et al. (2012) were able to analyze F1, F2, and F3 hydrocarbon fractions within the leaching study, limitations are posed with measuring the F1 fraction and thus only the F2, F3 and F4 fractions were analyzed for the scope of this study.

4.5 Results and Discussion

Although the anticipated column packing density was desired to mimic the average field bulk density at the Aurora Soil Capping study site, issues were encountered with maintaining this bulk density throughout each of the columns. The final bulk density (ρb) and porosity (n) reported for each column prescription in replication one and two can be viewed in Table 4.1. Porosity was calculated as follows:

$$n=Vv/Vt \qquad \text{(Eq. 4.3)}$$

where Vv (cm^3) is the volume of voids and Vt is the total volume (cm^3).

Table 4.1: Bulk Density and Porosity for Each of the Columns in Replication One and Two

Column	Material	----Replication One---- ρb (g cm^{-3})	Porosity	----Replication Two---- ρb (g cm^{-3})	Porosity
1	LFH	1.27	0.522	1.27	0.522
	BC (2% AOSM)	1.55	0.397	1.59	0.381
2	LFH	1.27	0.522	1.27	0.522
	BC (5% AOSM)	1.55	0.369	1.57	0.359
3	LFH	1.27	0.522	1.27	0.522
	Bm (2% AOSM)	1.52	0.409	1.52	0.409
	Subsoil (2% AOSM)	1.56	0.393	1.59	0.382
4	LFH	1.27	0.522	1.27	0.522
	BC (0% AOSM)	1.52	0.428	1.53	0.422
5	LFH	1.27	0.522	1.27	0.522
	Bm (0% AOSM)	1.52	0.427	1.52	0.427
	Subsoil (0% AOSM)	1.56	0.412	1.56	0.412

Following completion of replication one and questions raised on the influence of varying bulk density and porosity, a different method was utilized in replication two. Coughlan et al. (1978) studied variations in the physical properties of non-compacted soil-sand aggregates by dispersing soil with varying clay percentage, mixing with sand, and then subjected to wetting and drying. It was observed that a significant increase in void ratio is evident when the clay content ranged from zero to 10%. At clay contents lower than 10%, the majority of the clay does not fill the pores between the sand particles but rather forms films around the sand particles, increasing void ratio and expanding the coarse matrix. Therefore as opposed to packing to a desired bulk density and potentially having increased void ratio, and thus porosity, in the soils containing clay, the second replication of column packing attempted to alleviate differences in porosity between treatments.

Although differences are evident between treatments in terms of bulk density and porosity, the differences may be attributed to the presence and range in size of AOSM, along with slight variations in soil texture and sensitivity to the assumed particle density used in calculating the porosity.

4.5.1 Phase I: Soil Water Storage at Field Capacity

In replication one of the column study, the amount of time it took to saturate the columns with 36 liters of water was measured. Since sandy soil will reach steady-state infiltration under ponded conditions in a very short time, the average soil water flux at the soil surface was calculated as follows:

$$J_w = \frac{V}{A \cdot t} \qquad \text{(Eq. 4.4)}$$

The results obtained can be viewed in Table 4.2. The transient infiltration rate as a function of time was measured for replication two through calculating the amount of water that had been transported through the columns over a specified length of time. The results are shown in Table 4.3. The TDR output data was monitored until the water content remained constant before saturation was presumed to be reached, as indicated in Section 4.4.1.

In addition to the infiltration rates calculated during the saturation phase for replication one, the volume of water was collected at the bottom of the columns for the time period from saturation to field capacity, or 48 hours (Table 4.4). These measurements were not taken for the columns in replication two of the study but flux under saturated conditions was measured (Table 4.5). This was achieved by measuring the volume of outflow from the bottom of the column over a 10 second period once the columns had reached saturation, as indicated with stable water content values reported through the TDR data.

Table 4.2: Steady-state Infiltration Rate for the Columns in Replication One

Column	Material	Volume (cm^3)	Area (cm^2)	Time (seconds)	Jw (cms^{-1})
1	LFH BC (2% AOSM)	36000	314.16	6300	0.0182
2	LFH BC (5% AOSM)	36000	314.16	7260	0.0158
3	LFH Bm (2% AOSM) Subsoil (2% AOSM)	36000	314.16	6780	0.0169
4	LFH BC (0% AOSM)	36000	314.16	5460	0.0210
5	LFH Bm (0% AOSM) Subsoil (0% AOSM)	36000	314.16	5940	0.0193

Table 4.3: Transient Infiltration Rate as a Function of Time for the Columns in Replication Two

Column	Material	Volume (cm^3)	Area (cm^2)	Time (seconds)	Jw (cms^{-1})
1	LFH BC (2% AOSM)	28150	314.16	14400	0.00622
2	LFH BC (5% AOSM)	27930	314.16	14400	0.00617
3	LFH Bm (2% AOSM) Subsoil (2% AOSM)	30800	314.16	14400	0.00681
4	LFH BC (0% AOSM)	36000	314.16	14400	0.00796
5	LFH Bm (0% AOSM) Subsoil (0% AOSM)	32600	314.16	14400	0.00721

Table 4.4: Volume of Water Collected from Saturation to Field Capacity (48 hours) for the Columns in Replication One

Column	Material	Volume (cm^3)
1	LFH BC (2% AOSM)	27400
2	LFH BC (5% AOSM)	23600
3	LFH Bm (2% AOSM) Subsoil (2% AOSM)	24575
4	LFH BC (0% AOSM)	27900
5	LFH Bm (0% AOSM) Subsoil (0% AOSM)	26300

The presence of AOSM appears to slow the infiltration rate relative to columns without AOSM present (Tables 4.2, 4.3). The presence of 5% AOSM concentration slows infiltration to a greater degree than treatments with 2% AOSM content.

Additionally, the presence of soil layering (Column 5) slowed the infiltration rate when compared to homogenous columns without AOSM (Column 4) for replication one and two (Table 4.2, 4.3). When 2% AOSM was implemented into the columns with soil layering schemes (Column 3) the infiltration rate was further reduced over the column with layering and 0% AOSM (Column 5) and the homogenous column with 2% AOSM (Column 1) in replication one (Table 4.2). The same trend was observed when reviewing the drainage data for replication one (Table 4.4).

It should be noted that when comparing the column with the texturally uniform 2% AOSM (Column 1) to the column with soil layering and 2% AOSM (Column 3) in replication two, the rate of infiltration is not reduced with soil layering and AOSM implementation over homogenous column with 2% AOSM (Table 4.3). This may be a function of the slight difference in bulk density and porosity between treatments when comparing the results for replication one and two. The BC with 2% AOSM was packed to 1.55 g cm^{-3} and the Bm and subsoil were packed to 1.52 g cm^{-3} and 1.56 g cm^{-3}, respectively, in replication one. In replication two, the BC with 2% AOSM was packed to 1.59 g cm^{-3} and the Bm and subsoil were packed to 1.52 g cm^{-3} and 1.59 g cm^{-3}, respectively. This indicates that the addition of layers to reduce infiltration flux may be offset by increasing the bulk density of a homogenous soil with AOSM.

The infiltration rates and drainage volume indicate the potential for the AOSM to act as a barrier to the downward flow of water under unsaturated conditions. This may be due to either the reduction in porosity from AOSM implementation or the water repellency characteristics of the AOSM as identified in 3.4.2.

The presence of soil layering acts as a capillary barrier by restricting the downward flow of water at the interface due to the lower hydraulic conductivity of the coarser textured material located below the finer material under unsaturated conditions (Aubertin et al., 2009). This results in water remaining in the fine-textured soil layer due to the capillary break and will only flow into the underlying coarse layer only when the critical soil water potential is reached (Si et al., 2011). Although the Bm and subsoil material fall into the same textural class, the Bm material has a greater fine soil fraction as compared to the subsoil material (Table 3.1). The results obtained coincide with soil layering studies performed by Huang et al. (2011) that reviewed layering with only slight textural differences. Huang et al. (2011) found that when a

finer textured sand is layered above a coarser textured sand, a capillary break occurs resulting in increased water content in the finer-textured layer and reduced percolation. Huang et al. (2013) also indicate that the presence of layers delays drainage and increases water storage with the amount of water stored increasing, and drainage rate slowing, with the greater number of textural breaks. It was found that columns with smaller layer thicknesses of 5 or 10 cm retain increased moisture over columns with 25 cm layers and those with a homogenous soil profile (Huang et al., 2013).

Confirmation that these scenarios are occurring is given by the visual progression of the wetting front, used as an indicator of infiltration rate, captured in Figure 4.2 for replication two. This progression was observed for both replicates one and two of the column study.

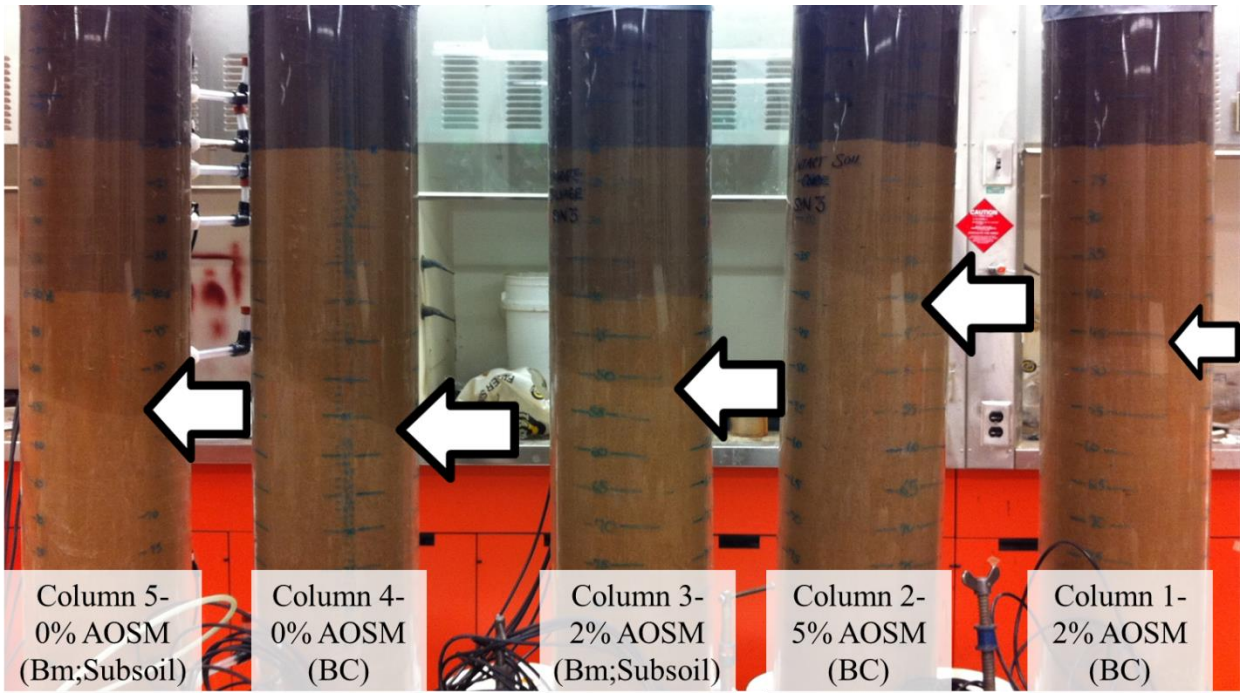

Figure 4.2: Observed Water Infiltration Fronts for Replication Two of the Column Study

Table 4.5: Flux Under Saturated Conditions for the Columns in Replication Two

Column	Material	Volume (cm^3)	Area (cm^2)	Time (seconds)	Jw (cms^{-1})
1	LFH BC (2% AOSM)	33.43	314.16	10	0.0106
2	LFH BC (5% AOSM)	33.73	314. 16	10	0.0107
3	LFH Bm (2% AOSM) Subsoil (2% AOSM)	34.57	314. 16	10	0.0110
4	LFH BC (0% AOSM)	28.33	314. 16	10	0.0090
5	LFH Bm (0% AOSM) Subsoil (0% AOSM)	38.77	314. 16	10	0.0123

Under saturated conditions for replication two, the presence of AOSM appears to increase the rate of water movement through the soil profile. However, these differences are small given the small range in flux values reported when comparing the 0%, 2% and 5% BC columns.

The potential for the slightly increased flux rates present under saturated conditions for the columns containing AOSM may be attributed to the potential formation of macropore channels around the AOSM due to the higher flow rates creating displacement between the soil particle and AOSM surface. Another possibility is that under saturated conditions, the AOSM are no longer water repellent and thus do not inhibit water movement as evident under unsaturated conditions. Observations made while unpacking the columns at the end of the study further support this theory as the AOSM material was wet throughout and broke apart easily.

The increased flux scenario for the columns containing AOSM under saturated conditions was not evident in the columns containing layering schemes. The inclusion of AOSM into layers appeared to reduce the downward flux in the column as compared to the layered column with 0% AOSM. In reviewing the bulk density and porosity for each of the layered columns, it is anticipated that if the bulk density was increased, and porosity decreased, for the layered column without AOSM the flux rate would be closer in comparison to the layered column with AOSM. Although the flux rates would be similar between the layered columns, this indicates the potential for layering schemes to reduce the increased flux rates associated with AOSM implementation.

In addition to the flow characteristics of the varying treatments, it is important to compare the soil water retained by each treatment at field capacity given the evidence that at field capacity the soil water content is considered to be ideal for plant growth (Brouwer et al., 1985). The resulting field capacity data after 18 hours, as indicated to be field capacity in field sites in close proximity to the Aurora Soil Capping study (Zettl et al., 2011) are shown in Figures 4.3 and 4.5 for replications one and two, respectively (See Appendix K for Raw Data). Field capacity reached after two days, as indicated to be field capacity by Veihmeyer and Hendrickson (1950), can be viewed in Figures 4.4 and 4.6 for replications one and two, respectively (See Appendix K for Raw Data).

The averaged field capacity measured from the TDR data for each of the specified column depths at 18 and 48 hours are presented in Tables 4.6 and 4.7 for replicates one and two, respectively.

Table 4.6: Average Water Content Measured at Field Capacity (18 and 48 hours) In the Columns for Replication One

	----------Average Soil Water Content (%)----------					
Column	**15 cm**	**30 cm**	**50 cm**	**80 cm**	**110 cm**	**130 cm**
1	9.65	6.15	7.00	8.90	10.85	32.40
2	10.10	4.55	7.75	9.55	10.05	32.75
3	9.45	7.30	7.60	12.35	15.05	26.45
4	8.40	5.15	6.25	8.25	12.15	26.15
5	9.45	8.00	5.75	9.90	16.15	23.10

Table 4.7: Average Water Content Measured at Field Capacity (18 and 48 hours) In the Columns for Replication Two

	----------Average Soil Water Content (%)----------					
Column	**15 cm**	**30 cm**	**50 cm**	**80 cm**	**110 cm**	**130 cm**
1	17.45	7.25	11.65	12.35	13.30	20.65
2	18.20	9.05	9.50	9.50	9.55	19.40
3	17.70	13.75	11.10	11.25	11.45	22.40
4	9.80	n.d.	9.60	9.10	13.10	14.50
5	14.75	11.90	8.95	11.50	13.00	23.20

Note : n.d. denotes not determined due to analytical error

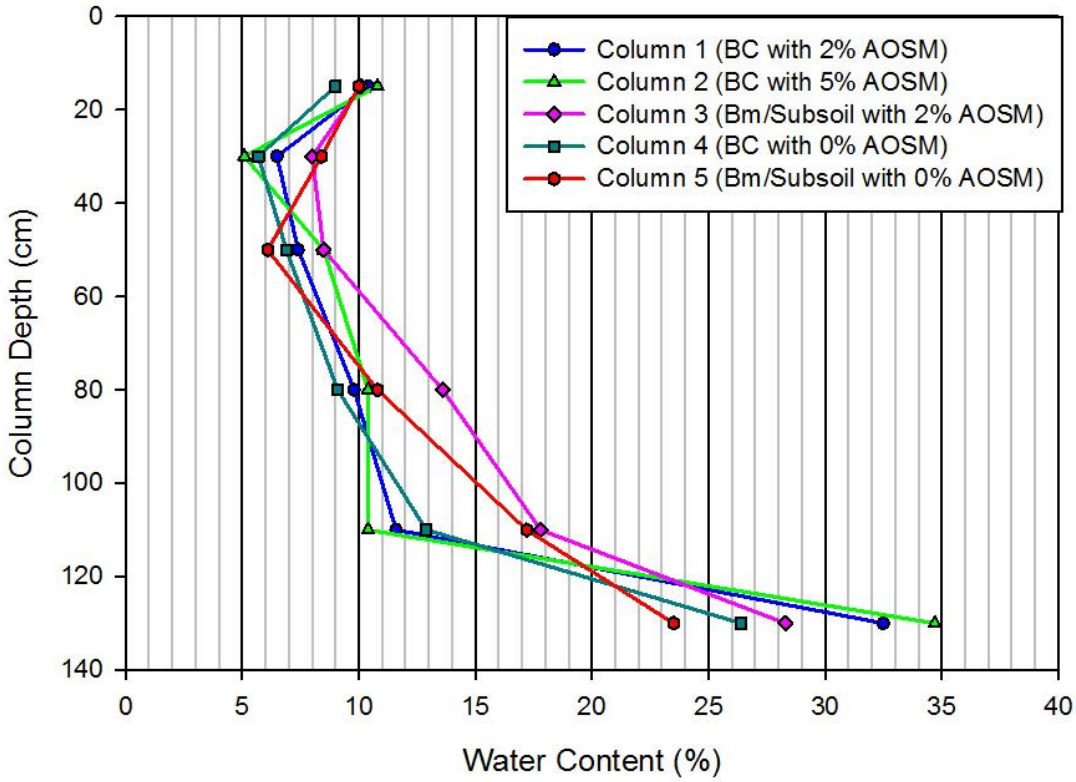

Figure 4.3: Water Content After 18 hours of Drainage for Replicate One

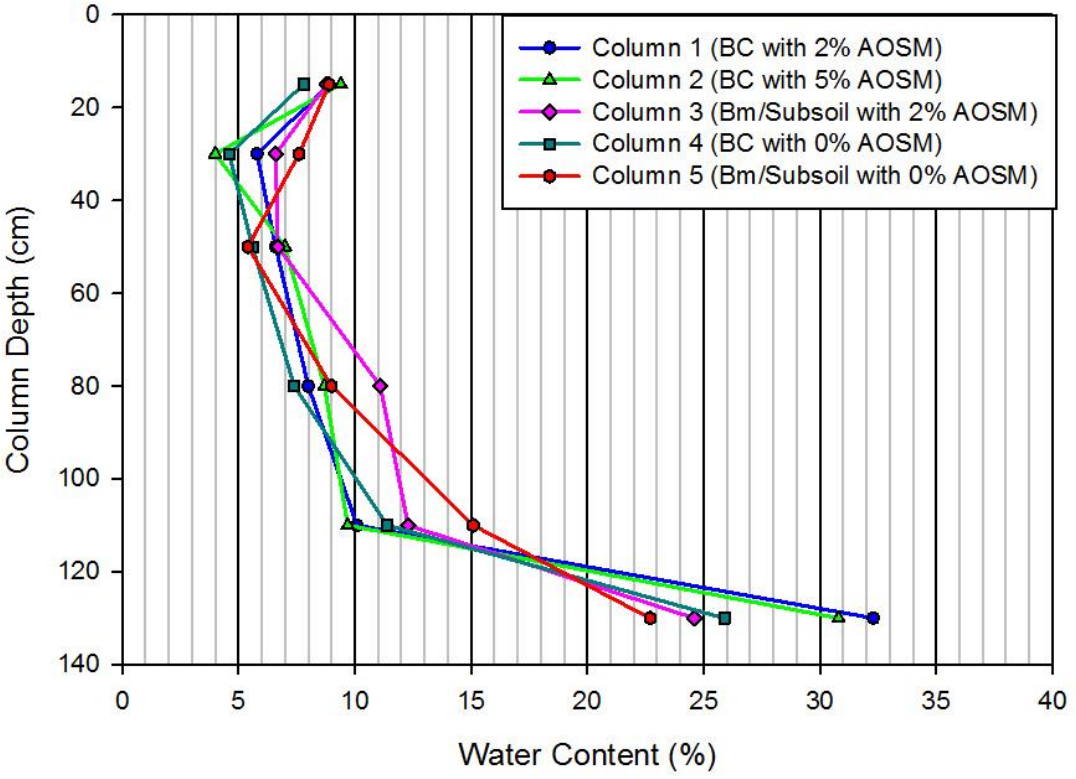

Figure 4.4: Water Content After 48 hours of Drainage for Replicate One

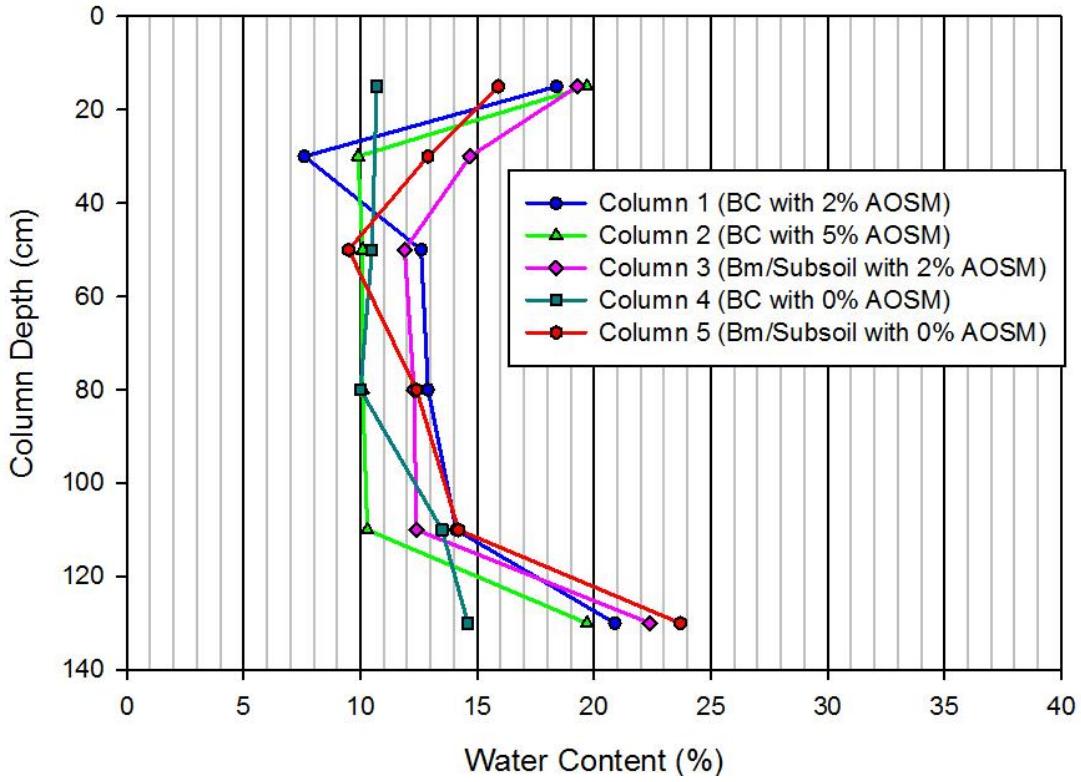

Figure 4.5: Water Content After 18 hours of Drainage for Replicate Two

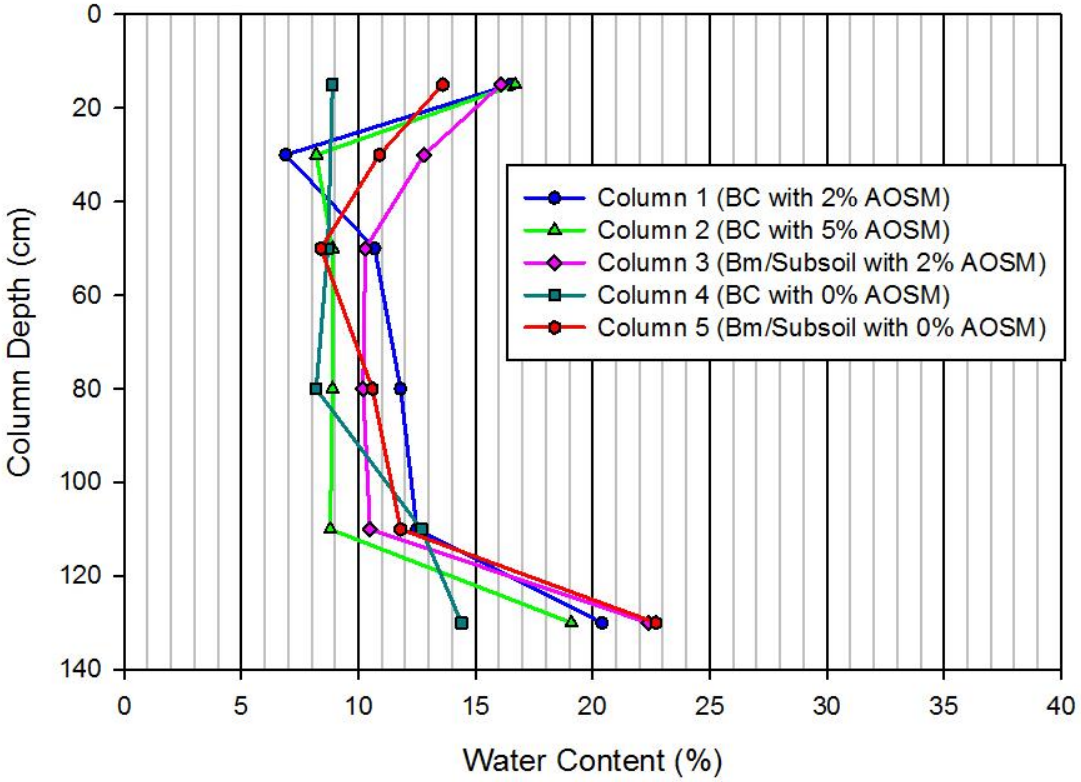

Figure 4.6: Water Content After 48 hours of Drainage for Replicate Two

As evident in Tables 4.6 and 4.7, there is no clear indication that hydrocarbon inclusions increase the water stored at field capacity. Although Fleming et al. (2012) concluded that AOSM soils retain more water due to an enriched silt and clay fraction of the AOSM material, a clear indication of this was not observed in this study. The absence of increased moisture storage from AOSM integration may potentially be attributed to the lack of an enriched silt and clay fraction in the AOSM material (Table 3.1).

Zettl et al. (2011) indicates that the laboratory methods currently utilized may not be able to replicate soil water dynamics in the field. It is therefore important to correlate laboratory derived data with results obtained from field scale studies. Zettl. et al. (2011) measured field capacity after 18 hours of drainage for sites located in close proximity to the Aurora Soil Capping study site, where the soil material was extracted from for this laboratory study. In reviewing the particle size analysis for the sites surveyed it can be identified that site SV10 was more comparable in the percentages of sand, silt and clay to the soil materials in the current study (Table 3.1). It should be noted that the SV10 site still had higher sand and clay percentage and lower silt percentage than the material extracted from the Aurora Soil Capping study site.

In comparing replications one and two after 18 hours of drainage (Figures 4.3 and 4.5) to the measured site field capacity results reported by Zettl et al. (2011), it can be concluded that the range in field capacity observed is similar. Site SV10 showed a range of around 0.05 cm^3 cm^{-3} to 0.1 cm^3 cm^{-3} for depths ranging from 10 to 100 cm (Zettl et al., 2011), which is comparable to the measured field capacity values in replication one (Figure 4.3) after 18 hours of drainage across the range of treatments studied in the columns at similar depths to Zettl et al. (2011) of 15 to 80 cm.

In replication two (Figure 4.5) the measured field capacity values after 18 hours were slightly higher than the reported ranges for SV10 but this replication was packed to a slightly higher bulk density then the columns in replication one. The range in field capacity for replication two is still comparable to the other sites studied by Zettl et al. (2011). These include SV62 which reported a range in field capacity of around 0.09 cm^3 cm^{-3} to 0.23 cm^3 cm^{-3} and SV60 which had a range of around 0.08 cm^3 cm^{-3} to 0.32 cm^3 cm^{-3} at depths of 10 to 100 cm.

4.5.2 Phase II: Artificial Rainfall and Enhanced Field Capacity Scenario

The field capacity at all depths within the columns after 48 hours of drainage, and prior to 'rainfall' applications, are shown in Table 4.8 and 4.9 for replications one and two, respectively. The values reported in Table 4.8 and 4.9 are both slightly higher and lower than the measured field capacity at 48 hours in Figures 4.4 and 4.6 for replications one and two, respectively. This may attributed to the columns being re-saturated and left until field capacity again before carrying out this part of the experiment.

Table 4.8: Measured Water Content at Field Capacity (48 hours) between the Columns for Replication One Prior to Artificial Rainfall Application

	----------Average Soil Water Content (%)----------					
Column	**15 cm**	**30 cm**	**50 cm**	**80 cm**	**110 cm**	**130 cm**
1	9.90	5.60	6.30	8.30	10.40	31.30
2	10.10	4.60	6.70	8.30	10.10	30.70
3	9.70	6.30	7.10	11.10	12.80	23.40
4	8.10	4.30	6.00	7.90	10.70	25.20
5	9.50	6.40	4.80	9.40	13.90	23.40

Table 4.9: Measured Water Content at Field Capacity (48 hours) between the Columns for Replication Two Prior to Artificial Rainfall Application

	----------Average Soil Water Content (%)----------					
Column	**15 cm**	**30 cm**	**50 cm**	**80 cm**	**110 cm**	**130 cm**
1	15.60	6.80	10.30	11.70	12.60	20.50
2	15.40	7.10	8.70	9.50	9.20	19.20
3	12.00	9.00	9.80	12.30	14.00	24.80
4	7.60	n.d.	7.30	7.50	12.20	13.90
5	11.10	7.00	7.70	10.90	12.50	22.80

Note : n.d. denotes not determined due to analytical error

The resulting water retained for each of the columns at all depths following the 'rainfall events' can be viewed in Figures 4.7 and 4.8 for replicates one and two, respectively. The data obtained can be challenged, given the significant pressure of 20 KPa applied to the column with seemingly little effect, other than natural drainage, on the soil water at the lower depths in the column. Due to the uncertainty relating to the effect of the pressure applied, the data will be considered with more emphasis on reviewing the results as a function of drainage rather than an enhanced field capacity scenario.

Overall, it can be concluded from the observations that the columns with AOSM had higher retention, or reduced drainage rates, over the homogenous column without AOSM. In addition, for the majority of the column depths in replication one, the layered columns with AOSM had higher retention than the homogenous columns with AOSM. This same trend was not evident in replication two throughout the majority of the column depths studied. Although the BC columns with 2% AOSM showed greater moisture retention over the layered columns in replication two at many of the depths, the layered columns appear to be at an advantage in retaining water when compared to a homogenous BC treatment without AOSM in both replications one and two, indicating the advantage of treatment layering.

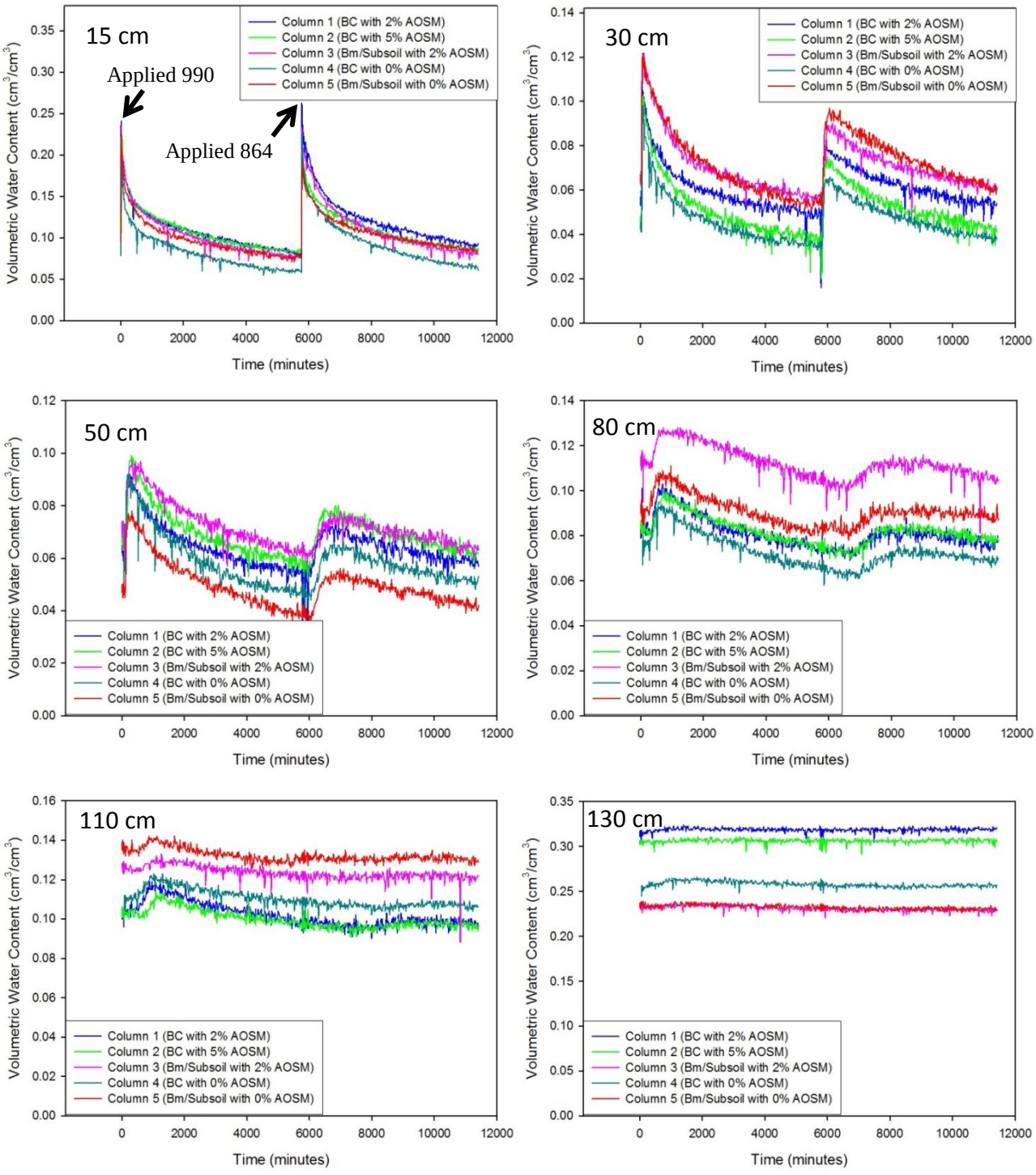

Figure 4.7: Water Content as a Function of Time at all Depths Following Two Rainfall Events in Replication One

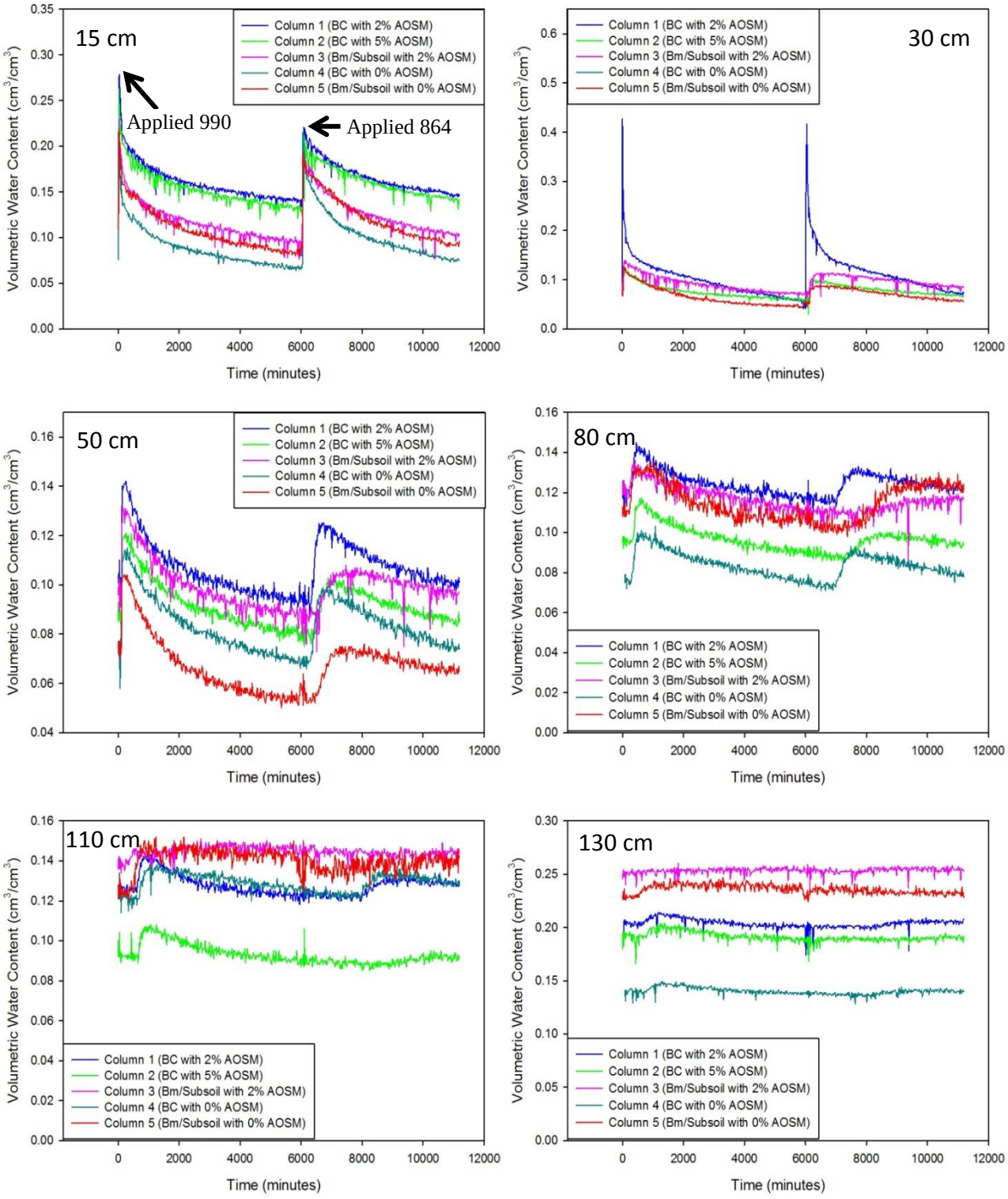

Figure 4.8: Water Content as a Function of Time at all Depths Following Two Rainfall Events in Replication Two

4.5.3 Phase III: Nutrient and Hydrocarbon Leaching Potential

The results for the chloride breakthrough curve as a function of time and cumulative infiltration can be viewed in Figures 4.9 and 4.10 for replications one and two, respectively.

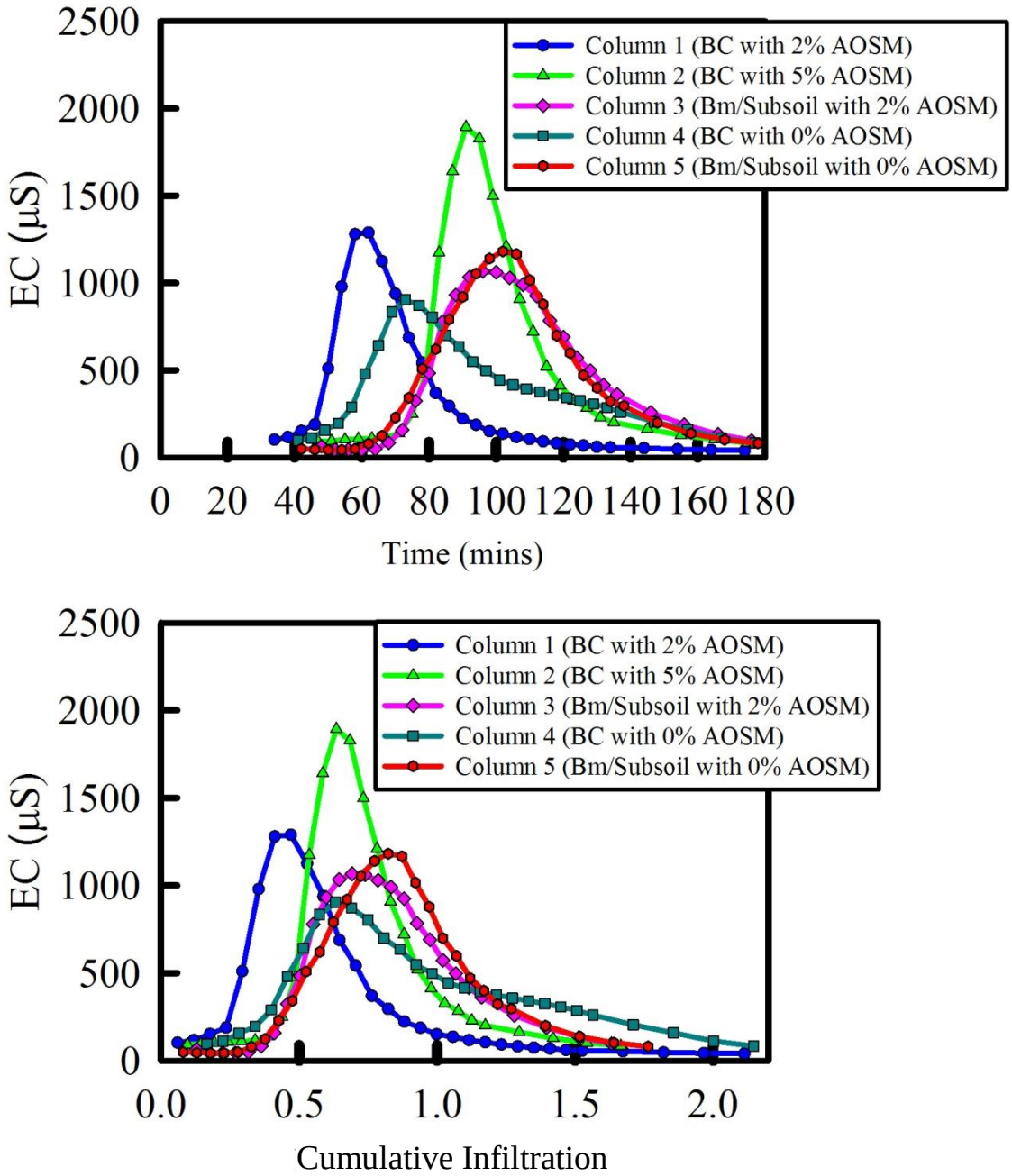

Figure 4.9: Chloride Breakthrough Curve for Replication One as a Function of Time (Top) and Cumulative Infiltration (Bottom)

In reviewing the chloride breakthrough curve versus time for replicate one it can be concluded that the presence of AOSM slows the chloride tracer travel time for the BC column containing 5% AOSM as compared to the BC column containing 0% AOSM. The presence of soil layering delays the chloride tracer travel time as shown by the delayed time for the peak to occur when compared to the homogenous soil treatments. This coincides with previous observations made on the presence of a finer textured layer over a coarser textured layer creating a capillary barrier that restricts percolation (Burgers, 2005). This leads to increased nutrient retention by the soil layers prolonging the concentration of chloride over a longer time period as compared to shorter peak times observed in the homogenous soil treatments.

It is also important to compare the curves for the columns as a function of cumulative infiltration given the variation in pore volume influencing transport rates. The same trend was observed with the presence of soil layering showing a delayed chloride peak over the homogenous soil treatments. A delayed chloride peak is still evident with the BC column containing 5% AOSM over the BC column with 0% AOSM but the difference is minimal under cumulative infiltration conditions.

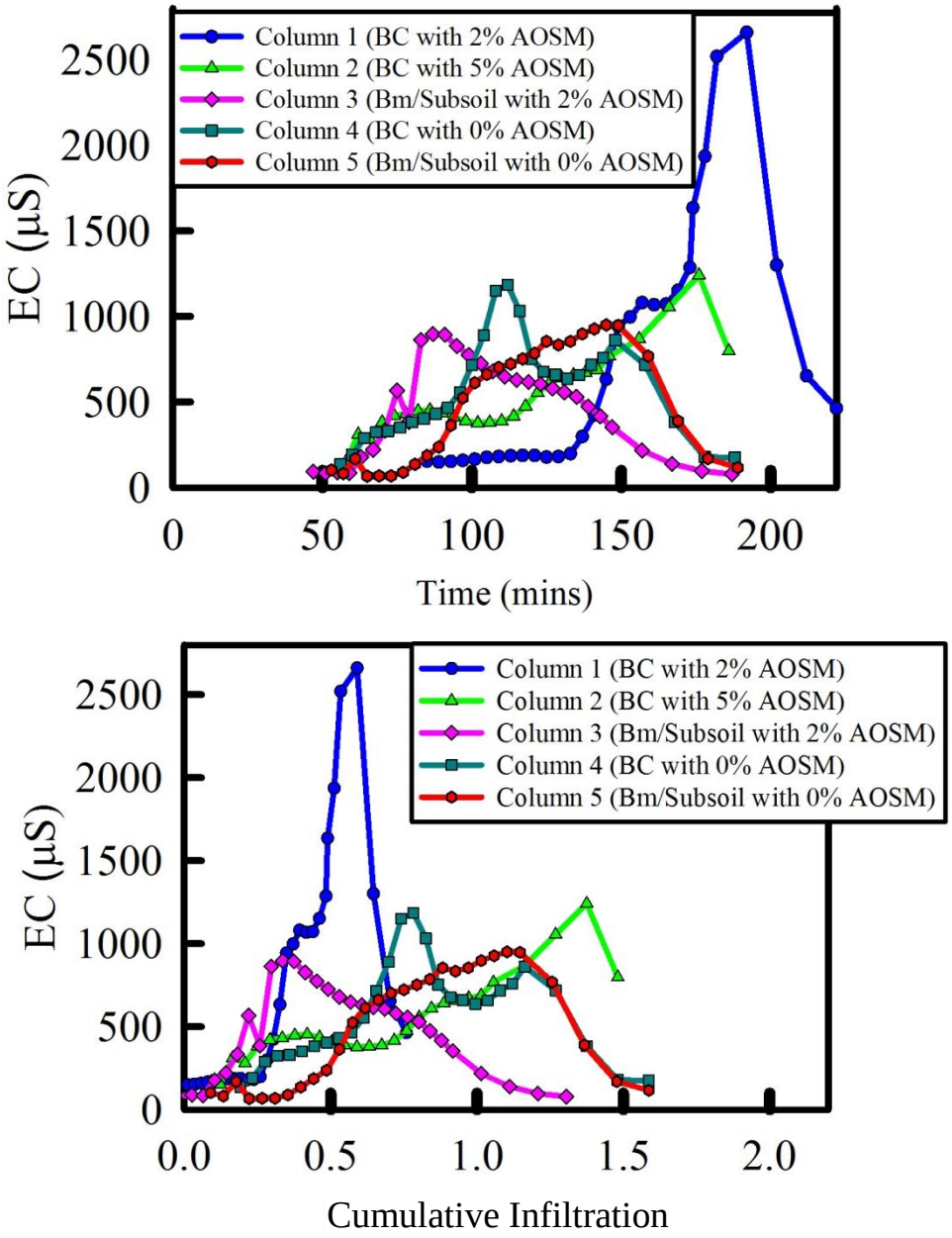

Figure 4.10: Chloride Breakthrough Curve for Replication Two as a Function of Time (Top) and Cumulative Infiltration (Bottom)

In comparison, the chloride breakthrough curve for replicate two (Figure 4.10) indicates that the implementation of 5% AOSM slows the chloride tracer peak under both time and cumulative infiltration when compared to homogenous and layered columns. As observed for replicate one, the presence of soil layers with 0% AOSM prolongs the BTC when compared to

the homogenous column with 0% AOSM. Although observations were made on the BTC for replicate two, concerns were raised on the accuracy of the data collected given the lack of clearly developed curves for each of the columns.

Hydrocarbon concentrations present in the column outflow solution (Table 4.10) indicate the potential for hydrocarbon leaching from the AOSM material contained within the reclamation prescriptions.

Table 4.10: Hydrocarbon Concentrations Present in the Outflow Solution

Column	Material	Replication	F2 (ppm)	F3 (ppm)	F4 (ppm)
1	LFH	1	0.6445	2.4826	0.3869
	BC (2% AOSM)	2	0.0087	6.5066	0.1871
2	LFH	1	0.0000	2.7335	0.0000
	BC (5% AOSM)	2	0.9327	5.8494	1.0651
3	LFH	1	0.8086	1.2851	0.3948
	Bm (2% AOSM)	2	0.6537	0.9379	0.5189
	Subsoil (2% AOSM)				
4	LFH	1	0.4438	1.4993	0.0266
	BC (0% AOSM)	2	0.5835	n.d.	0.5340
5	LFH	1	0.0000	2.6163	0.0000
	Bm (0% AOSM)	2	0.0000	1.0405	0.4488
	Subsoil (0% AOSM)				

Note : n.d. denotes not determined due to analytical error

The data obtained indicates that the outflow solution is dominated by F3 hydrocarbons. This is comparable to results of Fleming et al. (2012) in which the F1 and F2 fractions, or light hydrocarbons, represent less of the total AOSM hydrocarbons and the heavy hydrocarbons, consisting of F3 and F4 fractions dominate. The greater amount of F3 hydrocarbon fractions

indicates inhibition of weathering and degradation processes (Fleming et al., 2012) of the AOSM material studied that convert the heavier hydrocarbon fractions into lighter compounds.

Based on the Canada-Wide Standards (CWS) for Petroleum Hydrocarbons (PHC) in Soil published by CCME in 2001a which is illustrated in Table 4.11, all the fractions fall below the critical levels of concern identified, although CCME (2001a) indicates that the levels without parentheses do not include consideration of the soil-to-groundwater contamination pathway and levels within the parentheses do include protection of groundwater.

Table 4.11: Summary of Tier 1 Levels for Surface Soil by the Canadian Council of Ministers of the Environment

Land Use	Soil Texture	Fraction 1 (mg/kg)	Fraction 2 (mg/kg)	Fraction 3 (mg/kg)	Fraction 4 (mg/kg)
Agricultural	Coarse-grained soil	30[b]	150	300	2800
	Fine-grained soil	210 (170[a])	150	1300	5600
Residential/ Parkland	Coarse-grained soil	30[b]	150	300	2800
	Fine-grained soil	210 (170[a])	150	1300	5600
Commercial	Coarse-grained soil	320 (240[a])	260	1700	3300
	Fine-grained soil	320 (170[a])	260 (230[a])	2500	6600
Industrial	Coarse-grained soil	320 (240[a])	260	1700	3300
	Fine-grained soil	320 (170[a])	260 (230[a])	2500	6600

Overall, the hydrocarbon content observed in the outflow solution in this study does not appear to create concern for contamination as a result of the low levels of hydrocarbon fractions observed. This agrees with Fleming at al. (2012) in regards to results from column leachate studies in which the F1 hydrocarbons were not detected in the water while low concentrations of F2 and F3 hydrocarbons were detected. Fleming at al. (2012) further indicate that the F2 fractions were detected at concentrations of less than half of the clean water guidelines of 1.1 mg/L for the Province of Alberta and the F3 fractions, which were detected at concentrations

greater than the F2 hydrocarbons, are not regulated in groundwater. Although the F2 column leachate shows to be higher than half of the clean water guidelines of 1.1 mg/L for a few of the columns (Table 4.10), it still falls below the clean water guidelines identified. Fleming et al. (2012) concluded that the use of AOSM soil for reclamation would be expected to produce minimal environmental impact, based on the soil column leaching of hydrocarbons, to surface or groundwater. Hunter (2011) also supports the recommendation made by Fleming et al. (2012) in regards to implementing AOSM materials in reclamation covers.

4.6 Conclusion

In determining the capability of each reclamation treatment to increase soil water storage and reduce infiltration rates, each of the materials characteristics must be compared. Under steady state and transient conditions, the presence of AOSM appears to slow the rate of infiltration, with the higher concentrations of AOSM having a greater impact on slowing the rate further. The integration of soil layers over homogenous soils further slows the rate of infiltration. The integration of AOSM and layering shows the greatest potential in reducing infiltration rates over columns with layering and no AOSM under unsaturated conditions. Although the addition of layers reduces the infiltration rate, it may be offset by increasing the bulk density of a homogenous soil with AOSM. In the field it will be difficult to maintain packing bulk densities and thus soil layers with higher percentages of AOSM are expected to be the most beneficial in reducing infiltration rates and increasing water content. Similar trends were evident when reviewing the volume of water collected from saturation to field capacity, as well as following artificial rainfall simulations, further indicating the advantage of high AOSM concentrations and a soil layering design.

In addition to reduced infiltration rates, the presence of higher concentrations of AOSM delays the chloride tracer peak over the homogenous soil treatments with no AOSM present. The implementation of soil layers also shows a delayed chloride peak over the homogenous soil treatments, thereby increasing the nutrient retention time. Any concerns relating to hydrocarbon leaching from implementation of the AOSM are reduced given the low concentrations of hydrocarbon fractions observed in the outflow solution.

Under field capacity conditions, there is no clear indication that hydrocarbon inclusions increase the water stored at field capacity. This can potentially be correlated to the coarse nature of the AOSM material implemented within the column study which does not contain an increased silt and clay fraction over the other materials studied.

Under saturated conditions, although the presence of AOSM appears to increase the rate of water movement downward through the profile, these differences were minimal. The potential for slightly increased flux rates present under saturated conditions may be attributed to the potential formation of macropore channels around the AOSM. Another possibility includes that under saturated conditions, the AOSM are no longer water repellent and therefore cannot inhibit water movement through hydrophobic interactions between the water and AOSM material. The increased flux scenario for the columns containing AOSM under saturated conditions was not as clear in the columns containing layering schemes. Therefore, it is thought that although the AOSM may increase the flux under saturated conditions, its implementation within soil layers may offset the increased flux rates observed.

In conclusion, it is very important to identify the moisture status of the soil as AOSM may act differently depending on whether the soil is under saturated or unsaturated conditions. The potential for AOSM to act as a barrier to the downward flow of water, reducing infiltration

rates, in a soil profile is evident under unsaturated infiltration conditions. The ability of the AOSM to reduce water infiltration rates is further increased by the addition of greater percentages of AOSM and a soil layer. Although greater percentages of AOSM have the ability to increase flux under saturated conditions, it is unlikely that under natural field conditions this scenario will occur.

5. SYNTHESIS AND CONCLUSIONS

The largest oil sand deposits in the world are found in northern Alberta and Canada retains the only large-scale commercial oil sands industry. The bitumen contained within the oil sands is mined utilizing strip mining or open pit mining techniques leading to significant land destruction. The destruction involves removing the natural vegetation present, as well as disturbing and extracting the soil material from functioning ecosystems. The sand and other byproduct material, resulting from bitumen extraction, are returned to the mining site which is eventually reclaimed. Among the byproduct material from the bitumen extraction process, the uneconomical material to process from the bitumen oil remains in the form of oil embedded into sediments, known as aggregate oil sand material (AOSM) or hydrocarbon-affected material.

The Aurora Soil Capping study located in northern Alberta is a current multi-company effort led by Syncrude Canada Limited which was constructed to evaluate reclamation practices on lean oil sands dumps. The study focuses on utilizing available salvaged coarse textured reclamation soil, some of which contain residual bitumen in the form of AOSM, while evaluating varying soil capping depths and configurations in an attempt to increase the materials ability to store water and nutrients. Limited research into the impacts of AOSM material on soil water and nutrient dynamics within a soil ecosystem, raises key questions as to the impact this material will have on transport and retention processes, along with potential contamination from hydrocarbon leaching.

Although the Aurora Soil Capping project focuses on integrating various soil capping depths, configurations and reclamation materials on a larger scale, the individual materials must be characterized to assist in identifying the extent of water storage limitations and hydrophobicity issues. Further studies into the effect of material layering and varying

percentages of hydrocarbon material will indicate whether the presence of disturbed, naturally occurring aggregate oil sand material (AOSM) within a reconstructed reclamation soil profile will further impact nutrient and soil water dynamics. The specific objectives of this study included:

1.) Evaluating soil water retention, saturated hydraulic conductivity and water repellency of reclamation materials

2.) Determining the effect of hydrocarbons in the form of AOSM, and soil layering, on soil water retention, saturated hydraulic conductivity and water repellency

3.) Assessing transit times associated with leaching potential of nutrients and hydrocarbons in coarse textured, hydrocarbon affected soils

In order to meet these objectives, a series of laboratory studies were conducted on four soils; the upper organic LFH layer (0-15 cm), Bm (15-50 cm), BC (50-100 cm) and subsoil material (100-150 cm), while varying the amount of AOSM and implementing layering schemes. The studies included material characterization through organic carbon and particle size analysis as well as hydrophobicity studies on the AOSM and reclamation soil material through contact angle analysis and the water droplet penetration time (WDPT) test. Water retention studies were performed utilizing a tension table and pressure plates, along with columns equipped with Time Domain Reflectometry (TDR) probes to measure water content. Hydraulic conductivity was also measured through constant head methods on varying sample sizes. Lastly, to address hydrocarbon leaching concerns, chloride tracer studies were performed which allowed Breakthrough Curves (BTC) to be developed. The outflow solution was further analyzed using Gas Chromatography (GC) with FID (Flame Ionisation Detection) to detect the hydrocarbon type and concentration leached through the columns.

Through laboratory studies on material characteristics it is concluded that of the mineral reclamation materials studied, the subsoil appears to provide the best possibility for reclamation success. The subsoil has higher retained moisture levels, slower flux rates and lowest hydraulic conductivity, thereby increasing soil water storage for plant use. The ability of the subsoil material to exhibit these characteristics may be attributed to the greater susceptibility of the coarse material to water repellency due to smaller specific particle surface area and therefore reduced organic matter, or hydrocarbon material, required to coat the surface. The increased moisture may also potentially be attributed to the presence of a greater fine sand fraction within the subsoil material.

It should be noted that although water repellency exhibits the ability to restrict infiltration, and therefore increases water content, it also has the potential to cause reduced moisture storage. This is due to the residual hydrocarbons coating the soil particles as observed when comparing the BC material with hydrocarbons removed and the BC material with 0% AOSM in terms of water retention. It is anticipated that typically it has minimal occurrence and can only be detected when compared to a material where all hydrocarbons have been removed; as this trend of water repellency was not observed during water repellency studies on the BC reclamation material with 0% AOSM.

Results from water retention and hydraulic conductivity studies indicated that although the AOSM was hydrophobic with strong to very severe water repellency, its placement at varying concentrations and forms did not create consistent significant differences in the amount of moisture retained or transported. This indicates that the hydrocarbon material has minimal impacts on moisture storage. The absence of increasing moisture storage from AOSM

integration may potentially be correlated to the coarse nature of the AOSM material which does not contain an increased silt and clay fraction over the other materials studied.

Results from the large scale column studies showed that under steady state and transient conditions AOSM could result in decreased infiltration rates. The presence of higher concentrations of AOSM had a greater impact on slowing the infiltration rate and chloride tracer peak further. Additionally, the presence of soil layering slowed the infiltration rate when compared to homogenous columns without AOSM. When AOSM were implemented into the columns with soil layering schemes the infiltration rate was further reduced. Soil layering also delayed the chloride peak, thereby increasing nutrient retention time, as compared to the homogenous soil treatments.

Under saturated conditions the presence of higher concentrations of AOSM appeared to increase the rate of water movement. These differences were minimal and were not observed in the columns containing layering schemes.

Overall, it can be concluded that with appropriate material placement, the addition of layering schemes and hydrocarbon material, the potential exists to increase soil water content in the upper layers of the soil, thereby increasing soil water storage for plant use. Although concerns are raised on contamination from hydrocarbon leaching from AOSM integration into reclamation designs, low levels of hydrocarbon fractions were observed in the outflow solution. Therefore, given that the LFH and subsoil retained the highest moisture levels, slower fluxes and had the highest site gravimetric moisture contents for all the treatments studied, it is anticipated that a reclamation design with these soils, layering schemes and higher concentrations of AOSM would provide the best potential for increasing moisture content for revegetation success.

Caution should be used when extrapolating results of controlled laboratory studies to the field. Previous field studies indicate that although sites surveyed at the Athabasca oil sands exhibit highly similar soil textures, the natural occurrence of the coarse textured soil and highly variable moisture regimes are present. This indicates the importance of identifying the mechanisms governing soil water and nutrient dynamics in the field as the material has the capability of exhibiting varying results depending on the moisture status of the soil, along with AOSM placement within the reclamation profile.

Further studies are also required on AOSM behavior as it may act differently depending on whether the soil is under saturated or unsaturated conditions. In addition, although observations were made on the potential to increase soil water content with AOSM integration into reclamation designs, there was a lack of statistically significant differences attributed to inherently large variability associated with the hydrocarbons in the solid form.

6. LITERATURE CITED

Ali, M.H. 2010. 4.4.5.3 Moisture determination at high tension. *In* Fundamentals of irrigation and on-farm water management volume 1. New York, NY: Springer Science + Business Media, LLC.

Ancheyta, J. and J. G. Speight. 2007. 2.2.3 Density and specific Gravity. p. 19. *In* hydroprocessing of heavy oils and residua. CRC Press, Boca Raton, FL.

Aubertin, M., Cifuentes, E., Apithy, S.A., Bussière, B., Molson, J. and R.P. Chapuis. 2009. Analyses of water diversion along inclined covers with capillary barrier effects. Can. Geotech. J. 46(10):1146–1164.

Beckingham, J.D., Nielsen, D.G. and V.A. Futoransky. 1996. Field guide to ecosites of the mid-boreal ecoregions of Saskatchewan. UBC Press, Vancouver, BC.

Bonczek, J. 2007. Characterizing soil water [online]. Available at: http://soillab.ifas.ufl.edu/SOS%203022/Lectures%20pdf/Lecture%2011%20Characterizing%20Water.pdf (cited 3 Nov 2013).

Bossert, I. and R. Bartha. 1984. Chapter 10 The fate of petroleum in soil ecosystems. p. 435–473. *In* R.M. Atlas (ed.) Petroleum microbiology. Macmillan Publishing Company, New York, NY.

Bouma, J. 2008. Water movement. p. 822–824. *In* W. Chesworth (ed.) Encyclopedia of soil science. Springer, New York, NY.

British Columbia Ministry of Forests (BCMOF) Research Branch. 1998. Soil moisture regime classes and characteristics [online]. Available at: http://www.for.gov.bc.ca/hre/forprod/fordyn/projects/referenc/moisture.htm (cited 19 Feb 2015).

Brouwer, C., Goffeau, A., and M. Heibloem. 1985. Chapter 2 Soil and water. p. 31–52. *In* C. Brouwer et al. (ed.) Irrigation water management: Training manual no. 1 – Introduction to irrigation. Food and Agriculture Organization of the United Nations, Rome, Italy.

Burgers, T.D. 2005. Reclamation of an oil sand tailings storage facility: Vegetation and soil interactions. University of Alberta (Canada). ProQuest Dissertations and Theses, 134 p. http://search.proquest.com/docview/89118148?accountid=14739

Canadian Council of Ministers of the Environment (CCME). 2001a. Canada-wide standards for petroleum hydrocarbons (PHC) in soil. Canadian Council of Ministers of the Environment, Inc., Winnipeg, MB.

Canadian Council of Ministers of the Environment (CCME). 2001b. Reference method for the Canada-wide standard for petroleum hydrocarbons in soil - Tier 1 method, Publ. 1310. Canadian Council of Ministers of the Environment, Inc., Winnipeg, MB.

Chaikowsky, C.L.A. 2003. Soil moisture regime and salinity on a tailings sand storage facility. University of Alberta (Canada). ProQuest Dissertations and Theses, 135 p. http://search.proquest.com/docview/305261949?accountid=14739

Colwell, R. R., Mills, A. L., Walker, J. D., Garcia-Tello, P., and V. Campos-P. 1978. Microbial ecology of the Metula spill in the Straits of Magellan. J. Fish. Res. Board Can. 35:573–580.

Coughlan, K.J, Loch, R.J., and W.E. Fox. 1978. Binary packing theory and the physical properties of aggregates. Aust. J. Soil Res. 16(3):283–289.

Dane, J.H. and J.W. Hopmans. 2002a. 3.3.2.4 Pressure plate extractor. p. 688–690. In J.H. Dane and G.C. Topp (ed.) Methods of soil analysis part 4 physical methods. Soil Science Society of America, Inc., Madison, WI.

Dane, J.H. and J.W. Hopmans. 2002b. 3.3.2.1 Introduction. p. 675–680. In J.H. Dane and G.C. Topp (ed.) Methods of soil analysis part 4 physical methods. Soil Science Society of America, Inc., Madison, WI.

Decagon Devices, Inc. 2013. Pressure plates [online]. Available at: http://www.decagon.com/education/water-potential/measuring-water-potential/laboratory-instruments-for-measuring-water-potential/pressure-plates/ (cited 3 Nov 2013).

Dekker, L.W. and P.D. Jungerius. 1990. Water repellency in the dunes with special reference to the Netherlands. Catena 18:173–183.

Doerr, S.H. 1998. Short communication on standardizing the 'water drop penetration time' and the 'molarity of an ethanol droplet' techniques to classify soil hydrophobicity: A case study using medium textured soils. Earth Surf. Process. Landforms 23:663–668.

Doerr, S.H., Shakesby, S.H., and R.P.D. Walsh. 2000. Soil water repellency: Its causes, characteristics and hydro-geomorphological significance. Earth-Sci. Rev. 51:33–65.

Dyck, M.F., Kachanoski, R. G., and E. de Jong. 2003. Long-term movement of a chloride tracer under transient, semi-arid conditions. Soil Sci. Soc. Am. J. 67:471–477.

Fleming, M., Fleming, I., Headley, J., Jinglong, D. and K. Peru. 2012. Surficial bitumen in the Athabasca oil sands region, Alberta, Canada. Int. J. Mini. Reclamat. Environ. 26(2):134–147.

Fredlund, D.G. and A. Xing. 1994. Equations for the soil-water characteristic curve. Can. Geotech. J. 31(3):521–532.

Gosselin, P., Hrudey, S.E., Naeth, M.A., Plourde, A., Therrien, R., Van Der Kraak, G., and Z. Xu. 2010. The royal society of Canada expert panel: Environmental and health impacts of Canada's oil sands industry [online]. Available at: https://rsc-src.ca/sites/default/files/pdf/RSC%20Oil%20Sands%20Panel%20Main%20Report%20Oct%202012.pdf (cited 3 May 2012).

Government of Canada Climate Data. 2014. Accessing the data [online]. Available at: http://climate.weather.gc.ca/ (cited 5 Jan 2015).

Gureghian, A.B., Ward, D.S., and R.W. Cleary. 1979. Simultaneous transport of water and reacting solutes through multilayered soils under transient unsaturated flow conditions. J. Hydrol. 41:253–278.

Hillel, D. 1998. Environmental soil physics. Academic Press, San Diego, CA.

Horvath, S. (ed.). 2009. Oil and grease in water - Direct hexane extraction British Columbia environmental laboratory manual. Water and Air Monitoring and Reporting, Environmental Quality Branch, Ministry of Environment, Victoria, BC, Canada.

Huang, M., Barbour, S.L. Elshorbagy, A., Zettl., J.D., and B.C. Si. 2011. Infiltration and drainage processes in multi-layered coarse soils. Can. J. Soil Sci. 91:169–183.

Huang, M., Spies, J., Barbour, S.L., Si, B.C. and J. Zettl. 2013. Impact of textural layering on water retention within drained sand profiles. Soil Sci. 178(9):496–504.

Hunter, A. 2011. Investigation of water repellency and critical water content in undisturbed and reclaimed soils from the Athabasca Oil Sands Region of Alberta, Canada. (Master's thesis). Retrieved from University of Saskatchewan College of Graduate Studies Research. (URN etd-07072011-112233).

Itah, A.Y., and J.P. Essien. 2005. Growth profile and hydrocarbonoclastic potential of microorganisms isolated from tarballs in the Bight of Bonny, Nigeria. World J. Microbiol. Biotechn. 21:1317–1322.

Javaux, M. and M. Vanclooster. 2004. In situ long-term chloride transport through a layered, nonsaturated subsoil. 2. Effect of layering on solute transport processes. Vadose Zone J. 3(4):1331–1339.

Jensen, T. 2008. Nitrogen fertilizer, forms and methods of application [online]. Available at: http://www1.agric.gov.ab.ca/$department/deptdocs.nsf/all/ind10750 (cited 30 Dec 2013).

Johnson, D.W. and D.W. Cole. 1979. Anion mobility in soils: Relevance to nutrient transport from forest ecosystems. Environ Int. 3:79–90.

Jones, A.J. 1995. NF95-243 Soil compaction tips [online]. Available at: http://digitalcommons.unl.edu/extensionhist/1116/ (cited 5 Jan 2015).

King, P.M. 1981. Comparison of methods for measuring severity of water repellence of sandy soils and assessment of some factors that affect its measurement. Aust. J. Soil Res. 19:275–285.

Kramer, P.J. 1944. Soil moisture in relation to plant growth. The Botanical Rev. 10(9):525–559.

Leeper, G.W. and N.C. Uren. 1993. Soil science: An introduction. Melbourne University Press, Carlton, AU.

Letey, J., Carrillo, M.L.K., and X.P. Pang. 2000. Approaches to characterize the degree of water repellency. J. Hydrol. 231–232 (2000):61–65.

Lewis, J. and J. Sjöstrom. 2010. Optimizing the experimental design of unsaturated soil columns. In: Proceedings of the 19th World Congress of Soil Science “Soil Solutions for a Changing World”. Brisbane (Australia) 1–6 August 2010:51–54.

McCauley, A. and C. Jones. 2005. Soil & water management module 4 Water and solute transport in soils [online]. Available at: http://landresources.montana.edu/SWM/PDF/final_SW4_proof_11_18_05.pdf (cited 7 June 2012).

McMillan, R., Quideau, S.A., MacKenzie, M.D., and O. Biryukova. 2007. Nitrogen mineralization and microbial activity in oil sands reclaimed boreal forest soils. J. Environ. Qual. 36(5):1470–1478.

Miller, W. 2010. 10Lecture13WaterPotentialMeasurement [online]. Available at: http://www.learningace.com/doc/2292681/097f1cf84822dfe84ed1a3be7195fcfd/10lecture13waterpotentialmeasurement (cited 15 March 2013).

Mori, Y. and N. Higashi. 2009. Controlling solute transport processes in soils by using dual-porosity characteristics of natural soils. Colloids and Surfaces A: Physiochem. Eng. Aspects 347:121–127.

Murthy, V.N.S. 2003. 3.4 Comments on soil phase relationships. p. 25. *In* Geotechnical engineering principles and practices of soil mechanics and foundation engineering. Marcel Dekker, Inc., New York. NY.

Newman, D. 2002. Laboratory 3 hydraulic conductivity of a porous media [online]. Available at: www.eng.mu.edu/newmand/CEEN3160-F10-Lab3-HydCond.pdf (cited 27 Sept 2015).

NRCS East National Technology Support Center, NRCS National Soil Survey Center, ARS National Laboratory for Agriculture and the Environment, NCERA, University of Illinois and Department of Natural Resources and Environmental Sciences. 2011. Total organic carbon. Available at: http://soilquality.org/indicators/total_organic_carbon.html (cited 2 Jan 2013).

Oliviera, I.B., Demond, A.H. and A. Salehzadeh. 1996. Packing of sands for the production of homogeneous porous media. Soil Sci Soc Am J. 60 (1):49–53.

Ontario Ministry of the Environment. 2001. Protocol for analytical methods used in the assessment of properties under part XV.1 of the environmental protection act. Laboratory services branch ministry of the environment [online]. Available at: http://www.ene.gov.on.ca/stdprodconsume/groups/lr/@ene/@resources/documents/resource/stdprod_086546.pdf (cited 11 Nov 2013).

Paragon Soil and Environmental Consulting Inc. 2006. Hydrocarbons in natural oil sands soils: Field survey. Cumulative Environmental Management Association. Fort McMurray, AB.

Pennock, D., van Kessel, C. and M. Corre. 1995. Impact of agriculture and forestry on landscape-scale soil organic carbon storage in Saskatchewan. Soils and Crops Workshop Proceedings (1995). Extension Division, University of Saskatchewan, Saskatoon, SK.

Plummer, M.A., Hull, L.C. and D.T. Fox. 2004. Transport of carbon-14 in a large unsaturated soil column. Vadose Zone J. 3(1):109–121.

Pluske, W., Murphy, D., and J. Sheppard. 2014. Total organic carbon [online]. Available at: http://www.soilquality.org.au/factsheets/organic-carbon (cited 29 Dec. 2014).

Portage County Government. 2008. Soil & aquifer properties and their effect on groundwater [online]. Available at: http://www.co.portage.wi.us/groundwater/undrstnd/soil.htm (cited 30 Mar. 2012).

Reynolds, W.D. and D.E. Elrick. 2002. 3.4.2.2 Constant head soil core (tank) method. p. 804–808. In J.H. Dane and G.C. Topp (ed.) Methods of soil analysis part 4 physical methods. Soil Science Society of America, Inc., Madison, WI.

Reynolds, W.D., Elrick, D.E., Youngs, E.G., Booltink, H.W.G. and J. Bouma. 2002. 3.4.2 Laboratory methods. p. 802–804. In J.H. Dane and G.C. Topp (ed.) Methods of soil analysis part 4 physical methods. Soil Science Society of America, Inc., Madison, WI.

Ritter, M. E. 2009. The physical environment: An introduction to physical geography [online]. Available at: http://www4.uwsp.edu/geo/faculty/ritter/geog101/textbook/soil_systems/soil_development_soil_properties.html (cited 19 Apr. 2012).

Roberts, F.J. and B.A. Carbon. 1972. Water repellence in sandy soils of South-Western Australia. II. Some chemical characteristics of the hydrophobic skins. Aust. J. Soil Res. 10(1):35–42.

Robichaud, P. R., Lewis, S. A., and L.E. Ashmun. 2008. New procedure for sampling infiltration to assess post-fire soil water repellency Res. Note. RMRS-RN-33. United States Department of Agriculture, Forest Service, Rocky Mountain Research Station, Fort Collins, CO.

Romano, N., Hopmans, J.W. and J.H. Dane. 2002. 3.3.2.6 Suction table. p. 692–698. In J.H. Dane and G.C. Topp (ed.) Methods of soil analysis part 4 physical methods. Soil Science Society of America, Inc., Madison, WI.

Rowland, S.M., Prescott, C.E., Grayston, S.J., Quideau, S.A. and G.E. Bradfield. 2009. Recreating a functioning forest soil in reclaimed oil sands in northern Alberta: An approach for measuring success in ecological restoration. J. Environ. Qual. 38:1580–1590.

Scott, H.D. 2000. Soil physics Agricultural and environmental applications. Iowa State University Press, Ames, IA.

Sheoran, V., Sheoran, A.S. and P. Poonia. 2010. Soil reclamation of abandoned mine land by revegetation: A review. Int. J. Soil Sediment Water 3(2):1–20.

Si, B., Dyck, M. and G. Parkin. 2011. Flow and transport in layered soils. Can. J. Soil Sci. 91(2):127–132.

Skaggs, T.H., Wilson, G.V., Shouse, P.J. and F.J. Leij. 2002. 6.4 Solute transport: Experimental methods. p. 1381–1403. In J.H. Dane and G.C. Topp (ed.) Methods of soil analysis part 4 physical methods. Soil Science Society of America, Inc., Madison, WI.

Soil Classification Working Group. 1998. The Canadian system of soil classification (3rd ed). Agriculture and Agri-Food Canada, Publ. 1646 (revised). NRC Research Press, Ottawa, ON.

Soilmoisture Equipment Corp. 2008. FAQ: What are the procedures for saturating porous ceramic plates and soil samples? [online]. Available at: http://www.soilmoisture.com/FAQSaturateceramics.html (cited 3 Nov 2013).

Soilmoisture Equipment Corp. 2009. 1500F1 Operating instructions [online]. Available at: http://www.soilmoisture.com/PDF%20Files/81500.pdf (cited 3 Nov 2013).

Speight, J.G. 2000. 2.3 Density and specific gravity. p. 55. *In* The Desulfurization of heavy oils and residua. Marcel and Dekker, Inc, New York, NY.

Speight, J. 2005. Table 5.2 Solubilities of inorganic compounds and metal salts of organic acids in water at various temperatures. p. 5.17. In J.A. Dean (ed.) Lange's handbook of chemistry (15th ed.). McGraw-Hill Inc., Toronto, ON.

Speight, J.G. 2010.Table 3.3 Comparison of tar sand bitumen (Athabasca) and crude oil properties. p. 73. *In* The chemistry and technology of petroleum (5th ed.). Taylor and Francis Group, Boca Raton, FL.

Stalder, A.F., Melchior, T., Müller, M., Sage, D., Blu, T., and M. Unser. 2010. Low-bond axisymmetric drop shape analysis for surface tension and contact angle measurements of sessile drops. Colloids and Surfaces A: Physiochem. Eng. Aspects 364(1):72–81.

Stefano, C. D., Ferro, V., and S. Mirabile. 2010. Comparison between grain-size analyses using laser diffraction and sedimentation methods. Biosyst. Eng. 106:205–215.

Strong, W.L. and K.R. Leggat. 1981. Ecoregions of Alberta. Alberta Energy and Natural Resources Resource Information Services, Edmonton, AB.

Topp, G.C., Davis, J.L. and A.P. Annan. 1980. Electromagnetic determination of soil water content: Measurements in coaxial transmission lines. Water Resour. Res. 16(3):574–582.

UNEP. 2012. Chapter 12 Electrical conductivity [online]. Available at: http://www.rrcap.unep.org/male/manual/national/12Chapter12.pdf (cited 27 Mar. 2012).

University of Delaware Department of Chemistry and Biochemistry. n.d. Glassware care & cleaning [online]. Available at: http://www.udel.edu/chem/GlassShop/GlasswareCare.htm (cited 11 Nov 2013).

University of Nebraska-Lincoln. 2013. Plant & soil sciences eLibraryPRO soils - Part 6: Phosphorus and potassium in the soil: Losses of soil potassium [online]. Available at: http://passel.unl.edu/pages/informationmodule.php?idinformationmodule=1130447043&topicorder=13&maxto=15&minto=1 (cited 30 Dec 2013).

USDA. n.d. Soil quality indicators Bulk density. Available at: http://www.nrcs.usda.gov/wps/PA_NRCSConsumption/download?cid=nrcs142p2_051591&ext=pdf (cited 1 April 2014).

U.S. Department of the Interior, Bureau of Land Management (BLM). 2012. About tar sands [online]. Available at: http://ostseis.anl.gov/guide/tarsands/index.cfm (cited 26 April 2012).

Veihmeyer, F.J. and A.H. Hendrickson. 1950. Soil moisture in relation to plant growth. p. 285–304. *In* D.I. Arnon and L. Machlis (ed.) Annual review of plant physiology volume 1. Annual Reviews, Inc., Stanford, CA.

Wang, D. and D.W. Anderson. 1998. Direct measurement of organic carbon content in soils by Leco CR-12 carbon analyzer. Commun. Soil Sci. Plant Anal. 29(1&2):15–21.

White, P.J. and M.R. Broadley. 2001. Chloride in soils and its uptake and movement within the plant: A review. Ann. Bot. 88(6):967-988.

Yang, H., Rahardjo, H., Leong, E., and D.G. Fredlund. 2004. Factors affecting drying and wetting soil-water characteristic curves of sandy soils. Can. Geotech. J. 41(5):908–920.

Yarmuch, M. n.d. Reclamation challenges for Syncrude Canada Ltd. at the Aurora North mine and the Aurora soil capping study [PowerPoint slides]. Available at: http://www.albertaagrologists.ca/files/Presentation_8DEC2011.pdf (cited 8 May 2012).

Yarmuch, M. S. 2003. Measurement of soil physical parameters to evaluate soil structure quality in reclaimed oil sands soils, Alberta, Canada. University of Alberta (Canada). ProQuest Dissertations and Theses, 134 p. http://search.proquest.com/docview/305255060?accountid=14739

Zettl, J.D., Barbour, S.L., Huang, M., Si, B.C., and L.A. Leskiw. 2011. Influence of textural layering on field capacity of coarse soils. Can. J. Soil Sci. 91:133–147.

APPENDICES

Appendix A

Tabular data: Determining the Soil Moisture Content for the Material
Extracted from the Aurora Capping Study

Table A.0.1: Determining Site Soil Moisture for Each Soil Material

Material	Replication	Tin Weight (g)	Wet Sample+Tin (g)	Wet Weight (g)	Dry Sample+ Tin (g)	Dry Weight (g)	θw	Average θw	Average θw (%)
BC	1	1.23	13.36	12.13	12.98	11.75	0.0323		
	2	1.25	15.25	14	14.8	13.55	0.0332		
	3	1.54	15.42	13.88	14.99	13.45	0.0320	0.0325	3.2507
Bm	1	1.55	12.73	11.18	12.32	10.77	0.0381		
	2	1.23	15.79	14.56	15.25	14.02	0.0385		
	3	1.51	13.51	12	13.1	11.59	0.0354	0.0373	3.7320
Subsoil	1	1.24	16.36	15.12	15.61	14.37	0.0522		
	2	1.24	15.63	14.39	14.95	13.71	0.0496		
	3	1.25	14.12	12.87	13.48	12.23	0.0523	0.0514	5.1374
LFH	1	1.23	11.65	10.42	10.63	9.4	0.1085		
	2	1.19	9.37	8.18	8.84	7.65	0.0693		
	3	1.51	11.18	9.67	10.28	8.77	0.1026	0.0935	9.3471

**Formulas used to calculate data:*

$$\Theta w = \frac{(\text{Mass of Wet Soil + Tin}) - (\text{Mass of Dry Soil+Tin})}{\text{Mass of Dry Soil}}$$

Appendix B

Tabular data: Results Obtained from the LECO C632 Analyzer for Soil Organic Carbon Measurements

Table B.0.1: Soil Organic Carbon Results

Material	Replication	Sample Mass (g)	Organic Carbon Method	Carbon (mg)	Carbon (%)	Carbon Detector	Furnance Temp (^{0}C)	Carbon Low	Average Carbon (%)
BC	1	0.1021	5e19 low organic carbon	0.9572	0.9375	CO_2 Low	840	0.9375	
	2	0.1013	5e19 low organic carbon	0.7145	0.7053	CO_2 Low	839	0.7053	
	3	0.1038	5e19 low organic carbon	0.6369	0.6136	CO_2 Low	840	0.6136	0.7521
Bm	1	0.1097	5e19 low organic carbon	1.461	1.331	CO_2 Low	839	1.331	
	2	0.1082	5e19 low organic carbon	1.725	1.594	CO_2 Low	839	1.594	
	3	0.1054	5e19 low organic carbon	1.446	1.372	CO_2 Low	839	1.372	1.4323
Subsoil	1	0.1053	5e19 low organic carbon	0.7439	0.7065	CO_2 Low	839	0.7065	
	2	0.1087	5e19 low organic carbon	0.4723	0.4345	CO_2 Low	839	0.4345	
	3	0.103	5e19 low organic carbon	0.4925	0.4781	CO_2 Low	839	0.4781	0.5397
LFH	1	0.1021	5e19 low organic carbon	2.149	2.105	CO_2 Low	839	2.105	
	2	0.1063	5e19 low organic carbon	2.181	2.052	CO_2 Low	839	2.052	
	3	0.103	5e19 low organic carbon	2.122	2.06	CO_2 Low	839	2.06	2.0723

Appendix C

Tabular data: Results Obtained from Particle-Size Distribution Analysis for each of the Treatment Soil Types

Table C.0.1: Particle Size Analysis Results

Material	Replication	Sand (%)	Silt (%)	Clay (%)	Total (%)
----------*reclaimed site material*----------					
BC	Sonification-1	90.991	8.122	0.886	99.999
	Sonficication-2	91.766	5.991	0.106	97.863
	Sonification-3	95.333	4.672	0.000	100.005
	No Sonification-1	95.996	4.006	0.000	100.002
	No Sonficication-2	96.217	3.784	0.000	100.001
	No Sonification-3	98.401	1.600	0.000	100.001
Subsoil	Sonification-1	95.908	4.092	0.000	100.000
	Sonficication-2	93.783	6.218	0.000	100.001
	Sonification-3	94.943	5.055	0.000	99.998
	No Sonification-1	98.013	1.992	0.000	100.005
	No Sonficication-2	98.342	1.659	0.000	100.001
	No Sonification-3	96.909	3.092	0.000	100.001
Bm	Sonification-1	88.477	11.406	0.118	100.001
	Sonficication-2	84.015	12.404	0.124	96.543
	Sonification-3	92.962	7.043	0.000	100.005
	No Sonification-1	95.815	4.191	0.000	100.006
	No Sonficication-2	96.619	3.382	0.000	100.001
	No Sonification-3	96.855	3.144	0.000	99.999
LFH	Sonification-1	90.713	9.290	0.000	100.003
	Sonficication-2	93.403	6.599	0.000	100.002
	Sonification-3	92.350	7.651	0.000	100.001
	No Sonification-1	96.263	3.737	0.000	100.000
	No Sonficication-2	96.067	3.936	0.000	100.003
	No Sonification-3	95.559	4.445	0.000	100.004
AOSM (Crushed)	Sonification-1	93.988	6.013	0.000	100.001
	Sonficication-2	95.596	4.407	0.000	100.003
	Sonification-3	95.320	4.682	0.000	100.002
	No Sonification-1	96.623	3.383	0.000	100.006
	No Sonficication-2	97.017	2.985	0.000	100.002
	No Sonification-3	95.506	4.497	0.000	100.003
----------hydrocarbons removed----------					
BC	Sonification-1	98.221	1.782	0.000	100.003
	Sonficication-2	98.020	1.981	0.000	100.001
	Sonification-3	97.738	2.265	0.000	100.003
	No Sonification-1	98.623	1.380	0.000	100.003
	No Sonficication-2	98.173	1.829	0.000	100.002
	No Sonification-3	99.112	0.893	0.000	100.005

Appendix D

Tabular data: Results Obtained from Contact Angle Analysis for BC and AOSM

Table D.0.1: Contact Angle Analysis for the AOSM

Time Interval (seconds)	AOSM-Rep 1 (°)	AOSM-Rep 2 (°)	AOSM-Rep 3 (°)	AOSM-Rep 4 (°)	AOSM-Rep 5 (°)
0	137.129	138.591	142.736	140.017	152.021
6	136.659	138.591	142.561	140.017	152.021
12	136.360	138.591	142.392	140.017	152.021
18	136.360	138.303	140.538	140.017	152.021
24	136.360	138.303	140.654	140.017	152.021
30	136.360	138.303	140.747	140.017	152.021
36	136.360	138.303	140.017	140.017	152.021
42	136.360	138.303	140.017	140.017	152.021
48	136.360	138.303	140.017	140.017	152.021
54	136.055	138.303	140.017	140.017	152.021
60	136.055	138.303	140.017	140.017	152.021
66	136.055	138.303	140.017	140.017	152.021
72	136.055	138.009	140.017	140.017	152.021
78	136.055	138.176	140.017	136.659	152.021
84	136.055	138.009	140.017	136.659	152.021
90	134.644	138.009	140.017	136.659	152.021
96	134.644	138.009	140.017	136.659	152.021
102	134.644	138.009	140.017	136.659	147.582
108	134.317	138.009	140.017	136.659	147.582
114	134.644	138.009	140.097	136.554	147.582
120	134.317	138.009	140.017	136.554	147.582
126	134.317	136.758	140.097	136.554	147.582
132	134.317	136.554	140.017	136.554	147.582
138	134.317	136.554	140.178	136.554	147.582
144	134.317	136.554	140.017	136.554	147.582
150	134.317	136.554	140.017	136.554	147.582
156	134.317	136.554	140.017	136.554	147.582
162	134.317	136.239	140.097	136.554	147.582
168	133.983	136.239	140.017	136.554	147.582
174	133.983	136.239	140.017	136.554	147.582
180	133.983	136.239	140.017	136.554	147.582
186	133.983	136.239	140.097	136.554	149.657
192	133.983	136.239	140.097	136.554	149.657
198	133.983	136.239	136.659	136.554	149.657
204	133.983	135.915	136.554	136.554	149.657
210	133.983	135.915	136.554	136.554	149.657
216	132.536	135.915	136.554	136.554	149.657
222	132.178	135.915	136.554	136.554	149.657
228	132.178	135.915	136.554	136.554	149.657
234	132.178	135.915	136.554	136.554	149.657
240	132.178	135.915	136.554	136.554	149.657
246	132.178	135.915	136.554	136.554	149.657
252	132.178	135.915	136.439	136.554	149.657

Table D.0.1 Continued…:

Time Interval (seconds)	AOSM-Rep 1 (°)	AOSM-Rep 2 (°)	AOSM-Rep 3 (°)	AOSM-Rep 4 (°)	AOSM-Rep 5 (°)
258	132.178	134.096	136.554	136.554	149.657
264	132.178	134.019	136.554	136.554	149.657
270	132.178	134.174	136.554	136.554	149.657
276	132.178	134.427	136.439	136.554	149.657
282	132.178	134.427	136.439	134.317	149.657
288	132.178	134.427	136.439	134.317	149.657
294	132.178	134.427	136.439	134.317	145.278
300	131.115	134.079	136.439	134.317	145.278

Table D.0.2: Contact Angle Analysis for the BC Material

Time Interval (seconds)	BC-Rep 1 (°)	BC-Rep 2 (°)	BC-Rep 3 (°)	BC-Rep 4 (°)	BC-Rep 5 (°)
0	41.602	45.034	41.812	19.982	11.208
6	34.874	20.204	32.284	19.494	10.493
12	34.070	19.544	32.284	19.358	10.238
18	33.882	18.914	29.360	19.222	10.238
24	32.876	17.456	28.378	18.734	9.941
30	32.170	16.578	26.328	18.601	9.941
36	27.314	16.581	26.328	18.228	9.781
42	27.864	15.774	26.074	18.138	9.417
48	28.072	15.578	25.332	18.097	9.417
54	25.340	14.287	24.944	18.097	9.366
60	25.340	13.965	24.820	18.097	9.13

Appendix E

Tabular data: Results Obtained from Soil Water Retention Studies for each of the Treatment Soil Types

Table E.0.1: Gravimetric Water Retention for Saturated, -3 cm, -30 cm, -70 cm, -100 cm, -300 cm, -700 cm, and -5000 cm Suctions

Material	Soil+Core Weight (g)	Θw-0 cm (g/g)	Θw-3 cm (g/g)	Θw-30 cm (g/g)	Θw-70 cm (g/g)	Θw-100 cm (g/g)	Θw-300 cm (g/g)	Θw-700 cm (g/g)	Θw-5000 cm (g/g)	Soil+Core Weight (g)
LFH	253.10	0.3696	0.3370	0.2580	0.1491	0.1395	0.1156	0.0848	0.0636	31.56
	252.82	0.3649	0.3309	0.2641	0.1297	0.1162	0.1103	0.0962	0.0768	32.02
	253.11	0.3747	0.3362	0.2702	0.1278	0.1319	0.1298	0.1210	0.1003	32.03
	253.01	0.3764	0.3348	0.2709	0.1292	0.1109	0.1104	0.1024	0.0777	31.46
	252.96	0.3745	0.3424	0.2800	0.1381	0.1435	0.1399	0.1311	0.1142	31.64
Bm	272.65	0.2649	0.2341	0.1575	0.0591	0.0560	0.0477	0.0378	0.0218	36.77
	272.61	0.2680	0.2359	0.1624	0.0595	0.0544	0.0473	0.0354	0.0201	37.36
	272.66	0.2664	0.2346	0.1524	0.0439	*0.0228*	0.0257	0.0231	0.0180	36.55
	272.54	0.2681	0.2361	0.1540	0.0582	0.0558	0.0428	0.0315	0.0205	37.31
	272.63	0.2628	0.2333	0.1507	0.0523	0.0590	0.0429	0.0283	0.0200	36.63
Subsoil	272.66	0.2711	0.2292	0.1787	0.0610	0.0638	0.0599	0.0459	0.0170	37.31
	272.63	0.2631	0.2276	0.1759	0.0613	0.0635	0.0568	0.0452	0.0223	37.51
	275.31	0.2562	0.2319	0.1647	0.0541	0.0519	0.0497	0.0417	0.0237	37.14
	272.73	0.2674	0.2322	0.1721	0.0586	0.0512	0.0487	0.0353	0.0169	36.57
	272.74	0.2625	0.2316	0.1726	0.0575	0.0519	0.0491	0.0330	0.0197	38.31
----------BC Soil Material----------										
0% AOSM	272.57	0.2357	0.2164	0.1661	0.0616	0.0446	0.0098	0.0103	0.0207	36.98
	272.71	0.2543	0.2270	0.1384	0.0506	0.0333	0.0218	0.0159	0.0225	37.19
	272.58	0.2380	0.2160	0.1359	0.0431	0.0389	0.0284	0.0227	0.0244	36.80
	272.63	0.2567	0.2314	0.1328	0.0457	0.0290	0.0051	0.0059	0.0224	36.50
	272.65	0.2556	0.2285	0.1343	0.0467	0.0407	0.0307	0.0252	0.0201	37.40
2% AOSM	272.60	0.2489	0.2236	0.1643	0.0524	0.0420	0.0297	0.0223	0.0183	37.35
Powder	272.56	0.2569	0.2259	0.1575	0.0522	0.0478	0.0360	0.0285	0.0204	36.90
	272.67	0.2541	0.2250	0.1424	0.0440	0.0423	0.0326	0.0261	0.0214	36.95
	272.66	0.2596	0.2285	0.1442	0.0457	0.0221	0.0116	0.0045	0.0199	36.30
	272.55	0.2522	0.2212	0.1554	0.0517	0.0291	0.0177	0.0113	0.0224	36.99
2% AOSM	272.59	0.2488	0.2151	0.1467	0.0555	0.0392	0.0276	0.0208	0.0196	37.26
Solid	272.68	0.2627	0.2319	0.1460	0.0523	0.0428	0.0327	0.0242	0.0182	37.25
	272.58	0.2548	0.2253	0.1568	0.0523	0.0380	0.0266	0.0203	0.0212	36.60
	272.65	0.2484	0.2220	0.1430	0.0542	0.0474	0.0341	0.0272	0.0189	36.99
	272.58	0.2492	0.2255	0.1318	0.0491	0.0172	0.0063	*0.0003*	0.0197	35.99

Table E.0.1 Continued…: Gravimetric Water Retention for Saturated, -3 cm, -30 cm, -70 cm, -100 cm, -300 cm, -700 cm, and -5000 cm Suctions

Material	Soil+Core Weight (g)	Θw-0 cm (g/g)	Θw-3 cm (g/g)	Θw-30 cm (g/g)	Θw-70 cm (g/g)	Θw-100 cm (g/g)	Θw-300 cm (g/g)	Θw-700 cm (g/g)	Θw-5000 cm (g/g)	Soil+Core Weight (g)
5% AOSM	272.63	0.2507	0.2226	0.1566	0.0491	0.0447	0.0171	0.0195	0.0215	36.83
Powder	272.67	0.2514	0.2222	0.1538	0.0555	0.0452	0.0192	0.0214	0.0208	36.78
	272.57	0.2557	0.2219	0.1531	0.0513	0.0444	0.0167	0.0192	0.0205	37.03
	272.82	0.2570	0.2218	0.1481	0.0539	0.0471	0.0214	0.0225	0.0224	37.13
	272.45	0.2481	0.2192	0.1448	0.0487	0.0424	0.0219	0.0194	0.0205	36.41
5% AOSM	272.58	0.2551	0.2258	0.1429	0.0519	0.0480	0.0264	0.0236	0.0196	36.94
Solid	272.70	0.2623	0.2307	0.1389	0.0522	0.0487	0.0205	0.0238	0.0221	37.44
	272.68	0.2604	0.2312	0.1487	0.0585	0.0534	0.0333	0.0266	0.0208	37.55
	272.71	0.2616	0.2278	0.1493	0.0566	0.0519	0.0291	0.0257	0.0247	37.55
	272.62	0.2601	0.2261	0.1352	0.0500	0.0464	0.0257	0.0250	0.0211	39.99
----------hydrocarbons removed----------										
BC	273.02	0.2736	0.2449	0.1517	0.0580	0.0557	0.0497	0.0363	0.0189	36.82
	272.86	0.2718	0.2438	0.1582	0.0529	0.0450	0.0448	0.0379	0.0223	37.33
	272.62	0.2688	0.2388	0.1531	0.0485	0.0477	0.0399	0.0282	0.0187	25.94
	272.68	0.2667	0.2386	0.1506	0.0539	*0.0845*	*0.0818*	*0.0690*	0.0151	37.61
	272.62	0.2712	0.2413	0.1267	0.0448	0.0404	0.0360	0.0257	0.0139	33.79

****Note:** Soil+Core Weight (g) on Left of Table are for measurements from the large cores (5.08 cm Height; 2.54 cm Radius). This Soil+Core weight was used in calculating the gravimetric water content for suctions of 0, -3 cm, -30 cm, -70 cm, -100 cm, -300 cm, and -700 cm

Soil+Core Weight (g) on Right of Table are for measurements from the small cores (0.9 cm Height; 5.10 cm Radius). This Soil+Core Weight was used in calculating the gravimetric water content for suctions of -5000 cm

The Bulk Density of the LFH was 1.40 gcm^{-3} and for all other treatments the Bulk Density was 1.69 gcm^{-3}. Therefore, 144.14 g of dry soil material was packed into the large LFH cores and 163.71 g of dry soil material packed into all other treatments for the large cores. The smaller cores were packed to the same bulk density as previously indicated and the amount of soil required for each of the cores was calculated based on the moisture content reported at -700 cm suction immediately prior to re-packing to the smaller cores. Deviation in the specified amount of soil material for each of the cores is +/- 1 g. AOSM added on a percent weight basis

****Calculations to Determine Gravimetric Moisture Content:**

$$\frac{\text{(Measured Core+Soil Weight (g) at Specified Suction – Dry Core+Soil Weight (g))}}{\text{Dry Soil Weight (g)}}$$

Appendix F

Tabular data: Results Obtained from Saturated Hydraulic Conductivity Studies for each of the Treatment Soil Types

Table F.0.1: Saturated Hydraulic Conductivity for the Hydrocarbon Treatments

Material	ρb (gcm^{-3})	Head Height (cm)	Time Interval (seconds)	Water Weight in Flask (g)	Water Volume (cm^3)	Jw (cms^{-1})	Ksat (cms^{-1})
BC	1.69	7.9	300	76.36	76.36	0.0126	0.0047
	1.69	7.9	300	91.05	91.05	0.0150	0.0056
	1.69	8.3	300	93.04	93.04	0.0153	0.0056
	1.69	7.8	300	85.38	85.38	0.0140	0.0053
	1.69	7.6	300	111.42	111.42	0.0183	0.0071
BC-2% AOSM	1.69	6.9	300	71.98	71.98	0.0118	0.0048
Powder	1.69	7.2	300	84.36	84.36	0.0139	0.0055
	1.69	7.0	300	57.97	57.97	0.0095	0.0039
	1.69	7.3	300	82.35	82.35	0.0135	0.0054
	1.69	7.3	300	69.51	69.51	0.0114	0.0045
BC-2% AOSM	1.69	6.6	300	88.25	88.25	0.0145	0.0061
Solid	1.69	7.2	300	90.98	90.98	0.0150	0.0060
	1.69	6.9	300	49.53	49.53	0.0081	0.0033
	1.69	5.9	300	68.21	68.21	0.0112	0.0050
	1.69	6.7	300	109.29	109.29	0.0180	0.0075
BC-5% AOSM	1.69	7.3	300	59.97	59.97	0.0099	0.0039
Powder	1.69	7.4	300	85.50	85.50	0.0141	0.0055
	1.69	7.3	300	76.04	76.04	0.0125	0.0049
	1.69	7.3	300	76.29	76.29	0.0125	0.0050
	1.69	7.0	300	56.58	56.58	0.0093	0.0038
BC-5% AOSM	1.69	8.4	300	112.34	112.34	0.0185	0.0067
Solid	1.69	8.4	300	132.32	132.32	0.0218	0.0079
	1.69	7.9	300	74.93	74.93	0.0123	0.0046
	1.69	7.5	300	94.00	94.00	0.0155	0.0060
	1.69	7.4	300	104.47	104.47	0.0172	0.0067

Core Height= 4.78 cm
Core Radius= 2.54 cm

Table F.0.2: Saturated Hydraulic Conductivity for Organic and Mineral Material

Material	ρb (gcm^{-3})	Head Height (cm)	Time Interval (seconds)	Water Weight in Flask (g)	Water Volume (cm^3)	Jw (cms^{-1})	Ksat (cms^{-1})
Subsoil-1	1.51	4.7	300	158.28	158.28	0.0113	0.0070
	1.51	4.7	300	153.55	153.55	0.0110	0.0068
	1.51	4.7	300	151.83	151.83	0.0109	0.0067
Subsoil-2	1.61	3.9	300	165.60	165.60	0.0119	0.0078
	1.61	4.8	300	147.68	147.68	0.0106	0.0065
	1.61	4.9	300	146.27	146.27	0.0105	0.0064
Subsoil-3	1.60	4.0	300	149.20	149.20	0.0107	0.0070
	1.60	4.2	300	150.37	150.37	0.0108	0.0069
	1.60	4.1	300	151.78	151.78	0.0109	0.0071
BC-1	1.63	4.6	300	165.77	165.77	0.0119	0.0074
	1.63	4.7	300	160.27	160.27	0.0115	0.0071
	1.63	4.7	300	156.25	156.25	0.0112	0.0069
BC-2	1.60	4.8	300	179.86	179.86	0.0129	0.0079
	1.60	4.9	300	169.68	169.68	0.0121	0.0074
	1.60	4.8	300	167.14	167.14	0.0120	0.0073
BC-3	1.61	4.2	300	203.98	203.98	0.0146	0.0094
	1.61	4.0	300	190.08	190.08	0.0136	0.0089
	1.61	4.1	300	185.72	185.72	0.0133	0.0086
Bm-1	1.59	4.9	300	155.28	155.28	0.0111	0.0068
	1.59	4.9	300	126.55	126.55	0.0091	0.0055
	1.59	4.9	300	115.77	115.77	0.0083	0.0050
Bm-2	1.61	4.6	300	246.73	246.73	0.0177	0.0110
	1.61	4.5	300	238.52	238.52	0.0171	0.0107
	1.61	4.4	300	222.72	222.72	0.0159	0.0101
Bm-3	1.59	4.1	300	244.03	244.03	0.0175	0.0113
	1.59	4.1	300	234.86	234.86	0.0168	0.0109
	1.59	4.1	300	221.97	221.97	0.0159	0.0103

Table F.0.2 Continued…: Saturated Hydraulic Conductivity for Organic and Mineral Material

Material	ρb (gcm^{-3})	Head Height (cm)	Time Interval (seconds)	Water Weight in Flask (g)	Water Volume (cm^3)	Jw (cms^{-1})	Ksat (cms^{-1})
LFH-1	1.54	4.8	300	178.23	178.23	0.0128	0.0078
	1.54	4.8	300	169.41	169.41	0.0121	0.0074
	1.54	4.8	300	164.29	164.29	0.0118	0.0072
LFH-2	1.38	4.7	300	178.00	178.00	0.0127	0.0079
	1.38	4.8	300	175.19	175.19	0.0125	0.0077
	1.38	4.8	300	171.93	171.93	0.0123	0.0075
LFH-3	1.42	4.5	300	183.92	183.92	0.0132	0.0083
	1.42	4.3	300	176.64	176.64	0.0126	0.0081
	1.42	4.2	300	167.64	167.64	0.0120	0.0077
	----------hydrocarbons removed----------						
BC-1	1.61	4.2	300	382.25	382.25	0.0274	0.0176
	1.61	3.9	300	342.10	342.10	0.0245	0.0162
	1.61	3.9	300	312.90	312.90	0.0224	0.0148
BC-2	1.62	4.8	300	389.46	389.46	0.0279	0.0171
	1.62	4.9	300	366.70	366.70	0.0262	0.0160
	1.62	4.9	300	351.20	351.20	0.0251	0.0153
BC-3	1.62	4.4	300	420.00	420.00	0.0301	0.0190
	1.62	3.9	300	377.81	377.81	0.0270	0.0179
	1.62	4.7	300	353.50	353.50	0.0253	0.0156

Core Height= 7.6 cm
Core Radius= 3.85 cm

**Formulas used to calculate data:*

Core Area= *(π)*(Core Radius)^2*
Core Volume*= Core Height*Core Area*
ρb *= Soil Weight in Core / Core Volume*
Jw*= Water Volume / (Core Area*Time Interval)*
Ksat*= (Water Volume*Core Height) / (Core Area*((Time Interval)*(Core Height + Head Height))*

Appendix G

Calculations: Determining the Amount of AOSM Required for Packing Columns in 2000 gram Increments

Amount of AOSM Required for a 2% AOSM Concentration:

= 2000 g x 0.02
= 40 g

Amount of AOSM Required for a 5% AOSM Concentration:

= 2000 g x 0.05
= 100 g

Appendix H

Calculations: Determining the Amount of Water Required In Order to Achieve 5% Moisture Content During Column Packing

Amount of Water Required for 2000 g of Soil with a AOSM Concentration of 2%:

Amount of Dry Soil (g) = 2000 g

Amount of AOSM (g) = 40 g

Amount of Wet Soil (g) = (Amount of Dry Soil + AOSM x (1+θw))
= (2040 g x (1+0.05))
= 2142 g

Attributed Water Weight Difference (g)=Amount of Wet Soil(g)-(Amount of Dry Soil(g)+AOSM(g))
= 2142g - 2040g
= 102 g

**Given the assumption that 1 g=1 mL; it can be determined that 102 g of water, or 102 mL of water, is required to bring 2000 g of soil with a 2% AOSM concentration to 5% moisture capacity

Amount of Water Required for 2000 g of Soil with a AOSM Concentration of 5%:

Amount of Dry Soil (g) = 2000 g

Amount of AOSM (g) = 100 g

Amount of Wet Soil (g) = (Amount of Dry Soil + AOSM x (1+θw))
= (2100 g x (1+0.05))
= 2205 g

Attributed Water Weight Difference (g)=Amount of Wet Soil(g)-(Amount of Dry Soil(g)+AOSM(g))
= 2205g - 2100g
= 105 g

**Given the assumption that 1 g=1 mL; it can be determined that 105 g of water, or 105 mL of water, is required to bring 2000 g of soil with a 5% AOSM concentration to 5% moisture capacity

Appendix I

Tabular Data: Rainfall Patterns for the Fort McMurray Area

Table I.0.1: Data from Fort McMurray on Climate Patterns

Day	May 2009 Precip (mm)	June 2009 Precip (mm)	July 2009 Precip (mm)	Aug 2009 Precip (mm)	May 2010 Precip (mm)	June 2010 Precip (mm)	July 2010 Precip (mm)	Aug 2010 Precip (mm)	May 2011 Precip (mm)	June 2011 Precip (mm)	July 2011 Precip (mm)	Aug 2011 Precip (mm)
1	0.0	0.0	1.0	11.0	0.5	0.0	0.5	0.0	0.5	0.5	0.0	2.0
2	0.0	0.0	0.0	7.0	0.5	0.5	0.5	8.0	0.5	0.0	0.5	1.0
3	0.0	0.0	9.0	0.0	1.0	0.0	2.5	0.0	3.5	0.0	17.5	4.0
4	0.0	0.0	0.0	15.0	0.0	0.0	1.0	0.0	1.5	0.5	0.5	0.0
5	M	0.0	0.5	0.0	0.0	6.0	1.0	0.0	M	0.0	0.0	0.5
6	0.5	0.5	0.5	0.0	0.5	0.5	5.5	11.0	7.0	0.5	0.0	2.5
7	0.0	0.5	0.0	0.0	0.5	0.0	0.0	M	0.5	0.0	1.5	14.5
8	1.5	1.0	3.5	0.0	0.5	0.0	0.5	0.0	0.0	0.5	0.5	0.5
9	1.0	0.5	2.5	1.0	0.5	0.5	6.5	0.0	0.5	0.0	16.0	0.5
10	0.5	0.0	0.0	0.0	1.0	0.5	0.0	1.0	0.5	0.0	1.0	2.0
11	0.0	0.5	0.0	0.0	0.5	0.5	0.5	6.0	0.0	0.0	0.0	0.5
12	0.5	0.5	0.0	0.5	0.5	0.5	0.0	1.5	2.5	0.0	0.0	1.0
13	0.5	0.5	4.5	0.0	3.0	0.5	3.0	3.0	0.5	0.0	0.0	7.5
14	0.0	0.0	0.0	1.5	0.5	8.0	0.5	0.5	0.0	0.0	1.5	1.0
15	0.0	0.5	0.5	0.0	0.5	0.5	4.5	0.0	0.0	0.5	0.5	10.0
16	0.5	1.5	0.0	0.0	0.5	0.0	1.0	0.5	0.0	5.5	0.0	0.5
17	0.0	0.5	0.0	0.0	0.5	0.5	0.0	0.0	0.5	0.0	0.5	1.0
18	0.0	2.5	9.5	M	0.0	0.0	0.0	0.0	0.5	8.0	3.0	4.5
19	0.5	0.5	4.0	0.0	2.5	0.0	0.0	1.0	0.5	0.5	1.5	0.5
20	0.5	0.0	0.5	0.5	4.5	0.5	0.0	0.0	2.0	3.0	0.0	0.0
21	0.0	3.0	0.0	1.5	9.0	0.5	0.0	0.0	0.0	0.0	0.5	0.5
22	0.0	31.5	1.5	2.5	0.0	0.0	0.5	1.5	0.0	0.5	0.0	0.0
23	0.0	7.0	0.0	11.0	1.0	0.0	0.5	0.5	0.0	0.0	1.0	0.0
24	1.0	0.5	0.5	27.5	0.5	3.5	1.0	0.5	0.0	12.5	0.5	0.0
25	0.0	1.0	0.0	0.0	0.0	14.5	0.0	10.0	0.5	7.5	4.0	0.0
26	6.0	2.5	0.0	0.0	0.0	1.0	3.0	6.0	0.0	1.0	0.0	0.5
27	2.0	1.0	0.5	0.5	0.0	1.0	0.5	11.0	0.5	7.0	1.0	0.0
28	0.0	24.0	0.5	0.0	0.0	0.5	0.0	12.5	0.0	2.0	0.5	0.5
29	0.5	0.5	3.0	0.0	0.0	3.0	21.0	0.5	0.5	0.5	0.5	5.5
30	0.5	0.5	7.5	0.0	1.5	6.5	3.5	0.0	0.5	0.5	0.5	0.5
31	4.0	—	0.5	0.0	0.5	—	0.5	0.5	0.5	—	0.0	0.0

* M = Missing Data

**Obtained from the Government of Canada Climate Data (2014) for the FORT MCMURRAY AWOS A Location with monthly time intervals selected for each of the months studied

Appendix J

Calculations: Determining the Amount of Potassium Chloride Tracer for each Column

Column Area (m^2) = $2\pi r^2+2\pi rh$

$= 2(10\ cm)^2+2\pi(10\ cm)(150\ cm)$

$= 628\ cm^2 + 9420\ cm^2$

$= 10048\ cm^2$

$= 1.0048\ m^2$

Amount of KCl tracer required for the column based on 100 g/m^2 recommendation:

$$\frac{100\ g}{m^2} = \frac{x}{1.0048\ m^2}$$

$$x = 100.48\ g/m^2$$

Amount of water required for the Cl-tracer amount identified based solubility of 31.0 g KCl at 10°C in 100 g of water (Speight, 2005):

$$\frac{31.0\ g}{100\ mL} = \frac{100.48\ g}{x}$$

$$x = 324.13\ mL$$

Amount of Cl-tracer required for a 10 mL spike addition to the columns:

$$\frac{100.48\ g}{324.13\ mL} = \frac{x}{10\ mL}$$

$$x = 3.09999074\ g$$

$$x = 3.10\ g$$

\

Appendix K

Tabular Data: Water Content Measured at Field Capacity for Phase I

Table K.0.1: Measured Water Content Percentage throughout the Columns after 18 Hours for Replication One

Depth (cm)	Column 1	Column 2	Column 3	Column 4	Column 5
15	10.4	10.8	10.1	9.0	10.0
30	6.5	5.1	8.0	5.7	8.4
50	7.4	8.5	8.5	6.9	6.1
80	9.8	10.4	13.6	9.1	10.8
110	11.6	10.4	17.8	12.9	17.2
130	32.5	34.7	28.3	26.4	23.5

Table K.0.2: Measured Water Content Percentage throughout the Columns after 48 Hours for Replication One

Depth (cm)	Column 1	Column 2	Column 3	Column 4	Column 5
15	8.9	9.4	8.8	7.8	8.9
30	5.8	4.0	6.6	4.6	7.6
50	6.6	7.0	6.7	5.6	5.4
80	8.0	8.7	11.1	7.4	9.0
110	10.1	9.7	12.3	11.4	15.1
130	32.3	30.8	24.6	25.9	22.7

Table K.0.3: Measured Water Content Percentage throughout the Columns after 18 Hours for Replication Two

Depth (cm)	Column 1	Column 2	Column 3	Column 4	Column 5
15	18.4	19.7	19.3	10.7	15.9
30	7.6	9.9	14.7	—	12.9
50	12.6	10.1	11.9	10.5	9.5
80	12.9	10.1	12.3	10.0	12.4
110	14.1	10.3	12.4	13.5	14.2
130	20.9	19.7	22.4	14.6	23.7

Appendix K Con't….

Table K.0.4: Measured Water Content Percentage throughout the Columns after 48 Hours for Replication Two

Depth (cm)	Column 1	Column 2	Column 3	Column 4	Column 5
15	16.5	16.7	16.1	8.9	13.6
30	6.9	8.2	12.8	—	10.9
50	10.7	8.9	10.3	8.7	8.4
80	11.8	8.9	10.2	8.2	10.6
110	12.5	8.8	10.5	12.7	11.8
130	20.4	19.1	22.4	14.4	22.7

Appendix L

Tabular Data: Chloride Breakthrough Curve Results for the Five Soil Columns with Cumulative Infiltration

Table L.0.1: Calculated Cumulative Infiltration at the Corresponding Chloride Tracer Measurements for Columns in Replication One

Column 1- LFH; BC with 2% AOSM

Time (min)	EC (µS)	Ave Wgted θ (cm^3cm^{-3})	Pore Volume (m^3)	Cumulative Inflow (m^3)	Cumulative Infiltration
34	102.8	0.3039	0.0143	0.0008	0.0599
38	116.9	0.3035	0.0143	0.0017	0.1186
42	151.9	0.3034	0.0143	0.0025	0.1772
46	189	0.3036	0.0143	0.0033	0.2359
50	511	0.3000	0.0141	0.0042	0.2946
54	979	0.3020	0.0142	0.0050	0.3532
58	1280	0.3018	0.0142	0.0058	0.4119
62	1289	0.3031	0.0143	0.0066	0.4706
66	1125	0.3023	0.0142	0.0075	0.5292
70	938	0.3020	0.0142	0.0083	0.5879
74	688	0.3007	0.0142	0.0091	0.6466
78	543	0.2996	0.0141	0.0099	0.7052
82	370	0.3007	0.0142	0.0108	0.7639
86	295	0.2962	0.0140	0.0116	0.8226
90	223	0.2979	0.0140	0.0124	0.8812
94	187	0.3001	0.0141	0.0133	0.9399
98	151	0.2993	0.0141	0.0141	0.9986
102	136	0.2966	0.0140	0.0149	1.0572
106	117	0.3002	0.0141	0.0157	1.1159
110	105	0.2990	0.0141	0.0166	1.1746
114	92	0.2979	0.0140	0.0174	1.2332
118	82	0.2988	0.0141	0.0182	1.2919
122	74	0.2995	0.0141	0.0191	1.3506
126	69	0.3009	0.0142	0.0199	1.4092
130	61	0.3011	0.0142	0.0207	1.4679
134	58	0.2938	0.0138	0.0215	1.5266
144	53.5	0.2983	0.0141	0.0236	1.6732
154	47.2	0.2990	0.0141	0.0257	1.8199
164	43	0.2957	0.0139	0.0277	1.9666
174	39.6	0.2842	0.0134	0.0298	2.1132

Column 2- LFH; BC with 5% AOSM

Time (min)	EC (µS)	Ave Wgted θ (cm^3cm^{-3})	Pore Volume (m^3)	Cumulative Inflow (m^3)	Cumulative Infiltration
47	91.8	0.2735	0.0129	0.0012	0.0955
51	95.4	0.2749	0.0129	0.0018	0.1446
55	102.7	0.2740	0.0129	0.0025	0.1937
59	107.4	0.2755	0.0130	0.0031	0.2427
63	109.6	0.2751	0.0130	0.0037	0.2918
67	116.7	0.2739	0.0129	0.0044	0.3408
71	137.4	0.2740	0.0129	0.0050	0.3899
75	248	0.2753	0.0130	0.0056	0.4390
79	479	0.2737	0.0129	0.0062	0.4880
83	1174	0.2749	0.0129	0.0069	0.5371
87	1641	0.2754	0.0130	0.0075	0.5862
91	1893	0.2751	0.0130	0.0081	0.6352
95	1828	0.2750	0.0130	0.0087	0.6843
99	1498	0.2753	0.0130	0.0094	0.7333
103	1209	0.2742	0.0129	0.0100	0.7824
107	908	0.2742	0.0129	0.0106	0.8315
111	721	0.2738	0.0129	0.0112	0.8805
115	521	0.2737	0.0129	0.0119	0.9296
119	412	0.2666	0.0126	0.0125	0.9786
123	327	0.2650	0.0125	0.0131	1.0277
127	284	0.2643	0.0124	0.0137	1.0768
131	230	0.2651	0.0125	0.0144	1.1258
135	201	0.2609	0.0123	0.0150	1.1749
145	162.9	0.2639	0.0124	0.0166	1.2975
155	127.8	0.2641	0.0124	0.0181	1.4202
165	102.4	0.2633	0.0124	0.0197	1.5428
175	82.7	0.2632	0.0124	0.0213	1.6655

Table L.0.1 Continued…: Calculated Cumulative Infiltration at the Corresponding Chloride Tracer Measurements for Columns in Replication One

Column 3- LFH; Bm/Subsoil with 2% AOSM

Time (min)	EC (µS)	Ave Wgted θ (cm^3cm^{-3})	Pore Volume (m^3)	Cumulative Inflow (m^3)	Cumulative Infiltration
48	64.5	0.2876	0.0135	0.0017	0.1287
52	44.4	0.2720	0.0128	0.0024	0.1757
56	44.3	0.2904	0.0137	0.0030	0.2226
60	44.4	0.2914	0.0137	0.0037	0.2696
64	49	0.2905	0.0137	0.0043	0.3166
68	82.9	0.2887	0.0136	0.0049	0.3636
72	157.2	0.2887	0.0136	0.0056	0.4105
76	324	0.2899	0.0137	0.0062	0.4575
80	484	0.2899	0.0137	0.0068	0.5045
84	778	0.2911	0.0137	0.0075	0.5515
88	932	0.2920	0.0138	0.0081	0.5985
92	1034	0.2923	0.0138	0.0087	0.6454
96	1067	0.2904	0.0137	0.0094	0.6924
100	1061	0.2912	0.0137	0.0100	0.7394
104	1029	0.2905	0.0137	0.0107	0.7864
108	991	0.2895	0.0136	0.0113	0.8333
112	925	0.2779	0.0131	0.0119	0.8803
116	784	0.2879	0.0136	0.0126	0.9273
120	690	0.2884	0.0136	0.0132	0.9743
124	572	0.2881	0.0136	0.0138	1.0212
128	497	0.2895	0.0136	0.0145	1.0682
132	415	0.2878	0.0136	0.0151	1.1152
136	361	0.2870	0.0135	0.0157	1.1622
146	258	0.2880	0.0136	0.0173	1.2796
156	189	0.2880	0.0136	0.0189	1.3970
166	133.3	0.2881	0.0136	0.0205	1.5145
176	97.2	0.2690	0.0127	0.0221	1.6319

Column 4-LFH; BC with 0% AOSM

Time (min)	EC (µS)	Ave Wgted θ (cm^3cm^{-3})	Pore Volume (m^3)	Cumulative Inflow (m^3)	Cumulative Infiltration
41	96.4	0.2739	0.0129	0.0020	0.1663
45	110.7	0.2751	0.0130	0.0027	0.2245
49	156	0.2763	0.0130	0.0034	0.2828
53	195	0.2608	0.0123	0.0041	0.3411
57	289	0.2767	0.0130	0.0049	0.3993
61	479	0.2753	0.0130	0.0056	0.4576
65	642	0.2756	0.0130	0.0063	0.5159
69	834	0.2738	0.0129	0.0070	0.5741
73	904	0.2745	0.0129	0.0077	0.6324
77	871	0.2737	0.0129	0.0084	0.6907
81	804	0.2729	0.0129	0.0091	0.7489
85	699	0.2602	0.0123	0.0098	0.8072
89	635	0.2568	0.0121	0.0105	0.8655
93	548	0.2557	0.0120	0.0112	0.9237
97	497	0.2540	0.0120	0.0119	0.9820
101	444	0.2523	0.0119	0.0126	1.0403
105	415	0.2511	0.0118	0.0133	1.0985
109	393	0.2507	0.0118	0.0141	1.1568
113	375	0.2468	0.0116	0.0148	1.2151
117	357	0.2493	0.0117	0.0155	1.2733
121	341	0.2484	0.0117	0.0162	1.3316
125	325	0.2466	0.0116	0.0169	1.3899
129	307	0.2457	0.0116	0.0176	1.4481
133	286	0.2460	0.0116	0.0183	1.5064
137	260	0.2452	0.0115	0.0190	1.5647
147	205	0.2427	0.0114	0.0208	1.7103
157	159.1	0.2368	0.0112	0.0225	1.8560
167	112	0.2418	0.0114	0.0243	2.0017
177	82.7	0.2408	0.0113	0.0261	2.1473

Table L.0.1 Continued…: Calculated Cumulative Infiltration at the Corresponding Chloride Tracer Measurements for Columns in Replication One

Column 5- LFH; Bm/Subsoil with 0% AOSM

Time (min)	EC (µS)	Ave Wgted θ (cm^3cm^{-3})	Pore Volume (m^3)	Cumulative Inflow (m^3)	Cumulative Infiltration
42	49.2	0.2803	0.0132	0.0011	0.0797
46	45.2	0.2815	0.0133	0.0017	0.1292
50	42.8	0.2802	0.0132	0.0024	0.1787
54	43.2	0.2817	0.0133	0.0030	0.2283
58	48.6	0.2814	0.0133	0.0037	0.2778
62	79.2	0.2807	0.0132	0.0043	0.3274
66	124	0.2811	0.0132	0.0050	0.3769
70	229	0.2809	0.0132	0.0056	0.4265
74	342	0.2807	0.0132	0.0063	0.4760
78	508	0.2813	0.0132	0.0069	0.5256
82	621	0.2804	0.0132	0.0076	0.5751
86	791	0.2823	0.0133	0.0083	0.6247
90	920	0.2805	0.0132	0.0089	0.6742
94	1054	0.2804	0.0132	0.0096	0.7238
98	1140	0.2815	0.0133	0.0102	0.7733
102	1181	0.2811	0.0132	0.0109	0.8229
106	1166	0.2814	0.0133	0.0115	0.8724
110	1016	0.2817	0.0133	0.0122	0.9220
114	878	0.2799	0.0132	0.0128	0.9715
118	699	0.2796	0.0132	0.0135	1.0211
122	598	0.2804	0.0132	0.0142	1.0706
126	471	0.2798	0.0132	0.0148	1.1202
130	399	0.2802	0.0132	0.0155	1.1697
134	322	0.2797	0.0132	0.0161	1.2192
138	296	0.2812	0.0132	0.0168	1.2688
148	199.3	0.2791	0.0131	0.0184	1.3927
158	137.5	0.2798	0.0132	0.0200	1.5165
168	101.8	0.2807	0.0132	0.0217	1.6404
178	80.7	0.2804	0.0132	0.0233	1.7643

Appendix L Con't….

Table L.0.2: Calculated Cumulative Infiltration at the Corresponding Chloride Tracer Measurements for Columns in Replication Two

Column 1- LFH; BC with 2% AOSM

Time (min)	EC (µS)	Ave Wgted θ (cm^3cm^{-3})	Pore Volume (m^3)	Cumulative Inflow (m^3)	Cumulative Infiltration
85	154.7	0.2860	0.0135	-0.0001	-0.0100
89	149.4	0.2837	0.0134	0.0002	0.0125
93	152.9	0.2840	0.0134	0.0005	0.0349
97	158.3	0.2830	0.0133	0.0008	0.0574
101	166.3	0.2841	0.0134	0.0011	0.0798
105	176.3	0.2838	0.0134	0.0013	0.1023
109	181.1	0.2842	0.0134	0.0016	0.1247
113	185.6	0.2847	0.0134	0.0019	0.1472
117	187.5	0.2828	0.0133	0.0022	0.1696
121	187.4	0.2823	0.0133	0.0025	0.1921
125	178	0.2814	0.0133	0.0028	0.2145
129	181	0.2792	0.0132	0.0031	0.2370
133	198	0.2794	0.0132	0.0034	0.2594
137	298	0.2788	0.0131	0.0037	0.2819
141	424	0.2786	0.0131	0.0040	0.3043
145	633	0.2792	0.0132	0.0043	0.3268
149	943	0.2767	0.0130	0.0046	0.3492
153	997	0.2768	0.0130	0.0049	0.3717
157	1081	0.2773	0.0131	0.0052	0.3941
161	1068	0.2772	0.0131	0.0055	0.4166
165	1072	0.2762	0.0130	0.0058	0.4390
169	1152	0.2764	0.0130	0.0061	0.4615
173	1286	0.2757	0.0130	0.0064	0.4839
174	1635	0.2761	0.0130	0.0064	0.4895
178	1936	0.2759	0.0130	0.0067	0.5120
182	2520	0.2753	0.0130	0.0070	0.5344
192	2660	0.2735	0.0129	0.0078	0.5906
202	1301	0.2777	0.0131	0.0085	0.6467
212	653	0.2775	0.0131	0.0093	0.7028
222	463	0.2763	0.0130	0.0100	0.7589

Column 2- LFH; BC with 5% AOSM

Time (min)	EC (µS)	Ave Wgted θ (cm^3cm^{-3})	Pore Volume (m^3)	Cumulative Inflow (m^3)	Cumulative Infiltration
58	152.5	0.2489	0.0117	0.0014	0.1227
62	310	0.2504	0.0118	0.0019	0.1652
66	280	0.2497	0.0118	0.0024	0.2076
70	381	0.2499	0.0118	0.0029	0.2501
74	421	0.2484	0.0117	0.0034	0.2925
78	430	0.2471	0.0116	0.0039	0.3349
82	447	0.2466	0.0116	0.0043	0.3774
86	452	0.2451	0.0115	0.0048	0.4198
90	436	0.2461	0.0116	0.0053	0.4623
94	410	0.2461	0.0116	0.0058	0.5047
98	390	0.2450	0.0115	0.0063	0.5472
102	377	0.2452	0.0116	0.0068	0.5896
106	380	0.2447	0.0115	0.0073	0.6321
110	387	0.2441	0.0115	0.0078	0.6745
114	416	0.2431	0.0115	0.0082	0.7170
118	475	0.2430	0.0114	0.0087	0.7594
122	555	0.2423	0.0114	0.0092	0.8018
126	609	0.2425	0.0114	0.0097	0.8443
130	641	0.2424	0.0114	0.0102	0.8867
134	657	0.2411	0.0114	0.0107	0.9292
138	672	0.2406	0.0113	0.0112	0.9716
142	688	0.2410	0.0114	0.0117	1.0141
146	767	0.2398	0.0113	0.0122	1.0565
156	868	0.2403	0.0113	0.0134	1.1626
166	1054	0.2395	0.0113	0.0146	1.2687
176	1241	0.2401	0.0113	0.0158	1.3748
186	798	0.2401	0.0113	0.0170	1.4810

Table L.0.2 Continued…: Calculated Cumulative Infiltration at the Corresponding Chloride Tracer Measurements for Columns in Replication Two

Column 3- LFH; Bm/Subsoil with 2% AOSM

Time (min)	EC (µS)	Ave Wgted θ (cm^3cm^{-3})	Pore Volume (m^3)	Cumulative Inflow (m^3)	Cumulative Infiltration
47	92.7	0.2694	0.0127	-0.0007	-0.0516
51	83.4	0.2711	0.0128	-0.0002	-0.0128
55	88	0.2691	0.0127	0.0003	0.0259
59	85.5	0.2732	0.0129	0.0008	0.0647
63	177.9	0.2767	0.0130	0.0013	0.1034
67	221	0.2761	0.0130	0.0018	0.1422
71	333	0.2771	0.0131	0.0023	0.1810
75	566	0.2775	0.0131	0.0028	0.2197
79	385	0.2776	0.0131	0.0033	0.2585
83	862	0.2780	0.0131	0.0038	0.2973
87	897	0.2780	0.0131	0.0043	0.3360
91	893	0.2787	0.0131	0.0048	0.3748
95	827	0.2779	0.0131	0.0053	0.4136
99	774	0.2789	0.0131	0.0058	0.4523
103	725	0.2783	0.0131	0.0063	0.4911
107	679	0.2785	0.0131	0.0068	0.5299
111	648	0.2772	0.0131	0.0073	0.5686
115	629	0.2768	0.0130	0.0079	0.6074
119	616	0.2767	0.0130	0.0084	0.6461
123	606	0.2678	0.0126	0.0089	0.6849
127	579	0.2773	0.0131	0.0094	0.7237
131	557	0.2624	0.0124	0.0099	0.7624
135	530	0.2747	0.0129	0.0104	0.8012
139	473	0.2759	0.0130	0.0109	0.8400
143	416	0.2756	0.0130	0.0114	0.8787
147	353	0.2732	0.0129	0.0119	0.9175
157	217	0.2719	0.0128	0.0131	1.0144
167	138.7	0.2700	0.0127	0.0144	1.1113
177	96.6	0.2689	0.0127	0.0156	1.2082
187	78	0.2684	0.0126	0.0169	1.3051

Column 4-LFH; BC with 0% AOSM

Time (min)	EC (µS)	Ave Wgted θ (cm^3cm^{-3})	Pore Volume (m^3)	Cumulative Inflow (m^3)	Cumulative Infiltration
56	135.1	0.2798	0.0132	0.0024	0.1909
60	191	0.2832	0.0133	0.0029	0.2332
64	289	0.2714	0.0128	0.0035	0.2755
68	323	0.2793	0.0132	0.0040	0.3178
72	330	0.2792	0.0131	0.0045	0.3601
76	351	0.2774	0.0131	0.0051	0.4024
80	381	0.2789	0.0131	0.0056	0.4446
84	403	0.2742	0.0129	0.0061	0.4869
88	431	0.2750	0.0130	0.0066	0.5292
92	465	0.2766	0.0130	0.0072	0.5715
96	555	0.2734	0.0129	0.0077	0.6138
100	716	0.2726	0.0128	0.0082	0.6561
104	890	0.2741	0.0129	0.0088	0.6984
108	1149	0.2663	0.0125	0.0093	0.7406
112	1185	0.2612	0.0123	0.0098	0.7829
116	1031	0.2657	0.0125	0.0104	0.8252
120	753	0.2638	0.0124	0.0109	0.8675
124	676	0.2628	0.0124	0.0114	0.9098
128	659	0.2594	0.0122	0.0120	0.9521
132	636	0.2607	0.0123	0.0125	0.9943
136	657	0.2601	0.0123	0.0130	1.0366
140	717	0.2540	0.0120	0.0135	1.0789
144	759	0.2519	0.0119	0.0141	1.1212
148	861	0.2586	0.0122	0.0146	1.1635
158	717	0.2591	0.0122	0.0159	1.2692
168	382	0.2489	0.0117	0.0173	1.3749
178	178.3	0.2401	0.0113	0.0186	1.4806
188	174.5	0.2556	0.0120	0.0199	1.5863

Table L.0.2 Continued…: Calculated Cumulative Infiltration at the Corresponding Chloride Tracer Measurements for Columns in Replication Two

Column 5- LFH; Bm/Subsoil with 0% AOSM

Time (min)	EC (µS)	Ave Wgted θ (cm^3cm^{-3})	Pore Volume (m^3)	Cumulative Inflow (m^3)	Cumulative Infiltration
53	102	0.2744	0.0129	0.0011	0.0896
57	81.8	0.2734	0.0129	0.0017	0.1336
61	169.2	0.2739	0.0129	0.0023	0.1777
65	66.4	0.2741	0.0129	0.0028	0.2217
69	68.3	0.2732	0.0129	0.0034	0.2658
73	68.4	0.2699	0.0127	0.0039	0.3098
77	88.7	0.2734	0.0129	0.0045	0.3539
81	135.7	0.2744	0.0129	0.0051	0.3979
85	186.4	0.2674	0.0126	0.0056	0.4420
89	237	0.2681	0.0126	0.0062	0.4860
93	364	0.2706	0.0127	0.0067	0.5301
97	524	0.2747	0.0129	0.0073	0.5741
101	612	0.2717	0.0128	0.0079	0.6182
105	661	0.2720	0.0128	0.0084	0.6622
109	702	0.2690	0.0127	0.0090	0.7063
113	722	0.2717	0.0128	0.0096	0.7504
117	752	0.2692	0.0127	0.0101	0.7944
121	785	0.2732	0.0129	0.0107	0.8385
125	854	0.2681	0.0126	0.0112	0.8825
129	834	0.2714	0.0128	0.0118	0.9266
133	854	0.2649	0.0125	0.0124	0.9706
137	898	0.2717	0.0128	0.0129	1.0147
141	927	0.2706	0.0127	0.0135	1.0587
145	950	0.2699	0.0127	0.0140	1.1028
149	947	0.2691	0.0127	0.0146	1.1468
159	768	0.2667	0.0126	0.0160	1.2570
169	389	0.2629	0.0124	0.0174	1.3671
179	168.7	0.2618	0.0123	0.0188	1.4772
189	116	0.2672	0.0126	0.0202	1.5874